2011-01-01

Accumulation, Speciation, And Distribution Of Metal(loids) In Plants: Applications Of Synchrotron Techniques In Environmental Sciences

Hiram Castillo-Michel
University of Texas at El Paso, hiramcm79@gmail.com

ACCUMULATION, SPECIATION, AND DISTRIBUTION OF METAL(LOIDS) IN PLANTS: APPLICATIONS OF SYNCHROTRON TECHNIQUES IN ENVIRONMENTAL SCIENCES

HIRAM CASTILLO-MICHEL

Environmental Science and Engineering

Approved

_____
Jorge L. Gardea-Torresdey, Ph.D., Chair

_____
Kristine Garza, Ph.D.

_____
John Walton, Ph.D.

_____
Alejandro Martinez-Martinez, Ph.D.

_____
Patricia D. Witherspoon, Ph.D.

Dean of the Graduate School

DEDICATORIA

Doy gracias a dios por darme la oportunidad de ver la vida atravez de la ciencia y llenar mi vida de oportunidades y aventuras. Dedico este trabajo a mi familia que es mi tesoro invaluable por compartir siempre mis logros y darme aliento en mis derrotas. A mis padres y mi hermano por bindarme siempre su apoyo y amor incondicional y haber sembrado en mi los valores que son la base de mi vida diaria. A mis hermosas ahijadas por darme momentos tan felices y amor sincero. A mi esposa por todas las cosas buenas que ha traido a mi vida. Priscila te amo, eres mi mayor fortaleza, gracias por estar siempre conmigo y demostrarme que no hay distancia ni obstaculo que no podamos superar. Tambien dedico este trabajo a mi hija aun no nacida por ser el regalo mas maravilloso que hay en el mundo.

DEDICATION

I thank god for giving me the opportunity to see life through the eyes of science and giving me a life full of opportunities and adventures. I dedicate this work to my family, my invaluable treasure, for always being there to celebrate my success and offering support during bad times. To my parents and brother for giving me unconditional love and support and for founding in me the values that are the basis of everyday journey. To my beautiful nieces for giving me all those happy moments and sincere love. To my wife for all the good you have brought to my life. Priscila I love you, you are my strength, thanks for always being with me and showing me there is no distance or obstacle that we cannot overcome. Also, I dedicate this work to my unborn daughter for being my most wonderful gift.

ACCUMULATION, SPECIATION, AND DISTRIBUTION OF METAL(LOIDS) IN PLANTS: APPLICATIONS OF SYNCHROTRON TECHNIQUES IN ENVIRONMENTAL SCIENCES

by

HIRAM CASTILLO-MICHEL, B.Sc., M.Sc.

DISSERTATION

Presented to the Faculty of the Graduate School of
The University of Texas at El Paso
in Partial Fulfillment
of the Requirements
for the Degree of

DOCTOR OF PHILOSOPHY

Environmental Science and Engineering
THE UNIVERSITY OF TEXAS AT EL PASO

May 2011

ACKNOWLEDGEMENTS

I would like to acknowledge all the people that throughout my years as a Ph.D student have contributed in one way or another to the realization of this dissertation work. First of all, I would like to express my most sincere gratitude to my mentor, Dr. Jorge Gardea-Torresdey, for letting me work under his supervision, for his advice, support and friendship. Thank you Dr. Gardea for supporting me in my scientific quests, without your mentoring this work would have never been possible. Thanks to all present and former members of Dr. Gardea's Lab; you have made me feel like home, I have always been happy to work side by side with all of you. Thanks for your friendship and kind support. I also would like to thank Dr. Peralta for his guidance during the past years, for his helpful ideas and suggestions throughout the course of this research. I would like to acknowledge Dr. Lopez and Dr. De la Rosa for teaching me so much while they were part of Dr. Gardea's lab; you are great scientists but greater persons. Also, I would like to acknowledge Alia Servin, Kenneth Dokken and Jose Hernandez for taking care of my experiments while I was gone for my fellowship at the ALS. Thanks for your friendship and for being there during my long hours of no sleep during my beamtimes. Thanks for listening me when I was in my maximum state of sleep deprivation. I hope we can continue having long hours of no sleep at the synchrotrons together. Thanks to Dr. Mathew Marcus for your great support during my beamtimes at the ALS and for helping me get valuable beamtime when I needed it the most.

I would like to acknowledge Dr. Kristine Garza, Dr. John Walton, and Dr. Alejandro Martinez-Martinez for being part of my dissertation committee. Thanks Dr. Garza and Dr. Walton I have enjoyed the experience of having you as my professors and committee members. I

want to give special thanks to Dr. Martinez for opening the doors of his lab at UACJ and letting me conduct experiments and get trained in the field of molecular biology.

With my entire heart I thank to my family, they are my inspiration and the strength that I need to continue. Thank you for always being there for me, for filling my life with love and respect and for having always a good advice for me.

I would like to acknowledge the financial support from the US Department of Energy under proposal # 31406 number, the USDA grant number 2008-38422-19138**,** the Toxicology Unit of the BBRC (NIH NCRR Grant # 2G12RR008124-16A1), the NSF Grant # CHE-0840525, and the ALS Doctoral Fellowship in Residence Program (ALS-LBNL). Portions of this research were carried out at the Stanford Synchrotron Radiation Laboratory, a national user facility operated by Stanford University on behalf of the U.S. Department of Energy, Office of Basic Energy Sciences. The SSRL Structural Molecular Biology Program is supported by the Department of Energy, Office of Biological and Environmental Research, and by the National Institutes of Health, National Center for Research Resources, Biomedical Technology Program. I acknowledge the operations of the Advanced Light Source at Lawrence Berkeley National Laboratory. The Advanced Light Source is supported by the Director, Office of Science, Office of Basic Energy Sciences, of the U.S. Department of Energy under Contract No. DE-AC02-05CH11231. I also acknowledge the Consejo Nacional de Ciencia y Tecnologia of Mexico (CONACyT) for its financial support.

ABSTRACT

In the last two decades synchrotron based techniques have gained popularity and been increasingly used in environmental sciences. The present dissertation has relied significantly in the use of synchrotron based techniques to study the speciation, coordination, and distribution of toxic metal(loids) in plants.

Parkinsonia florida is a plant species native to the semi-desert regions of North America. The cultivation characteristics of this shrub/tree suggest that it could be used for phytoremediation purposes in semiarid regions. *P. florida* plants were grown in two types of soils spiked with As at 20 mg kg^{-1}. Plants grown in the SS and SCL soil accumulated detectable amounts of As mainly in roots. Linear combination μXANES data analysis from the roots exposed to As(V) treated soil showed that As was reduced to As(III). Also, a fraction of the reduced As was found coordinating to S in a form consistent with As-Cys_3. *P. florida* has demonstrated the ability to stabilize As in roots in the form of a less toxic and more stable compound.

Plants modify the bioavailability of As in the rhizosphere. This research investigated As speciation in the rhizosphere of mesquite (*Prosopis juliflora*) plants using synchrotron techniques. The selected soil for this study was a sandy clay loam treated with As(III) and As(V). Rhizosphere soil and freeze dried root tissues of one month old plants were analyzed using bulkXAS. Arsenic was found as As(V) in all soils whereas in the roots it was found as As(III). μXAS and μXRF studies of thin sections (1mm thick) from resin embedded soil cores confirmed the presence of As(III)-S interactions in the root tissues and a strong As-Fe interaction in the soil.

The uptake and speciation of Cd in corn plants and its effects on nutrient uptake was studied in this research. The link between S concentration, Cd uptake, and the synthesis of Low molecular weight thiols (LMWT) was investigated. ICP/OES determinations demonstrated that Cd concentration was higher in the roots compared to the shoots. Nutrient absorption of Mo, Mn, and P remained normal in comparison to the control plants. However, the concentration of S in roots and shoot tissues increased with increasing uptake of Cd. The production the LMWT also increased upon exposure to Cd. XAS analyses was performed to demonstrate the link between Cd and sulfur ligands. The results indicate that Cd inside the corn roots and shoots is bound to sulfur ligands with interatomic distances of 2.51-2.52 Å. These results confirm a strong link between S uptake and the production of LMWT upon exposure to Cd.

The rapid development of nanotechnology has created an urge for the assessment of possible health and environmental hazards caused by metal NPs. In this reserach we studied the effect on DNA stability of ZnO and CeO_2 NPs in soybean plants using the RAPD assay. RAPD profiles from treated plants were compared to control plants. Results showed that ZnO at 4000 mg/L and CeO_2 at 2000 and 4000 mg/L did affect the stability of the DNA with new bands appearing. Roots treated with ZnO NPs at 4000 mg/L presented a new band at 519bp. Roots treated with CeO_2 NPs at 2000 mg/L presented four new bands (1516, 581, 544, and 353bp), while three new bands appeared at 4000 mg/L (581, 411, and 353bp). RAPD has shown that the ZnO and CeO_2 NPs do affect the DNA integrity in soybean plants.

TABLE OF CONTENTS

Page

LIST OF TABLES

Page

LIST OF FIGURES

Page

CHAPTER 1

Introduction

In the last two decades synchrotron based techniques have gained popularity and been increasingly used in environmental sciences. The present dissertation has relied significantly in the use of synchrotron based techniques to study the speciation, coordination, and distribution of toxic metal(loids) in plants. Aiming to elucidate mechanisms of accumulation, translocation and toxicity of these elements, the use of synchrotron techniques has proved to be of great help. This chapter is an effort to provide an overview of synchrotrons and synchrotron-based techniques and their application in the study of plant-soil-metal interactions.

1.1 Introduction to synchrotron radiation

Synchrotron radiation (SR) sources are based on technology developed for high energy physics experiments. Synchrotrons are use to accelerate charged particles (mainly electrons) to velocities approaching the speed of light. Charged particles generate electromagnetic radiation when they are being accelerated, and they do this as they are directed around a curved pattern by magnetic fields. Charged particles moving close to the speed of light generate an electromagnetic spectrum dramatically altered compared to slower particles. Large amounts of power are radiated, the electromagnetic spectrum is shifted to higher energies (frequencies), and the pattern of radiation becomes highly directional. During the 1970s the field of SR was completely parasitic of the high energy physics experiments [1]. High energy physicists considered the

emitted radiation a loss, because it steals energy from their particle beams. However, over the last three decades the use of SR has been found to have extremely beneficial properties for X-ray experimenters. Due to the success of SR research dedicated second generation facilities such as the National Synchrotron Light Source (NSLS) were built. After, the development of the called insertion devices (wigglers and undulators) the third generation facilities such as the advanced light source (ALS) and the European synchrotron radiation facility (ESRF) were built. Today there are about 50 synchrotrons (http://www.lightsources.org/) located all over the world being used by a growing number of scientists from different fields (e.g. physics, chemistry, geosciences/environmental).

The main component of a synchrotron is the storage ring where SR is emitted tangentially to the electron's orbit in the form of a narrow cone. With increasing speed of the electrons the emission cone becomes narrower and the emitted radiation shifts towards higher energies (shorter wavelengths) [2]. In the so called third-generation light sources, the storage ring has a polygonal shape where in the straight sections special magnetic structures called insertions devices are accommodated. Bending magnets are still used in the corners to bend the electron's path around the storage ring. Insertion devices (undulators and wigglers) generate magnetic fields specially shaped to drive electrons in an oscillating trajectory, each bend acts like a source radiating along the axis of the insertion device. The light emitted from insertion devices becomes very intense sometimes with near laser-like brightness. The properties that make SR so unique include:

1. High brightness: SR is hundreds of thousands times more intense than that from conventional X-ray tubes [2]. Measured as flux (number of photons/ sec in a beam) or as intensity (photons/sec/area incident on a target) [1].

2. Wide energy spectrum: SR is emitted with energies ranging from infrared light to hard X-rays (Fig. 1.1). Furthermore, the emitted light is tunable with the use of monochromators. This allows selection of the incident X-ray energy required to perform experiments of X-ray absorption spectroscopy (XAS). Resolutions lower that 1ev are required for XAS and achieved with the use of silicon crystal monochromators.

3. Highly polarized: The emitted SR is highly polarized, which can be linear, circular or elliptical depending on the magnetic structure used to guide the path of the electrons.

4. Time structure: Electrons in the storage ring are not uniformly spaced around its periphery, they are concentrated in bunches (one to several hundred). This can offer important benefits for some experiments. The beam is like a stroboscope that enables time-resolved studies.

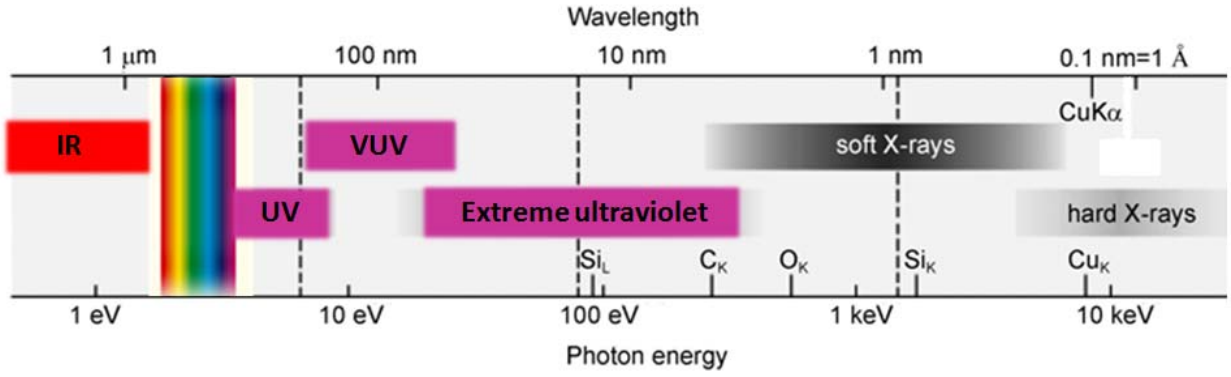

Figure 1.1 Electromagnetic spectrum in wavelength and in photon energy with some L and K shell electron binding energies [1].

Due to the above mentioned properties, a significant number of spectroscopic methodologies are available for the study of environmental samples. The following section will cover the description of the techniques employed in this dissertation work: X-ray absorption and fluorescence (unfocused and focused) techniques.

1.2 X-ray absorption and fluorescence techniques

The physical basis of X-ray absorption spectroscopy relies on the energy of the X-rays interacting with the element of interest. When the energy of the X-ray is sufficiently high to eject core electrons from an atom, via the photo-electric effect, a sharp increase in the absorption of X-ray photons occurs. This is called the absorption edge. The X-ray absorption coefficient (μE) is measured while the energy of the incoming X-ray is scanned across the binding energy of the element of interest. Each core electron has a specific binding energy depending on the atom's electronic configuration. With increasing number of electrons in the atom the binding energy of the core electrons increases and higher energy X-rays are required to produce the photoelectric effect. A consequence of the photoelectric effect is fluorescence, this occurs as the atom relaxes back to the ground state. An electron from a higher energy level fills the vacancy left by the photoelectron and the difference in energy between the two electrons is emitted as fluorescence (Fig.1.2). The specific energies involved in both absorption and fluorescence processes and the ability of the synchrotron source to provide energy-tunable X-rays confer the element-specificity to these techniques.

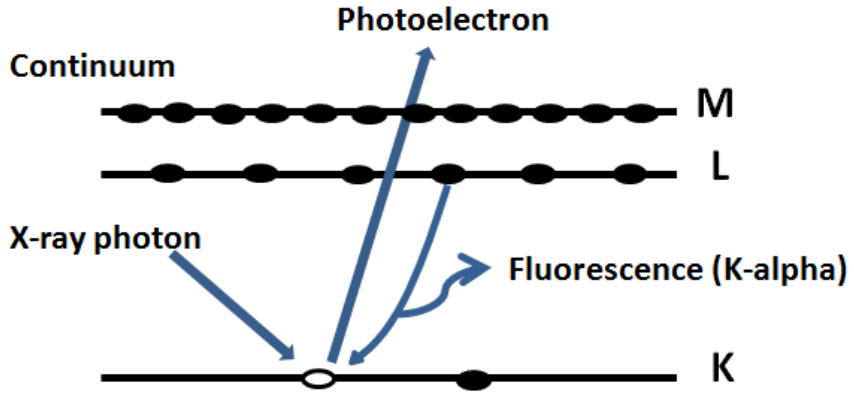

Figure 1.2 Schematic representation of the excitation of an atom by an X-ray photon and the corresponding relaxation process by X-ray fluorescence. K,L and M are the core electron levels.

XAS is a powerful technique that provides information about the oxidation state, three-dimensional geometry and coordination environment of the element of interest. The main advantage of this technique is the ability to investigate both crystalline and amorphous portions of samples which facilitates sample preparation [3]. However, this technique requires high X-ray fluxes and tunability that are generally only achievable with a SR source. The XAS spectrum can be divided in two energy regions that give the name to the two complimentary XAS techniques: X-ray absorption near-edge spectroscopy (XANES) and extended X-ray absorption fine structure (EXAFS) (Fig. 1.3). The XANES region extends from the pre-edge region to about 50 eV above the absorption edge. The main XANES feature is represented by an intense resonance feature originated by the production of photoelectrons. The position of the edge increases with each electron that is removed from the valence shell by 1-3 eV. The binding energy of the core levels increases when the atom losses one valence electron. Also, the position of the absorption edge is affected by the bonding environment of the absorber. This allows distinguishing for instance As coordinating to O from As coordinating to S. Hence, XANES provides important information about the oxidation state and chemical environment of the absorber. The shift of the edge of absorption can be observed in Fig. 1.3A. The mineral arsenolite ($As(III)_2O_3$) has its absorption edge at a lower energy compared to the mineral pharmacosiderite ($KFe_4(As(V)O_4)_3(OH)_4 \cdot 6\text{-}7H_2O$).

In order to understand EXAFS the photoelectrons ejected from the atom should be considered as waves. The interaction of the outgoing and backscattered wave generates oscillations in the absorption coefficient product of constructive and destructive interferences. Since the backscattered wave is caused by first and second order neighboring atoms the frequency of the oscillation is inversely related to the bond distance. The amplitude is related to

the characteristics of the neighboring atom and their number (coordination number). The physics behind the EXAFS signal is well understood and can be modeled with the aid of computer programs to obtain information about the surrounding atoms, bond distances and coordination numbers. The information obtained from EXAFS analysis is limited to neighboring atoms, typically within 10 Å from absorbing atom.

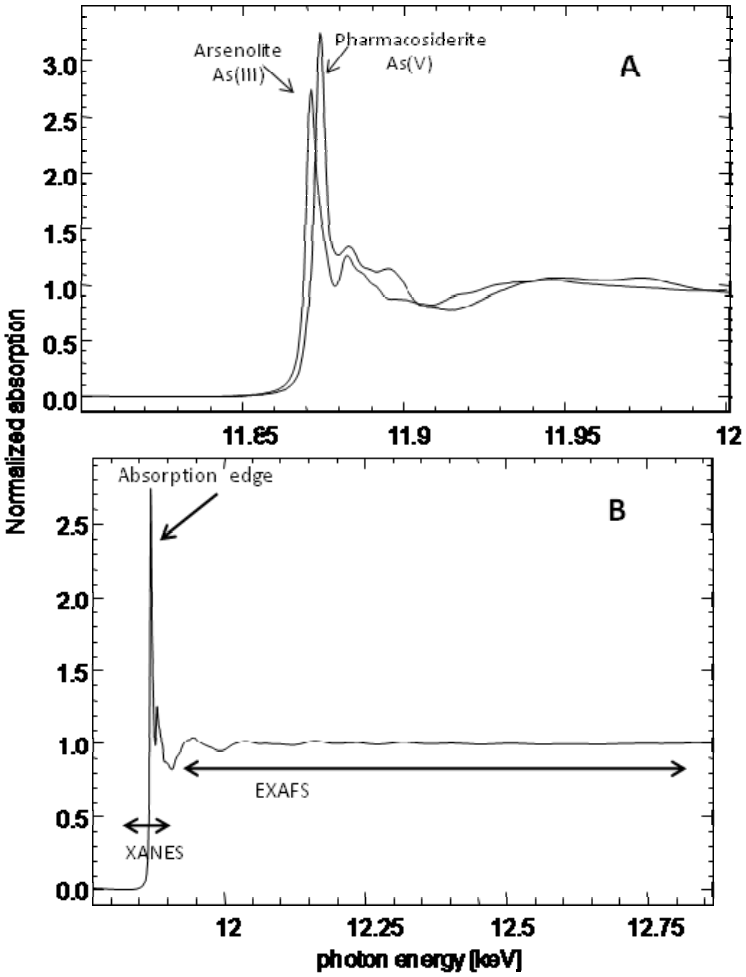

Figure 1.3 XAS spectra from As minerals. A) Absorption edge position of arsenolite ($As(III)_2O_3$) and pharmacosiderite ($KFe_4(As(V)O_4)_3(OH)_4 \cdot 6\text{-}7H_2O$). B) XAS spectrum of the mineral arsenolite showing XANES and EXAFS pertinent regions.

The high photon flux from a SR source allows the focusing of X-rays with the use of mirrors, crystals or Fresnel zone plates to beam sizes of a few micrometers and even the sub-micron range [2]. With the aid of a microfocused beam SR analyses such as μXAS and μXRF

can be conducted in a laterally resolved manner. In this fashion, experiments conducted with microfocused X-rays involve the use of μXRF to generate maps of distribution of elements in a sample followed by μXAS analysis conducted at selected spots of interest in the sample. In contrast to bulkXAS a μXAS experiment allows identifying chemical species that do not contribute significantly to the bulk signal. For instance, the presence of a mineralized form of arsenic in a sample where arsenic adsorbed to iron oxides is the predominant form (Chapter 2). It is important to mention that the size of the beam defines lateral resolution but the depth resolution depends on the nature of the sample, the element of interest and the energy of the incident X-ray [2]. In comparison to other non-synchrotron methods with similar capabilities, such as scanning electron microscopy with energy dispersive x-ray analysis (SEM-EDXA), μXRF has better sensitivity due to the high photon flux. This is important for the study of trace metals in the environment. A significant amount of applications in environmental science have taken advantage of μXRF and μXAS. The following section will provide an overview of the application of these techniques in the study of metal(loids) in plants.

1.3 Applications of μXAS and μXRF

This section will focused on the main applications of μXAS and μXRF in the investigation of As, Cd and ZnO nanoparticles in plants. Arsenic and cadmium are higly toxic for plants and humans. Hyper accumulator plants have been identified for both As and Cd opening the possibility for phytoremediation applications [4, 5]. On the other hand, the accumulation of As and Cd in edible plants presents a threat for human health. Thus, it is important to understand the mechanisms involved in their tolerance, trafficking, and accumulation by plants.

Isaure et al. 2006 [6] studied the distribution and speciation of Cd in the model plant *Arabidopsis thaliana*. Plants (14 day old) were exposed to Cd concentrations of 200 μM in agar enriched media for 4 days. Elemental distribution of Cd in roots and leaves was performed by two comparable and complimentary techniques SEM-EDX and μXRF. The speciation of Cd was studied for the first time using Cd L_{III}-edge μXANES. In roots Cd was found coordinated to S ligands and localized in the vascular bundles. The leaves of *A. thaliana* accumulated Cd in the epidermal hairs bound to O and N ligands most likely from the cell wall. One of the critical points in the analysis of biological specimens is sample preparation. The authors compared the two most common methods for plant samples: freeze dried vs. frozen hydrated (-170ºC). The results obtained were similar for both sample preparation methods and the authors suggest the freeze drying treatment does not induce redistribution of Cd in the plant cells. However, these results should not be interpreted as a general rule for all elements in plant samples. It is worth noting that in Isaure et al. 2006 [6] the results from SEM-EDX and μXRF both confirmed the accumulation of Cd in the epidermal hairs of *A. thaliana*. The advantage of μXRF is the highly improved sensitivity that allows mapping elements in the tens of ppm [2]. In addition to this, speciation studies (μXANES) on the same sample can only be performed with the use of SR. However, SEM-EDX images provide structural details that are complimentary to synchrotron based techniques.

A recent study by Isaure et al. 2010 [7] reports on the elimination of Cd via the production of Ca containing grains at the top of tobacco leaf hairs (trichomes). With the use of SEM-EDX and synchrotron based X-ray diffraction (μXRD) and μXANES. Some synchrotron beamlines have incorporated detection modes for XRD analysis. The beam size for microfocused XRD is the same as for μXANES (.3 to 30 μm). The main advantage of performing XRD

analysis with SR is again the high photon flux that allows studying the crystal properties of micro structures. Tobacco plants produced more grains per mass of dry matter under high exposure to Cd and Ca. Supplemented Ca in high molar ratio (Ca/Cd = 131 mol ratio) increased the elimination of Cd via the production of Cd containing vaterite. The speciation of Cd was studied by Cd L_{III}-edge μ-XANES. Using the least-squares fitting procedure best one component fittings from several grains were obtained with the use Cd containing calcites and Cd vaterite. The results from μXANES were confirmed by μXRD, this approach is applicable in this case as the samples were crystal grains. The work presented by Isaure et al. 2010 [7] is an excellent example of how two powerful synchrotron based techniques complement each other to provide very accurate results.

The toxicity of As depends on its chemical form. The studies of As accumulation in plants have focused mainly in hyperaccumulator plants and rice cultivars. Pickering et al. 2006 [8] presented the first application of μXRF and μXAS in the study of As accumulation in *Pteris vittata* plants. The unusual amounts of As this plant species is able to accumulate in the fronds revealed it as an excellent candidate for phytoremediation. *P. vittata* spores were germinated and grown for one month in 1mM potassium arsenate (As(V)) liquid and agar medium. Rather than using microspectroscopy at selected spots of interest the authors demonstrated the strength of using μXAS at multiple energies (chemical mapping). In this application, the sample is raster scanned at maximum peaks of absorption energies of selected chemical species. A detailed description of this methodology is offered by Marcus 2010 [9]. In the work by Pickering et al. 2006, the energies chosen were 11 869.8, 11 871.4, and 11 874.8 eV for As(glutathione)$_3$, arsenite, and arsenate, respectively. The final outcome of chemical mapping is As distribution maps that are specific for the tested chemical species (e.g. distribution maps of As(V) and As(III)

in the same sample). Results provided compelling evidence of As(V) transport to the frond tissues of *P. vittata* plants and stored in leaf tissues as neutral As(III). A significant result is the lack of As-thiolate species, despite of the great affinity of As to thiol groups. The presence of As-thiolates was confirmed in the form of cylindrical sheaths (5—50 μm thick) around As(V) in the leaf veins. The formation of As-thiolates seems to be in response to As(V) active transport to the veins and part of a reduction mechanism. The low amount of As coordination to thiolates (<5%) agrees with the low synthesis of phytochelatins in response to As(V) in *P. vittata*. Metal hyperaccumulators share this lack of thiol coordination in comparison to non-adapted plants where the thiolates play an important role in metal detoxification. In this work by Pickering et al. 2006 [8] the importance of combining bulkXAS and μXAS is demonstrated. The bulkXAS results showed a minimum contribution of As-thiolates in the signal from leaf tissues. This might lead to the conclusion that this is a non-relevant species in the trafficking and accumulation of As by *P. vittata*. However, the use of μXAS demonstrates the mechanistic relevance of As-thiolates suggesting that the formation of this complex is in response to active transport of As(V) and takes place in special cells.

Due to the concerns about As high levels in rice grains several studies using μXAS and μXRF have been conducted that either study the distribution of As in the grains [10, 11] or the biogeochemical processes that control As uptake in rice [12- 14]. Meharg et al. 2008 [10] provided the first report in the use of SR to study speciation and distribution of As in brown and white rice grains from US, China and Bangladesh. The rice specimens were bisected along its latitudinal axis and the germless half was analyzed. No embedding procedure was utilized alleging the embedding might affect the As speciation. However, this approach does not allow thin sectioning (< 100μm) which is what determines the depth resolution of the technique.

Hence, areas within the grain which are of higher density or thickness will provide a stronger XRF signal. In brown rice As was found localized in the pericarp and aleurone layer. Also, co-localization of Cu, Fe, Mn, and Zn with As is reported in brown rice. μXANES analysis revealed the presence of As in the grains as inorganic and dimethylarsinic acid (DMA). White rice had lower levels of arsenic (mainly in the form of DMA) revealing that polishing rice reduces the total arsenic burden of the grain and its inorganic content. Lombi et al. 2009 [11] performed studies in rice grain samples this time in 70μm thick cross and longitudinal sections. The distribution and speciation of As varied among husk, bran and endosperm. In contrast to Meharg et al. 2008, μXANES results shown As(III)-thiol complexes in the rice bran and endosperm. The two studies [10, 11] agree that As is located mainly in the outer layers of the grain (aleurone and pericarp). This confirms that polishing rice grains decreases As content but raises a concern about the use of the bran as food additive and "premiere health food product". The findings by Lombi et al. 2009 and Meharg et al. 2008 suggest that the translocation from the maternal to filial tissues may be a bottleneck for As accumulation in the grain. This result is also supported by the work done by Smith et al. 2009 [12] where As was found mainly accumulated in the pericarp and aleurone layer of dehusked grains. The speciation and distribution of As in roots of rice plants grown in paddy fields irrigated with As contaminated water was also studied by Smith et al 2009 [12]. Cross sections of root and leaf resin embedded tissues (3- 5 μm thick) were used for this study. The results from μXRF suggest the formation of Fe plaques in the root surface with adsorbed As(V). In the leaf, As was primarily distributed along the vascular tissues and this distribution of As was similar to that of Cu in the leaf material. Results from μXANES revealed the two major species of As in the root where As(V) and As(III). Whereas As(III) is the main species found in the leaf tissues. It is hypothesized that the formation of Fe plaques in the root

surface of rice plants limits As uptake. Both As species (mainly As(V)) have great affinity for Fe amorphous oxides that are deposited in the root surface under certain environmental conditions. As rice plants deliver oxygen to roots that diffuses to the rhizosphere and may oxidize Fe(II) that precipitates on the exterior of rice roots [13]. Seyfferth et al. 2010[13] investigated the formation of Fe plaque around the rice roots. The co-location of As and Fe was confirmed in the roots of rice plants. However, it was determined that this is not the main factor limiting As uptake in the roots as this plaque did not encapsulate the entire root systems. Moreover, μXRF images of the young roots showed no presence of Fe plaque. The two dominant As species observed in the roots were inorganic As(V) and As(III), and only minor amounts of DMA and As-tris gluthatione. The influence of rice roots in the surrounding soil (rhizosphere) geochemistry in paddy fields was studied by Frommer et al. 2010 in soil thin sections. μXRF studies demonstrated the root influence in soil Fe, Mn and As distribution up to 1mm away from the root-soil interface. Roots with different thickness influenced differently the distribution of these elements. Thick roots (around 500μm) concentrated Mn closer to the surface without associated As. On the other hand, thin roots (< 100 μm) showed As and Fe enrichments next to the root surface. The results from μEXAFS suggest Fe is present mainly in the form of a two-line ferrihydrite-like phase with the associated As in the form of mostly As(V). Mn enrichments consisted of Mn(III/IV) oxyhydroxides.

The field of nanotechnology has grown very rapidly in the last decade. However, little is known about the potential effects of these materials for the environment and human health. Zinc oxide nanoparticles (NPs) have unique properties for a variety of applications such as UV absorbing and antibiotics. Recently, the first application of μXRF and μXANES in field of nanotoxicology was reported by Hernandez-Viezcas et al. 2010 [15]. Mesquite plants exposed to

ZnO nanoparticles in hydroponic culture showed increased uptake of Zn compared to control plants. μXRF maps of Zn in the root thin sections (30 μm) showed Zn accumulated mainly in the vascular region. Freeze-dried leaves were also analyzed; the ZnO treated leaves had more Zn in the vascular system compared to the control. The results from μXANES and bulkXANES analysis showed Zn has a different coordination environment compared to the ZnO NPs. These results suggest different Zn ligands inside the plants that might be organic acids. Whether the ZnO NPs are being transformed in the root-solution interface or inside the plant cells is yet to be elucidated. However, the results from this study clearly showed the ZnO NPs treatments increased the Zn pool inside the plants.

1.4 Research objectives

The objectives of this research were:

1) To investigate the capacity of *Parkinsonia florida* and *Prosopis Juliflora* plants to accumulate As from As-containing soils, as well as to study the speciation and distribution of As in plant tissues.

2) To study the As speciation in the root-soil interaction of *Prosopis juliflora* plants and to assess the availability of As in soils with different physico-chemical properties.

3) To evaluate uptake and speciation of Cd in corn plants and its effect over the production of low molecular weight thiols.

4) To evaluate the genotoxic effects of CeO_2 and ZnO nanoparticles in soybean plants with the use of the random amplified polymorphic DNA method.

5) Overall, the main goal was to utilize synchrotron techniques to determine the speciation and localization of As in desert plants and soils.

CHAPTER 2

Accumulation, distribution, coordination, and speciation of arsenic in the desert plant *Parkinsonia florida*: A synchrotron based study

Abstract

Parkinsonia florida is a plant species native to the semi-desert regions of North America. The cultivation characteristics of this shrub/tree suggest that it could be used for phytoremediation purposes in semiarid regions. This work describes, for the first time through the use of synchrotron μXRF and μXANES techniques and ICP-OES, the arsenic (As) accumulation and distribution in 8 week-old *P. florida* plants grown in two types of soils spiked with As at 20 mg kg^{-1}. A loamy sand soil (SS) and a sandy clay loam (SCL) were used as proxies for low and high As sorption capacity soils, respectively, based on the clay and Fe content. Plants grown in the SS soil accumulated in roots (mg As kg^{-1} dry tissue) 164.4 ± 5.4 from As(V) treatment and 102.2 ± 30.0 from As(III) treatment. The corresponding numbers for roots grown in the SCL soil were 53.2 ± 4.8 mg As kg^{-1} from As(V) treatment and 35.2 ± 2.6 mg As kg^{-1} from As(III) treatment. Linear combination XANES data analysis from the roots exposed to As(V) treated soil showed that As was reduced to As(III). Also, a fraction of the reduced As was found coordinating to S in a form consistent with As-Cys_3. The percentage of As coordinated to sulfur was smaller for plants grown in the SCL soil when compared to the SS soil. *P. florida* has demonstrated the ability to stabilize As in roots in the form of a less toxic and more stable compound.

2.1 Introduction

Arsenic (As) is an element widely distributed in the earth's crust. Despite the low abundance of As (0.0001%), it is easily found in nature with ores of lead, copper, and gold [1]. Arsenic can exist in four oxidation states: As(-III), As(0), As(III), and As(V), being the latter two forms the most toxic and predominant. Natural and anthropogenic activities contribute to the mobility of As, often increasing its availability to living organisms [2]. The toxicity of inorganic As depends on its chemical form. Arsenate [As(V)] enters plant cells as a molecular analog of phosphate [2], whereas arsenite [As(III)] does it via aqua-glyceroporins and is even more broadly toxic [3] than As(V). In the US, the EPA has established 20 mg As kg^{-1} as the limit for residential soil. However, certain arid regions in the Southwest and Midwest US have As concentrations above this limit [4, 5]. One way to reduce the risk of As contamination is by removing it from the soil. Phytoremediation is an *in situ* remediation method to remove pollutants from the environment by the use of plants that is cheaper than other remediation techniques [6, 7]. In order to make As phytoremediation a more suitable technology, researchers have investigated the As absorption, metabolism, and toxicity in many plant species [8]. However, only a few plant species have been identified as As hyperaccumulators. The most studied As hyperaccumulator plant species belong to the *Pteris* genus (brake ferns) [9, 10] which grows well in tropical and subtropical environments, but are not adapted to the harsh conditions of the Southwestern USA. *Parkinsonia* species are shrubs/trees native to semi-arid regions of the US that being studied for their phytoremediation potential by the Gardea-Torresdey research group. *P. florida* was identified as the *Parkinsonia* species with the best potential to remediate

As(III) and As(V) in soil [11]. Arsenic was accumulated in the root tissues of this plant which revealed its phytostabilization potential.

Arsenic bioavailability in soils depends on several factors such as pH, soil texture, and iron and manganese concentrations [12, 13]. For this reason, the accumulation of As in *P. florida* was studied in two types of soils: loamy sand and sandy clay loam. A loamy sand soil (SS) and a sandy clay loam (SCL) serve as good proxies for low and high As sorption capacity soils, respectively, based on the clay and Fe content. Also, As spatial localization and speciation were studied in fresh sectioned *P. florida* plant roots using synchrotron based microfocused X-ray absorption spectroscopy (μXAS) and micro X-ray fluorescence (μXRF). Synchrotron μXAS and μXRF have been previously used to study As distribution and speciation in *P. vittata* and *O. sativa* Quest [14- 16]. However, to our knowledge, this is the first time these techniques are used to investigate As speciation and distribution in a shrub/tree desert plant species grown in soils endemic to the southwestern US. Additionally, the speciation of As in the soil water soluble fraction and As concentrations in the plant tissues were studied by LC-ICP-MS and ICP-OES, respectively.

2.2 Materials and Methods

2.2.1 Soil preparation

Two types of soil were used for this study, a loamy sandy soil (SS) and a sandy clay loam soil (SCL). Samples of top soil (0-30 cm) were collected from a region in El Paso, TX free of arsenic contamination (<5 mg As kg^{-1}). The soil was dried for 2 days at 60 °C in a Fisher

Scientific Isotemp oven (Pittsburgh, PA) and passed through a 2-mm-mesh stainless steel sieve to have homogeneous grain size. The properties of both types of soils are shown in Table 2.1.

Table 2.1 Physico-chemical properties of the loamy sand (SS) and sandy clay loam (SCL) soils used in this study.

Parameter	Units	SS soil	SCL soil	Method
Texture		**Loamy sand**	**Sandy clay loam**	**Bouyoucos (*17*)**
Sand	**%**	**82.59**	**56.52**	
Silt	**%**	**16.59**	**10.97**	
Clay	**%**	**0.81**	**32.5**	
Water holding capacity	**mL kg^{-1}**	**200**	**220**	**Oven-dry**
pH		**7.9**	**7.9**	**pH meter**
Total S	**mg kg^{-1}**	**52.4**	**1159.6**	**ICP-OES (*18*)**
Total P	**mg kg^{-1}**	**18.6**	**181.24**	
Total Al	**mg kg^{-1}**	**4258.7**	**7310.3**	
Total Fe	**mg kg^{-1}**	**4590.2**	**8379**	
Total Mn	**mg kg^{-1}**	**65.9**	**185.4**	

Three sets of 2.5 kg of soil were placed in plastic pots and watered with deionized (DI) water (control), or a solution containing either As(V) (from $Na_2HAsO_4 \cdot 7H_2O$) or As(III) (from As_2O_3) to obtain a final concentration of 20 mg As per kg of soil. The As solutions were adjusted to pH 5.8 ± 0.1 and the water-holding capacity of the soil was determined by adding enough water to saturate the soil without leaching. The soil was left in the pots for one month to allow adsorption and equilibration of As. Then the soil from each replicate was removed from the pots and homogenized by crushing the aggregates and mixing the soil.

2.2.2 Plant sowing

Seeds of *P. florida* from Granite seed company (Lehi, UT, USA) were first immersed in concentrated sulfuric acid for 2.5 h for scarification, triple rinsed with DI water and finally soaked for 24 h in DI water to speed up germination. Five seeds were sown in each pot and watered with 150 mL of DI water. After that, plants were watered daily with 20-30 mL of DI water to maintain soil moisture. All treatments were arranged in a completely random design with three replicates per treatment. The pots were set at 25 ± 2ºC, a light–dark cycle of 12/12 h, and illumination of 53 μmol m^{-2} s^{-1}. The plants were harvested 2 months after sowing and washed with 0.01M HNO_3 twice and twice with DI to remove any soil particles or metal bound to the root surface. Plant material was separated into roots, stems, and leaves for ICP-OES analysis. One set of plants was transported alive to the Advanced Light Source (ALS, Berkeley National Laboratories, Berkeley, CA) for μXAS studies.

2.2.3 ICP-OES Elemental analysis

For the ICP analysis, the plant samples were digested in a CEM MarsX microwave oven (CEM, Mathews, NC) with 5mL trace-pure HNO_3 (SCP Science, NY) and diluted to 25mL using double-DI water. The total As concentration in the tissues was determined using ICP-OES (Perkin Elmer Optima 4300 DV with a Perkin-Elmer AS-90plus autosampler rack; Perkin Elmer, Shelton, CT). For QC/QA of the ICP readings, every 10 samples, the blank and a spiked sample containing As at 0.1 mg L^{-1} were read. The average reading for As in the spiked sample was 0.106 ± 0.003 mg L^{-1} (n=5). The ICP-OES parameters used were: nebulizer flow, 0.80 L min^{-1}; power, 1450 W; peristaltic pump rate, 1.5 mL min^{-1}; flush time, 15 s; delay time, 20 s; read time, 10 s; wash time, 60 s; and every sample was read in triplicate. Soil samples were analyzed for

Mn, Al, Fe, P and S using the above mentioned ICP-OES parameters after digestion with concentrated HNO_3 following EPA method 3051 [18]. The Mn average recovery from San Joaquin soil certified reference material (SRM 2709a) treated in the same way as samples was 77% (n=6).

2.2.4 LC-ICP-MS As speciation

For As speciation in soil, 1 g of a homogenized sample was added to 20 mL of Millipore water in rocking motion for 1 h. After that, the sample was centrifuged at 3,000 g on a benchtop centrifuge for 5 min. The supernatant was filtered through a 0.22 μm Durapore (PVDF, Millipore Corporation, Bedford, MA). A Perkin Elmer series 200 LC coupled to an ELAN DRC II (dynamic cell reaction) 6000 ICP-MS axial field technology (PerkinElmer, Shelton, CT) were used for the separation of the arsenic species. The LC-ICP-MS operating parameters used were those previously reported by Lopez-Moreno et al. [19]. Blank and standards were analyzed at the beginning and at the end of the analysis. The As species [As(III) and As(V)] were separated using a PRP-X-100 anion exchange column (150×4.6 mm, Hamilton). The ICP-MS DRC was operated using oxygen as auxiliary gas to eliminate $^{40}Ar^{35}Cl^{+}$ interference (the As ion was monitored at *m*/z 90.92) [19]. Integrated peaks areas from chromatographic peaks were imported into Microsoft Excel and correlation coefficients from calibration curves were between 0.99999 and 1 for As(III) and As(V). Six spiked soil samples (500 ppb) were treated as samples and analyzed using LC-ICP-MS in order to obtain the recovery percentage for arsenic species. The average recovery (for *n*=4) of the spikes was 91.4%, demonstrating that the total quantification for As species was accurate. The As recovery from San Joaquin soil (SRM 2709a) treated in the same way as samples was 90% (n=4).

2.2.5 µXAS data acquisition

Roots of *P. florida* plants treated with 20 mg L^{-1} of As were washed with 0.01M HNO_3 and three times with DI water to eliminate any excess of As on root surface. Roots were then cross sectioned at the beamline with a stainless steel blade and mounted onto a Mo foil sample holder on top of a freeze pack block. Root samples were dissected 2-4 cm from the root-stem intersection. The µXRF mapping of the distribution of As and relevant elements in the roots was performed at beamline 10.3.2 at the ALS [20]. Root sections were fixed on an x–y translation stage, cooled down to -20C to reduce radiation damage, and scanned under a micro focused beam. Maps were recorded using a 5 × 5 µm (H × V) beam at 12keV with a 10 × 10 µm pixel size and a 100 ms dwell time. The fluorescence yield was measured with a seven-element germanium (Ge) solid-state detector and normalized by I_0 and the dwell time. Several spots of interest were selected from the µXRF maps for As K-edge µXANES analysis. XANES spectra were processed using a suite of programs available at beamline 10.3.2. Briefly, spectra were energy-calibrated with respect to the white line max feature of Na_2HAsO_4 (11873.7 eV) and the pre-edge background was subtracted and normalized using a linear pre-edge. XANES model compounds were aqueous Na_2HAsO_4 (pH 2, 5.8, 7.5 and 12) and As_2O_3 (pH 3), and solid Na_2HAsO_4, As_2O_3, As_2S_3, and As-Cys_3. The As-Cys_3 model compound was synthesized by reacting L-cysteine hydrochloride and $AsCl_3$ (Sigma Aldrich, St. Louis, MO) at a 3-1 molar ratio in 50 mL of ethanol at room temperature. The mixture was stirred on a hot plate using low heat. After several minutes, a white precipitate was formed. The precipitate was collected by vacuum filtration and dried overnight. The dried product was then ground using mortar and pestle and stored in microcentrifuge tubes in the dark until analyses were performed.

2.3 Results and Discussion

2.3.1 Arsenic speciation in the soil water soluble fraction

The most immediately bioavailable As pool in soils is the water soluble fraction (WSF). Arsenic found in this fraction is mobilized by the presence of water in the soil pores and can easily reach the root surface to be further taken up by plants. The As concentrations found in the WSF of the SS and SCL soils are shown in Table 2.2.

Table 2.2 Concentration of As(V) in the soil water soluble fraction as determined by LC-ICP-MS. Capital letters stand for mean comparison in SS soil and lower case letters for mean comparison in SCL soil (Tukey test α=0.05). *Significantly different for the same As treatment in different type of soil (t-test 0.05).

		µg As(V) L^{-1}	**mg As(V) kg^{-1} soil**	**% of total**
Loamy sand (SS)				
	Control	1.64 ± 0.18^{A}	0.032 ± 0.003	
	As(V)	417 ± 14^{B}	8.4 ± 0.5	42 ± 1.4
	As(III)	310 ± 63^{C}	6.2 ± 0.15	31 ± 0.7
Sandy clay loam (SCL)				
	Control	$12.5 \pm 1.5^{a*}$	0.25 ± 0.03	
	As(V)	$158 \pm 13.5^{b*}$	3.2 ± 0.3	15.8 ± 1.3
	As(III)	$158 \pm 9.6^{b*}$	3.2 ± 0.2	15.8 ± 1

In the WSF all the As was found in the form of As(V), which indicates that As(III) was oxidized to As(V) in the soil. Mn oxides are effective As(III) oxidants and the SS and SCL soils used in the present study had 65.9 and 185.4 mg Mn kg^{-1} soil, respectively (Table 2.1) [21]. In the oxidation process, As(III) is changed to As(V), producing soluble Mn^{+2} or $Mn^{+3}OOH$ [21]. Future X-ray absorption spectroscopic analysis of As and Mn in the soil can provide useful

information about the formation of Mn arsenate precipitates and the oxidation of As(III) in the soil.

The concentration of As in the WSF of the SS was significantly higher compared to the SCL soil (Table 2.2). This could be explained by higher amount of Fe and Al found in the SCL (almost twice compared with SS soil) (Table 2.1). According to Manning at al. [22] the adsorption of As to Fe and Al oxides is an important process that affects As mobility in soils. The Fe(III) oxides have high affinity for As(V) and As(III) capable of forming inner-sphere (covalent linkages with no hydration water) and bidentate binuclear As(V)-Fe(III) complexes [22].

The concentration of As found in the WSF of SS soil was similar to those reported in poultry waste samples collected from two locations in Mississippi between 1997 and 2000 [23]. The percentage of As found in the WSF of those soils varied between 36–75% from total concentrations ranging between 11-36.2 mg As kg^{-1} soil. In contrast, the values found in the WSF of the SCL soil were similar to the concentration of As found in floodwater close to the soil surface in paddy soils from Bangladesh (40–120 μg As L^{-1}) [24]. The arsenic concentration in the WSF of the As(V) treated SS soil (417.96 ± 13.95 μg As(V) L^{-1}) was significantly higher ($\alpha = 0.05$) than the concentration found in the As(III) treated soil (309.77 ± 2.51 μg As(V) L^{-1}). One possible explanation is that reduction of poorly crystalline MnO_2 by As(III) liberates Mn^{+2} leading to increased binding sites for As(V) and greater As retention in the As(III) treated SS soil. The oxidation/sorption mechanisms can increase the As retention in the soil, As(III) entering a soil with Mn-oxides may exhibit increased retention compared to AsV entering the same soil [21]. This result was not observed in the SCL soil, which suggests that a different biogeochemical process was taking place in this soil.

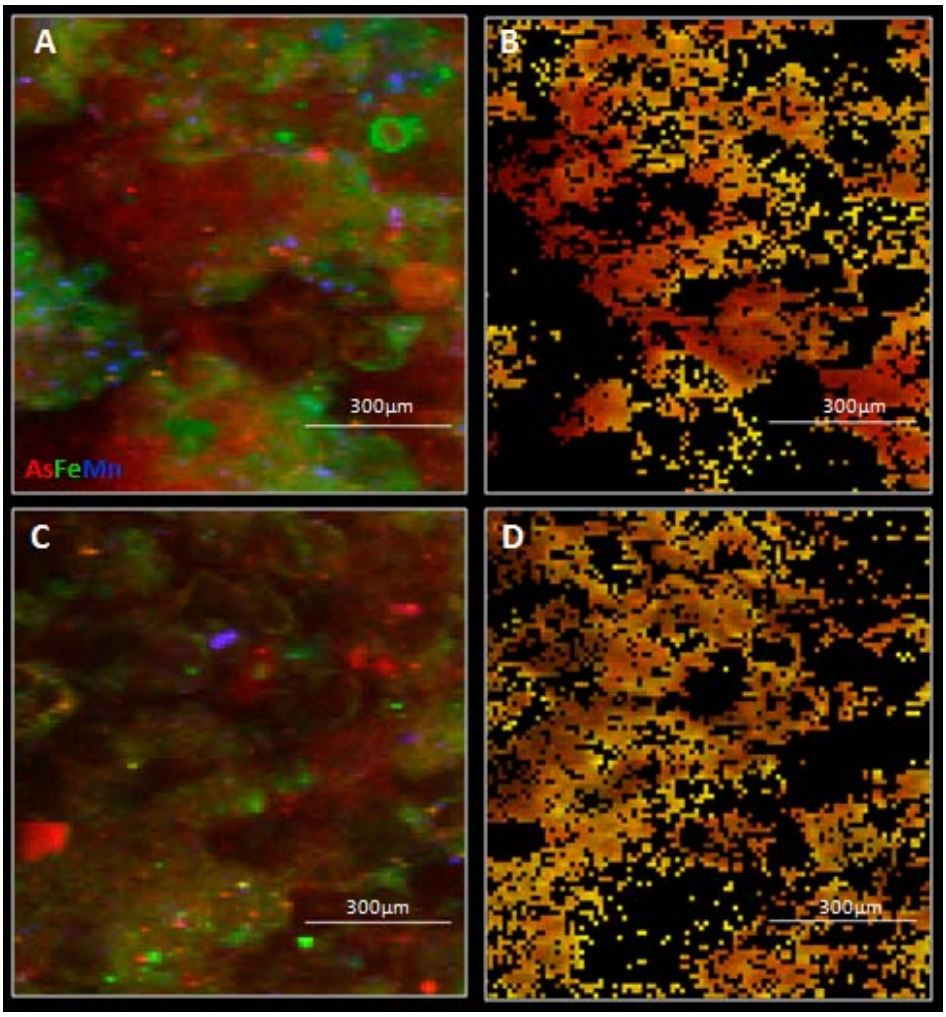

Figure 2.1 µXRF maps of As contaminated sandy clay loam (SCL) soil. (A) As(III) contaminated soil, (B) As-Fe correlation map (Pearson= 0.811). (C) As(V) contaminated soil. (D) As-Fe correlataion map (Pearson= 0.857). Map acquisition performed at 12 KeV with 10 µm pixel size and a 100 ms dwell time (As = red, Fe = green) (Mn = blue in A and C).

The spatial distribution of As, Fe, and Mn was investigated only in the SCL soil due to limited beam time availability. Samples of soil were collected 2 cm below the surface and 2 cm away from the roots and flattened between layers of polypropylene windows. Fluorescence maps were collected from the As(III) and As(V) contaminated soils in which the fluorescence signals for As, Fe and Mn were assigned the colors red, green and blue, respectively. The color coded fluorescence signals are superimposed and the resulting mixing of colors representative of metal associations. For example, the combination of As (red) and Fe (green) would appear on the map

as a yellow point, while a combination of Fe (green) and Mn (blue) would appear in cyan color. A strong spatial correlation between As and Fe was observed in the μXRF maps from both As(III) and As(V) contaminated SCL soil (see Fig. 2.1 and Fig. 2.2).

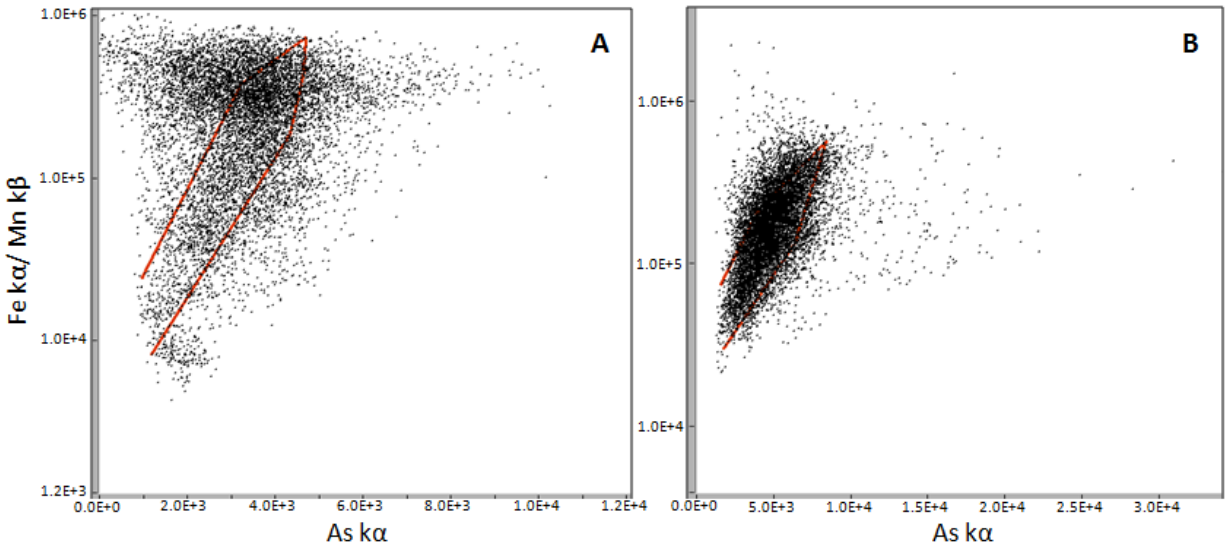

Figure 2.2 As-Fe scatter plot from μXRF maps of As contaminated SCL soil. (A) As(III) contaminated soil, (B) As(V) contaminated soil. Area inside the red lines covers the pixels shown in Figure 1B and 1D.

These results suggest that the As adsorption onto Fe oxides is a main geochemical process occurring in the SS and SCL soils. This also explains the low concentration of As in the WSF of both soils. The distribution of Mn in the SCL showed the sites where As(III) oxidation could be taking place in the SCL soil. The adsorption of As onto Fe oxides and the oxidation of As(III) by Mn oxides have been previously studied by XAS [21, 22, 25, 26]. The speciation of As by XAS should be further studied to confirm the presence As adsorbed onto Fe oxides and the oxidation of As(III) to As(V) in the SS and SCL soils.

2.3.2 As accumulation in the roots of P. florida

Arsenic accumulation in the tissues of *P. florida* was determined 2 months after germination and growth in As contaminated soil. The concentration of As in the stems and leaves

of *P. florida* was below the detection limits of the ICP-OES. Similar results were previously reported for *Parkinsonia aculeata* and *Parkinsonia microphylla* [11]. Accumulation of As (from As(V) treatments 0-500 µg L^{-1} in hydroponics) in castor bean (*Ricinus communis* cv. Guarany) showed As accumulation only in the root tissues [27]. Considering the concentration of As in the water soluble fraction in the treatments from the present experiment (1-417 µg L^{-1}) it can be concluded that the As accumulation in *P. florida* was similar to that reported in roots of castor bean plants (226 mg kg^{-1} root dry biomass at 500 µg L^{-1}).

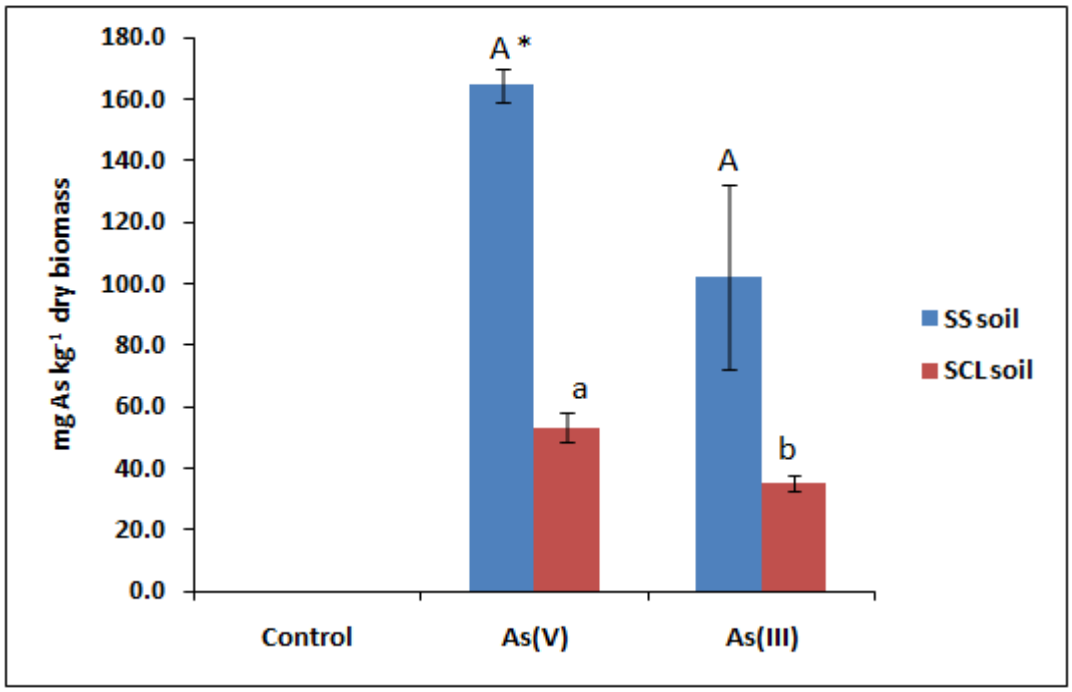

Figure 2.3 Accumulation of As in the root tissues of *P. florida* plants germinated and grown for 2 months in As contaminated soil (40 mg As kg^{-1} soil). Error bars are standard errors of n=3. Capital letters stand for mean comparison in SS and lower case letters for mean comparison in SCL soil (Tukey test α=0.05. *significantly different for the same As treatment in different type of soil (Tukey test α=0.05).

The As accumulation in roots of *P. florida* grown in SS soil was lower in As(III) treated plants compared to As(V) treated plants (Fig. 2.3). This was an expected result since the concentration of As in the WSF from the As(III) treated SS soil was significantly lower compared to the As(V) treated SS soil (Table 2.2). Accumulation of As from the As(III) treated

SCL soil was also significantly lower compared to the As(V) treated SCL soil. A similar result was reported for mesquite plants grown in soil for 45 days [19]. Arsenic accumulation in the mesquite roots from the As(III) treated soil was lower in comparison to the As(V) treated soil [19]. The soil used for the mesquite experiments was similar to the SS soil used in the present study.

Two mechanisms have been proposed for As absorption by roots. One of the mechanisms involves the active absorption of inorganic As(V) via phosphate carriers into the root symplast [28, 29]. The other mechanism involves the passive absorption of neutral species (pH < 9.2) of inorganic As(III) via aquaporin channels [30]. These oxidation state specific mechanisms could lead to differential uptake of inorganic As(III) and As(V); however, in the present study, As(V) was the predominant form in the WSF and the most likely predominant form in the soil. The reduced accumulation of As from the As(III) treated SS soil is then better explained in terms of its decreased availability as indicated by the concentration of As in WSF (Table 2.2). The formation of an insoluble As-Mn solid phase from the oxidation of As(III) by Mn oxides is a possible explanation for the decreased As concentration in the WSF. This corresponds well with the reduced accumulation in roots of *P. florida* plants grown in the As(III) treated SS soil (Fig. 2.3). On the other hand, differential As uptake was observed for the plants grown in the SCL soil. Accumulation of As from the As(V) treated SCL soil (about 50 mg As kg^{-1}) was significantly higher compared to the As(III) treated soil (about 30 mg kg^{-1}) (Fig. 2.3). This is an interesting result since a similar concentration of As was found in the WSF of both As(III) and As(V) treated SCL soil. Reduced accumulation from As(III) treated SCL soil may be due to a competition between As(III) and silicic acid. Silicic acid has been found to decrease the absorption of As(III) in rice plants, as both chemical species are transported into the roots via

aquaporin channels [31]. In general, silicic acid concentration in soil solution ranges from 0.1 to 0.6 mM and it is twice as bioavailable than P in soils [32]. In general, arsenic accumulation in the roots of *P. florida* was higher in the SS soil compared to the SCL soil. The higher Fe, Al, Mn and clay content in the SCL soil can explain the decreased availability of As in this soil.

2.3.3 Sulfur accumulation in the roots of P. florida

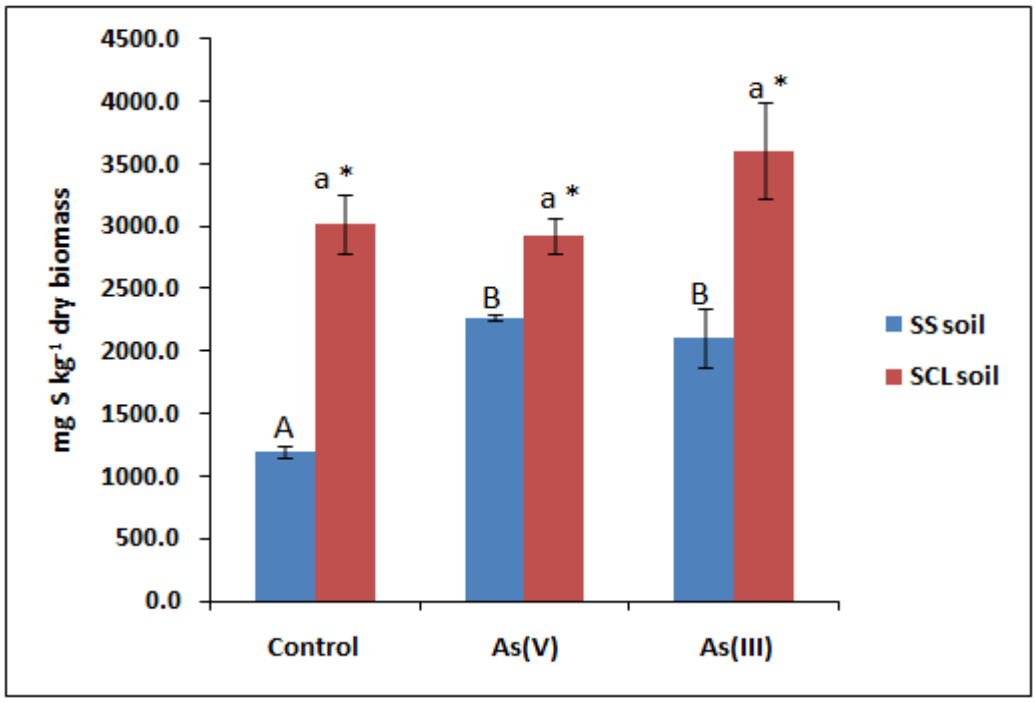

Figure 2.4 Accumulation of S in the root tissues of *Parkinsonia florida* plants germinated and grown for 2 months in As contaminated soil (40 mg As kg^{-1} soil). Error bars are standard errors of n=3. . Capital letters stand for mean comparison in SS soil and lower case letters for mean comparison in SCL soil (Tukey test α=0.05). *significantly different for the same As treatment in different type of soil (t-test 0.05).

Sulfur, an important element for As detoxification and tolerance, is present in plant molecules such as thiol groups and phytochelatins. Thiol groups (–SH) are present in the cysteine residues of the antioxidant glutathione (GSH) and the metal-induced binding peptides phytochelatins (PCs) and metallothioneins. Increased S absorption can lead to enhanced As tolerance and accumulation in plants due to a positive effect on thiol metabolism and antioxidant

capacity [33- 35]. The S accumulation in roots of *P. florida* under the exposure to As is shown in Fig. 2.4. Accumulation of S in roots of *P. florida* plants grown in all SCL soil treatments was significantly higher compared to the SS soil treatments. Accumulation of S in roots was statistically similar for both As(V) and As(III) treated plants grown in the SCL soil. However, S accumulation significantly increased ($\alpha \leq 0.05$) in both As(V) and As(III) treated plants grown in SS soil. The significant increase in S accumulation in the SS soil grown plants corresponded to a higher As accumulation (Fig. 2.3). Plants grown in the SCL soil accumulated more S and less As compared to plants grown in the SS soil. These results suggest that plants grown in SCL soil had more S available, and that the As concentration in roots was not enough to promote an increase in S accumulation. On the other hand, increased accumulation of As in roots of plants grown in the SS soil corresponded to lower S accumulation (compared to plants grown in SCL soil) and a significant increased in S accumulation compared to control plants grown in SS soil (Fig. 2.3 and Fig. 2.4). Similarly, experiments performed with *Prosopis sp.* and *Hydrilla verticillata* showed an increase in S accumulation with increasing accumulation of As in the tissues [33, 34]. The increase in S accumulation was correlated with more production of total thiols and a positive effect in the antioxidant status of *H. verticillata*. Also an increased production of low molecular weight thiols and gluthatione S-transferase activity was observed. Results from the present study suggest that *P. florida* plants absorbed more S in response to As accumulation to maintain their antioxidant capacity.

2.3.4 Arsenic speciation and distribution in the roots P. florida

The spatial distribution and speciation of As in the roots of *P. florida* plants was studied using synchrotron μXRF and μXANES. The distribution of As in root tissues and the spots

chosen for XANES data collection are shown in Fig. 2.5. The fluorescence signal from Ca and K was used to provide better contrast for the μXRF images (Fig. 2.5A-D).

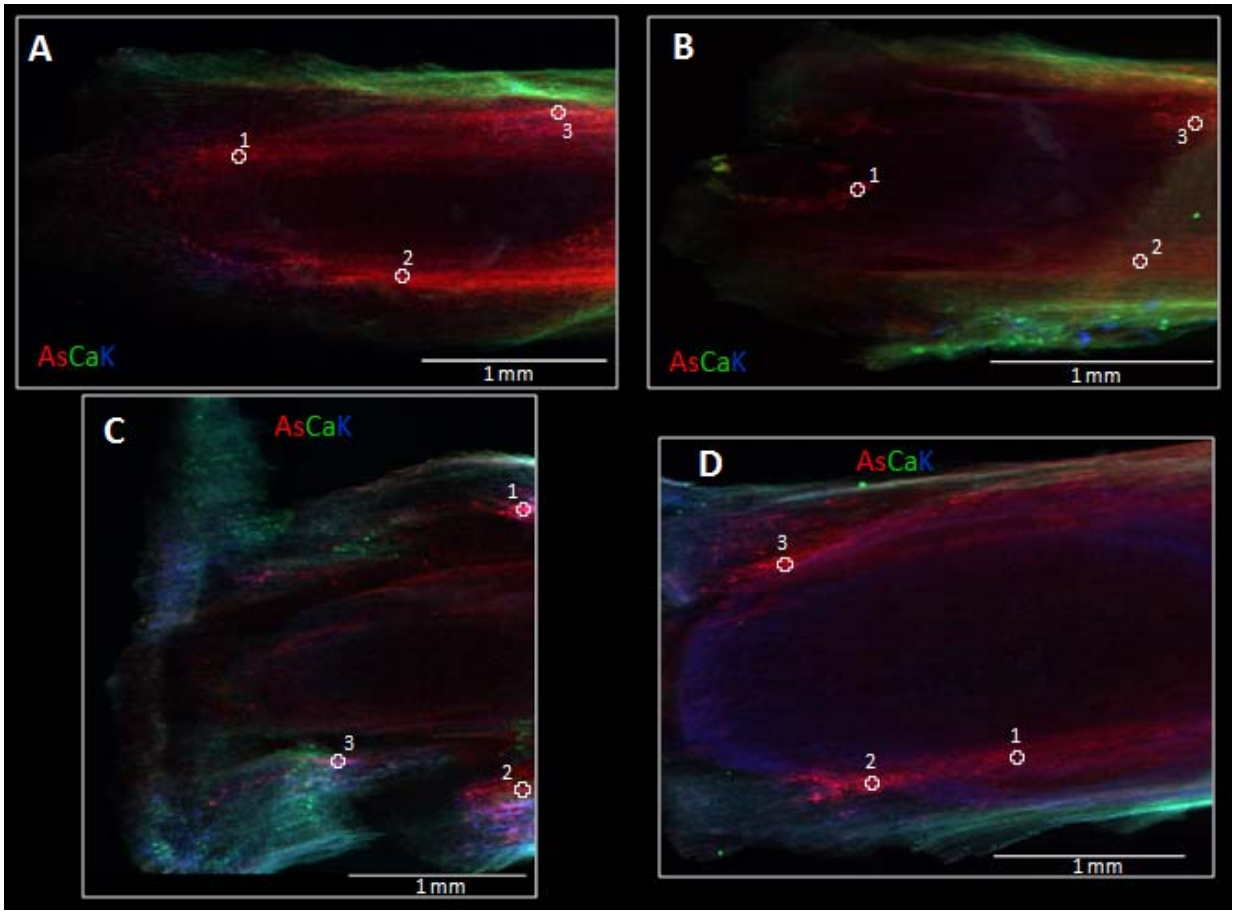

Figure 2.5 μXRF maps of *Parkinsonia florida* roots grown in As contaminated soil. (A) loamy sand soil As(V), (B) loamy sand soil As(III), (C) sandy clay loam As(V), (D) sandy clay loam As(III). Map acquisition performed at 12 KeV with 10μm pixel size and a 100ms dwell time. Numbers in the figures correspond to spots where As K-edge XANES data were collected. (As = red, Ca = green, K = blue).

From Fig. 2.5 it can be observed that Ca was mainly accumulated in the epidermis of the roots and K in the vascular region. In contrast, As fluorescence signal (Fig. 2.5 A-D) was from a region between the epidermis and the vascular tissues, as it is not perfectly co-located with either Ca or K (this could be the procambium region). These results corroborate the absence of As in the aerial tissues of *P. florida* plants, because the vascular tissue is where the transport from roots to shoots of soil solution with elements takes place, and As was not found in the vascular tissue.

The present results demonstrate that *P. florida* retained As in the roots tissues. This makes *P. florida* a good candidate for As phytostabilization (a long-term remediation process where contaminants are accumulated in roots and rhizosphere reducing their bioavailability and mobility) [36].

The results from linear combination XANES (LC-XANES) analyses are shown in can be Table 2.3. LC-XANES fittings showed that the spectra from all the spots fit to linear combinations of those from inorganic As(V), As(III) and As-Cys_3 model compounds. The predominant form of As within the root tissues of *P. florida* is consistent with As-Cys_3 (used as a proxy for As-thiolate species). This is in contrast with what is reported for rice, in which inorganic As(V) and As(III) are the predominant species found in the root tissues [15]. The reduction of As(V) to As(III) followed by coordination to thiol containing groups such as GSH or phytochelatins is a well reported mechanism for As detoxification in plants and other organisms [19, 31, 33]. This is a litle bit contradictory because the reduction process can lead to As toxicity since As(III) has a high affinity for the thiol groups found in the amino acid cysteine [31]. Some of the As in the roots has an XAS spectrum consistent with As-Cys3 and may be any As-S organic form, such as As bound to thiolate groups in GSH, phytochelatins or proteins. The binding of arsenic to cysteine residues from proteins can disrupt the structure and protein–protein interactions affecting key metabolic processes in the cell. Also, the antioxidant status of the cell can be affected by depletion of GSH once it is bound to As(III). Since no visual symptoms of toxicity such as chlorosis, necrosis, wilting or stunting were observed in *P. florida* plants, it is hypothesized that GSH and/or phytochelatins play an important role in the accumulation of As in roots of this plant species.

Table 2.3 LC-XANES fitting results of *P. florida* roots exposed to As contaminated soil. Reference compounds used are aqueous solutions from As_2O_3 (pH= 3.0) and $Na_2HAsO_4 \cdot 7\ H_2O$ (pH=5.8) for As(III) and As(V), respectively. As-Cys_3 was analyzed as a dry fine powder.

	As-Cys_3 %	As(III) %	As(V) %
Florida As(V) Loamy sand			
Spot 1	68	22	11
Spot 2	74	18	8
Spot 3	85	4	11
Florida As(III) Loamy sand			
Spot 1	64	9	27
Spot 2	74	15	11
Spot 3	67	15	18
Florida As(V) Sandy clay loam			
Spot 1	81	16	4
Spot 2	43	30	26
Spot 3	50	33	16
Florida As(III) Sandy clay loam			
Spot 1	69	15	17
Spot 2	52	24	23
Spot 3	75	10	16

The percentage of As found in plants as an As-thiolate species (As grown in the SS soil (67%- 85%) was higher compared to the percentage found in plants grown in the SCL soil (43%-81%), as can be seen in Fig. 2.6. These results correspond to the plants where a significant increase in S accumulation compared to control plants was observed (Fig. 2.4).

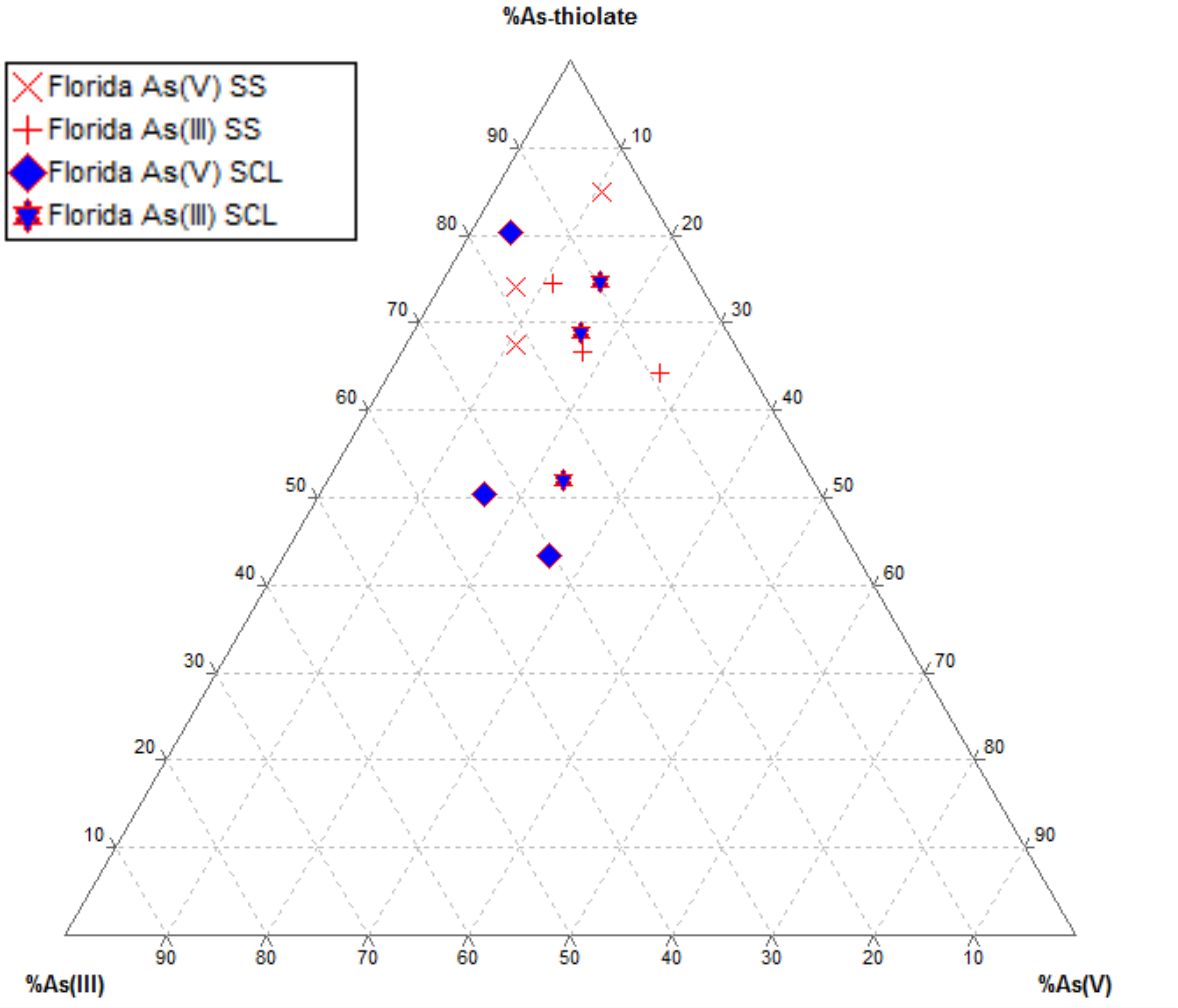

Figure 2.6 Ternary plot of LC-XANES fitting results from spots where As K-edge XANES data was collected. Reference compounds used were aqueous solutions from As_2O_3 (pH= 3.0) and $Na_2HAsO_4 \cdot 7\ H_2O$ (pH=5.8) for As(III) and As(V), respectively. As-Cys_3 was used as proxy for As-thiolate species and analyzed as a dry fine powder.

Plants from SS soil treatments also accumulated more As in the tissues compared to the ones from the SCL soil. A relationship between S and As accumulation and the coordination to thiol groups was confirmed in this work supporting the working hypothesis of this study that LMWT (GSH or phytochelatins) are essential for As tolerance in *P. florida* plants. The role of LMWT in As tolerance and detoxification has been demonstrated in other desert plant species [33, 37].

2.4 Conclusions

The results from the present study have depicted the differential response to As of *P. florida* grown in soils with different physico-chemical properties. The desert plant species *P. florida* has demonstrated the ability to accumulate As in the root tissues from As contaminated soil. Furthermore, the results have shown that *P. florida* stores As in the form of a less toxic and more stable species ($As\text{-}Cys_3$) [38], which makes this plant a possible candidate for phytostabilization of As in arid regions. Phytostabilization is a long-term remediation process where the contaminant is accumulated in root plant tissue and in the soil around the roots reducing its bioavailability and mobility [36]. *P. florida* has demonstrated As tolerance and limited shoot metal accumulation. Therefore it satisfies most of the criteria required for phytostabilization applications; drought-, salt-, and metal-tolerant plant [36]. Further studies in multi-element contaminated soils (e.g. mine tailings) with longer periods of exposure can help to confirm the As phytostabilization capacity of *P. florida* in arid regions.

CHAPTER 3

Local coordination and speciation of arsenic in the root-soil interface of the desert plant *Prosopis juliflora*

Abstract

Plants modify the bioavailability of As in the rhizosphere. Biogeochemical processes differ between the bulk and the vegetated soil. Synchrotron X-ray fluorescence (μXRF) and X-ray Absorption μXAS allow to create a detailed profile of As speciation and spatial relationships between As and other elements in the rhizosphere. We are investigating As speciation in the rhizosphere of mesquite (*Prosopis juliflora*) plants. The capacity of mesquite plants to accumulate As from soil (50mg As kg-1 soil) has been demonstrated in a previous study. The selected soil for this study was a sandy clay loam spiked with As(III) and As(V). The concentration of As after one month of equilibration and mixing was 37±1.68 mg kg-1 soil and 59±7.65 mg kg-1 soil for As(V) and As(III), respectively. Arsenic did not inhibit the germination rate of the plants. Rhizosphere soil and freeze dried root tissues of one month old plants were analyzed using bulkXAS. Arsenic was found as As(V) in all soils whereas in the roots it was found as As(III). μXAS and μXRF studies of thin sections (1mm) from resin embedded soil cores confirmed the presence of As(III)-S interactions in the root tissues and a strong As-Fe interaction in the soil.

3.1 Introduction

Arsenic bioavailability in soils depends on several factors such as pH, organic matter content, ion exchange capacity, and the concentration of oxides and clay minerals such as iron and aluminum[1]. Plants modify the bioavailability of As in the rhizosphere, therefore As biogeochemical processes differ between the bulk and the vegetated soil. Arsenic speciation and bioavailability in the rhizosphere depend on biogeochemical gradients in pH, redox potential and organic ligand concentration induced by plants. These induced modifications differ with plant species and soil type, and vary in both space and time. Previous studies in the rhizosphere of several plant species show no consensus as to whether or not rhizospheric processes increase or decrease the bioavailable metal pool [2].

The use of micro-focused synchrotron-based X-ray fluorescence allows us to generate elemental distribution maps in the micro scale. Rhizosphere plant induced As speciation changes can be monitored using this technique combined with X-ray Absorption Spectroscopy [3]. The combination of the μXRF microprobe and μXANES allows to create a detailed profile of As speciation and spatial relationships between As and other relevant elements. We have previously explored the uptake of As and the effects on elemental uptake and amylolitic activity in the mesquite plants [4, 5]. Our previous soil experiments have demonstrated the ability of mesquite to tolerate and accumulate As up to a concentration of 40 mg kg^{-1} of soil [6]. Results from XAS analysis have demonstrated the oxidation of As(V) to As(III) in the soil matrix and the reduction and coordination of As to S ligands possibly from glutathione and/or phytochelatins [4, 7]. These thiol containing molecules are used by plants to bio-inactivate heavy metals and arsenic [8-10]. Reduction of As(V) to As(III) and further coordination to sulfur containing groups, specially low

molecular weight thiols (LMWT), has been reported as a successful strategy for arsenic tolerance and hyperaccumulation in the plant species *Pteris vittata* [11]. We have also shown the induction in the production of low molecular weight thiols after exposure to As in mesquite plants [7]. The present work studied the induced changes in As speciation in the rhizosphere of mesquite (*Prosopis juliflora velutina*) plants. *Prosopis spp.* is an endemic plant species in the arid southwestern US lands. Previous studies have focused their attention in coastal plants (*Pteris vittata*), rhizosphere of riparian soils, or bulk non-vegetated soils [2, 3, 12, 13]. Our experimental approach looked at As speciation using arid soils in the presence of a desert plant species, to our knowledge no other similar studies have been reported. The objective of this study was to further study As accumulation in the mesquite plants, and As distribution and speciation in the rhizosphere zone. Additionally, the distribution and speciation of As in the root tissues were studied in root cryo-sectioned tissues using μXAS techniques.

3.2 Materials and Methods

3.2.1 Soil preparation

A sandy clay loam soil was selected for this study (Table 2.1, Chapter 2). The soil was top soil (0-30 cm) collected from a region in El Paso, Tx free of arsenic contamination. Soil was dried at 60°C in a Fisher Scientific Isotemp oven (Pittsburgh, PA, USA) 2 days and passed through a 2-mm-mesh stainless steel sieve to have homogeneous grain size. Three sets of 2.5 kg of soil were placed in plastic pots and watered with deionized (DI) water (control), or a solution containing either As(V) (from $Na_2HAsO_4 \cdot 7H_2O$) or As(III) (from As_2O_3) to obtain a final concentration of 40 mg As per kg of soil. The As solutions were adjusted to pH 5.8±0.1 and the

water-holding capacity of the soil was determined by adding enough water to saturate the soil without leaching. The soil was left in the pots for one month to allow adsorption and equilibration of As. Then the soil from each replicate was removed from the pots and homogenized by crushing the aggregates and mixing the soil.

3.2.2 Plant sowing

Seeds of *Prosopis juliflora velutina* from Granite seed company (Lehi, VT, USA) were first immersed in a 4% hypochlorite solution for 20 minutes, triple rinsed with DI water and finally soaked for 24 hours in DI water to speed up germination. Five seeds were sown in each pot and watered with 150 mL of DI water. Plants were watered daily with 10-20mL of DI water to maintain soil moisture. All treatments were arranged in a completely random design with three replicates per treatment. The pots were set at 25±2ºC, a light–dark cycle of 12/12 h, and irradiation of 53 $\mu molm^{-2}\ s^{-1}$. After one month, core samples with the root tissues placed in the center of the core were collected from a set of pots. Avoiding any disturbance of the sample the section of the core 2.5 cm away from the top was freeze dried and embedded in LR white resin (SPI supplies, Westchester, PA). Sections of approximately 1mm thick were prepared using a diamond saw and kept at room temperature to be further studied. A set of plants was harvested 2 months after sowing in the treatments, washed with 0.01M HNO_3 (twice) and with DI twice to remove any soil particles or metal bound to the root surface. Plant material was separated into shoots, stems and leaves for ICP-OES analysis.

3.2.3 ICP-OES Elemental analysis

P. juliflora plants were washed with 0.01M HNO_3, rinsed with DI, separated into roots and shoots and subsequently freeze dried. Samples were then digested in a CEM Marsx microwave oven (CEM Corporation, Mathews, NC) with 5mL trace-pure HNO_3 (SCP Science, NY) and diluted to 25mL using double-deionized water. The total S concentration in the tissues was determined using ICP-OES (Perkin-Elmer Optima 4300 DV with a Perkin-Elmer AS-90plus autosampler rack; Perkin Elmer, Shelton, CT). For QC/QA of the ICP readings, a spiked sample containing S at 20.0 mg L^{-1} were read. The average reading for S in the spiked sample was 19.46 ± 0.35 (n=3). The ICP-OES parameters used were as follows: nebulizer flow, 0.80 L min^{-1}; power, 1450 W; peristaltic pump rate, 1.5 mL min^{-1}; flush time, 15 s; delay time, 20 s; read time, 10 s; wash time, 60 s; and every sample was read in triplicate.

3.2.4 ICP-MS Elemental analysis

For the determination of As concentration in *P. juliflora* tissues an ELAN DRC II (dynamic cell reaction) 6000 ICP-MS axial field technology (PerkinElmer, Shelton, CT) was used. Blank and standards were analyzed at the beginning and at the end of the analysis. The ICP-MS parameters used were as follows: nebulizer flow, 0.90 L min^{-1}; power, 1200 W; auxiliary gas flow, 1.20 L min^{-1}; plasma gas flow, L min^{-1}; lens voltage, 8.50; CeO/Ce, <2%; and every sample was read in triplicate.

3.2.5 µXAS data acquisition

Soil cores (2.5cm diameter) containing roots from *P. juliflora* were sampled using a stainless steel core sampler. A section 2 cm below top soil was embedded in LR white resin (SPI

supplies, Westchester, PA) at 4ºC. Sections from the soil cores (aprox.1mm thick) were prepared using a diamond saw and stored at room temperature. Additionally, roots tissues from mesquite plants were sectioned with a cryotome (30 micron thick) and mounted onto kapton film. μXRF mapping of the distribution of As and relevant elements in the soil cores and root thin sections was performed at beamline 10.3.2 of the Advanced Light Source, Lawrence Berkeley National Laboratory, (ALS, Berkeley, CA) [14]. Samples were fixed on an x–y translation stage and scanned under a micro focused beam. Maps were recorded using a 10μm × 10μm beam and a 130 ms dwell time and a 5μm × 5μm and a 200ms dwell time for the soil cores and the root thin sections, respectively. The fluorescence yield was measured with a seven-element germanium (Ge) solid-state detector and normalized by I_0 and the dwell time. The incident energy was set at 12 keV. Several spots of interest were selected from the XRF maps for As K-edege XANES analysis. XANES spectra were processed using a suite of programs available at beamline 10.3.2. Briefly, spectra was energy-calibrated with respect to the whiteline max feature of Na_2HAsO_4 (11873.7 eV) and the pre-edge background was subtracted and normalized using a linear pre-edge. XANES model compounds were aqueous Na_2HAsO_4 (pH 2, 5.8, 7.5 and 12) and As_2O_3 (pH 3), and solid Na_2HAsO_4, As_2O_3, As_2S_3, and As-Cys_3.

3.2.6 BulkXAS data acquisition

The X-ray absorption spectra were collected at SSRL on the As K edge at beam line 7–3 with a beam current ranging between 80 and 100mA and energy of 3.0 GeV. Spectra of the samples were taken at room temperature and a Si (220, φ 90◦ orientation) double crystal monochromator and a 1.0-mm slit was used for data collection. An internal As standard (Na_2HAsO_4, whiteline max feature 11873.7 eV) was used for calibration purposes. A Canberra

30-element germanium detector (Canberra Instruments, Meriden, CT) was used to collect the fluorescence spectra of the As-laden plant samples and soils. Among the crystalline species were natural scorodite ($FeAsO_4 \cdot 2H_2O$), pharmacosiderite ($KFe_4(AsO_4)_3(OH)_4 \cdot 6\text{-}7H_2O$), and beudantite ($PbFe_3(AsO_4)(SO_4)(OH)_6$). Sorption samples were As(V) and As(III) sorbed on 2-line ferrihydrite (referred to as Fh-2L) synthesized following the procedures described by Cances et al, 2005 [15].

3.3 Results and Discussion

3.3.1 Arsenic concentration in mesquite tissues

Accumulation of As in roots and shoots from mesquite plants grown in As contaminated soil for two months is shown in Fig. 3.1. Mesquite plants accumulated As mainly in the root tissues with very low concentrations found in the shoots (< 6 mg kg^{-1} dry biomass). Similar findings are reported by Lopez et al. 2008 [16] where mesquite plants accumulated As mainly in the roots although the As concentrations in roots and shoots were higher (approx. 500 and 120 mg kg^{-1}, respectively) compared to the results presented herein. It is important to mention that the soil properties (Fe, Mn, Al, and clay content) from both experiments are significantly different. The soil properties from this experiment promote adsorption processes for As that limit its bioavailabilty. Soil used by Lopez et al. 2008 [8] is similar to the loamy sand (SS) soil used for the experiments with *Parkinsonia florida* plants reported in the previous chapter of this dissertation, whereas the soils for this experiments with mesquite is the same sandy clay loam (SCL) described in Table 2.1. As it was previously demonstrated As availability is decreased in the SCL soil resulting in decreased accumulation in plants. In contrast, As accumulation in

mesquite is significantly different when compared to hydroponic studies. Mogkalaka-Matlala et al. 2008 [7] reported As accumulation in mesquite roots exposed to 50 mg L^{-1} of As(III) and As(V) almost 10 and 20-fold higher than the results from this soil experiment. It is quite clear that availability of As in the soil is one of the main limiting factors of As accumulation in the mesquite plants. No significant difference in the As accumulation from As(III) and As(V) treatments was found. Most likely the oxidation of As(III) to As(V) in the soil makes As accumulation from both treatments comparable.

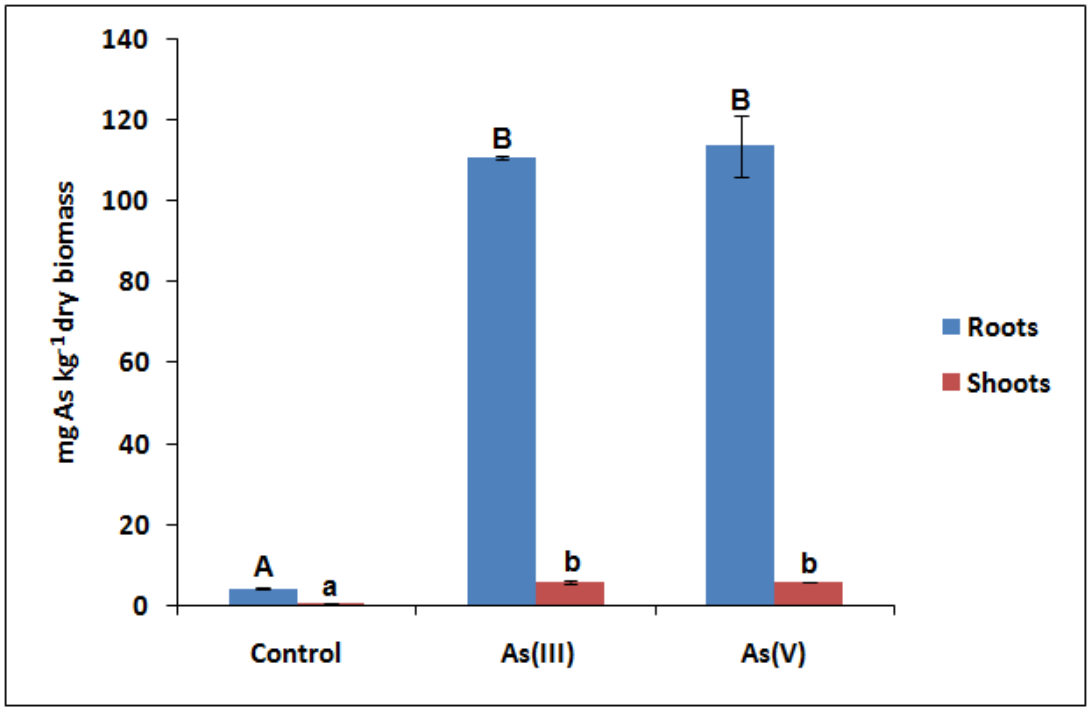

Figure 3.1 Accumulation of As in the tissues of *P. juliflora* plants germinated and grown in As contaminated soil (40 mg As kg^{-1} of soil) for 2 months. Error bars are standard error of n=3. Bars with different subscript letters are significantly different (tukey α=0.05). Capital letters= SS soil mean comparison, *significantly different for the same As treatment in different type of soil (tukey α=0.05).

3.3.2 Sulfur concentration in mesquite tissues

Sulfur (S) accumulation in mesquite plants exposed to As contaminated soil was studied in order to see the effect of As over S metabolism. It has been shown that As induces the production of low molecular weight thiols (LMWT) in plants as part of a detoxification

mechanism [16, 17]. Monitoring the concentration of S in the tissues of mesquite plants is a proxy to elucidate the role of LMWT in As detoxification in mesquite plants. Accumulation of S in roots and shoots from mesquite plants is shown in Fig. 3.2. Mesquite plants accumulated significantly higher amounts of S in the roots compared to the shoots. In contrast, Mogkalaka-Matlala et al. 2008 [7] reported an opposite result in mesquite plants exposed to As (50 mg L^{-1}) in hydroponics. Mesquite plants in hydroponics accumulated more S in the shoots than in the roots; however control roots had similar S concentration (7,000 mg kg^{-1} dry biomass) in both hydroponics and soil experiments. The higher accumulation of S in the roots corresponds with a higher accumulation of As suggesting the possible implication of As induced LMWT in the detoxification and accumulation of As in mesquite plants grown in As contaminated soils.

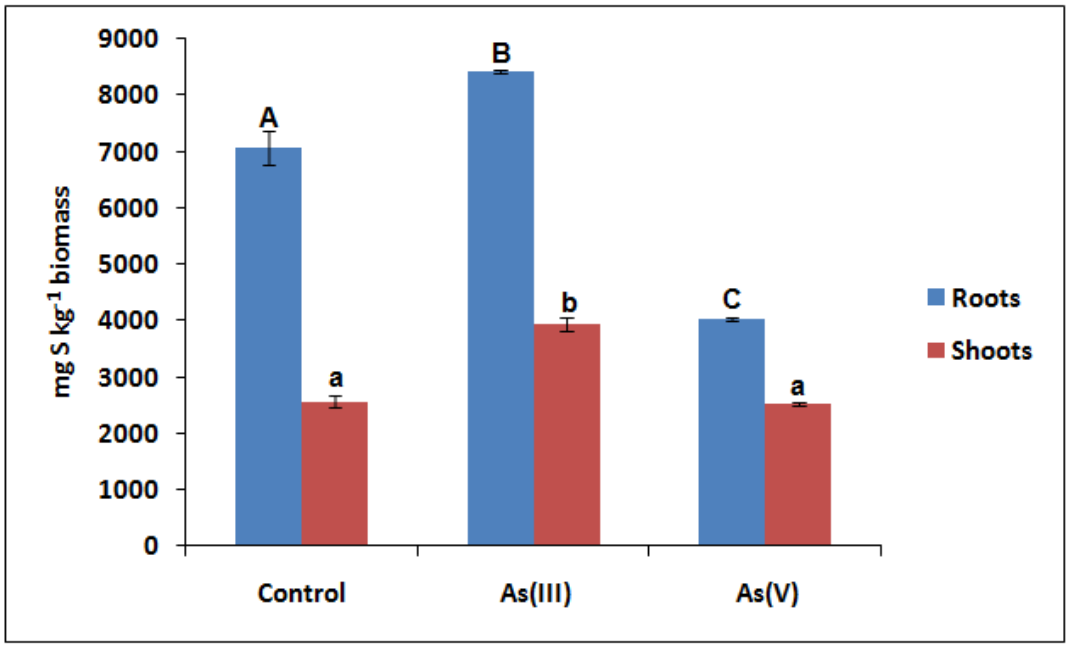

Figure 3.2 Accumulation of S in the tissues of *P. juliflora* plants germinated and grown in As contaminated soil (40 mg As kg^{-1} of soil) for 2 months. Error bars are standard error of n=3. Bars with different subscript letters are significantly different (tukey α=0.05). Capital letters= SS soil mean comparison, *significantly different for the same As treatment in different type of soil (tukey α=0.05).

Induction of LMWT in As treated mesquite plants was previously reported in hydroponics (50 mg L^{-1}) [9]. However, from Fig. 3.2 it can be observed that As(III) soil treatments significantly

increased S accumulation in roots whereas As(V) significantly reduced S accumulation in roots. This decreased in S accumulation might suggest As exposure is impacting the plant's health, however As accumulation was similar in both As(III) and As(V) treated plants and no signs of toxicity such as chlorosis, wilting, and stunting were observed.

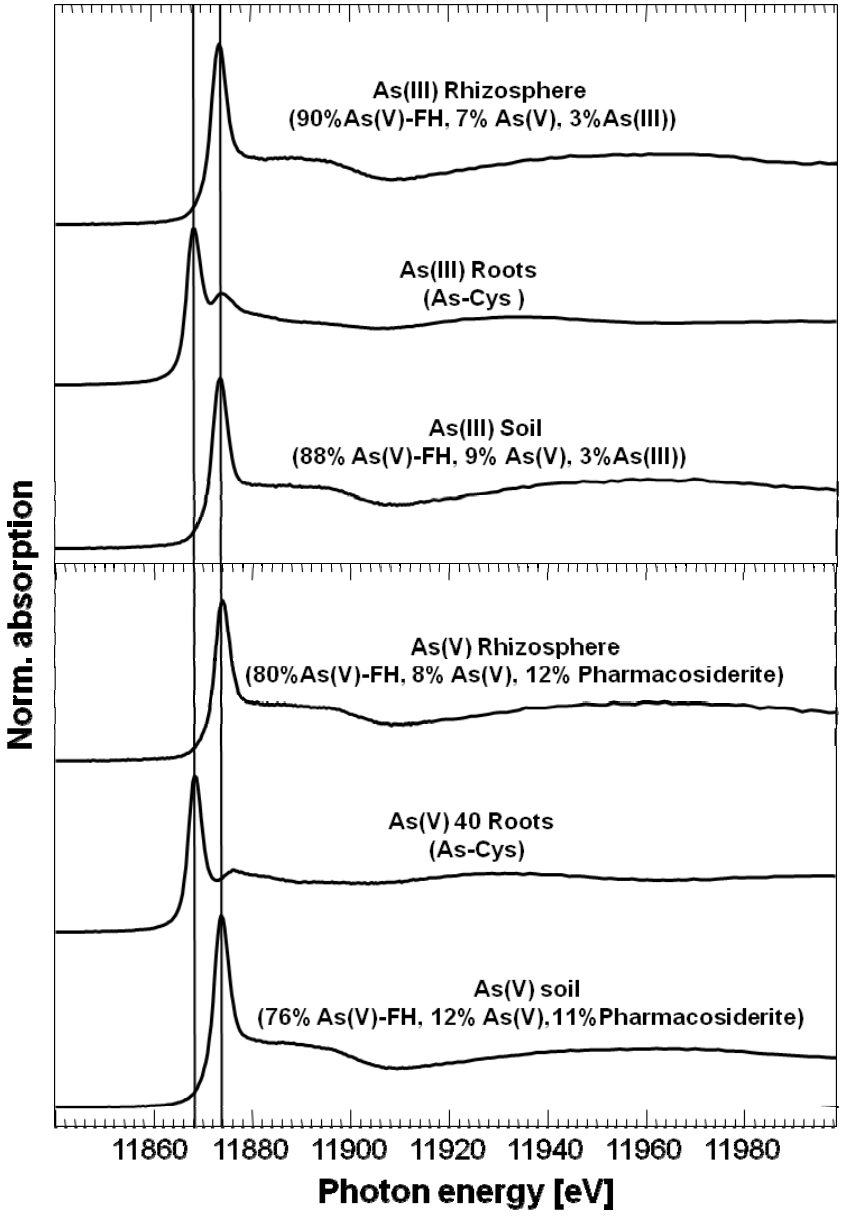

Figure 3.3 Bulk-XANES spectra from As(V) and As(III) roots, soil and rhizospheric soil. Vertical lines indicate the whiteline max energy of As(V) (11873eV) and As(III) (11869eV). Percentages inside parenthesis indicate results from linear combination fitting analysis.

3.3.3 Bulk XAS studies

Speciation of As in the rhizosphere soil, non-vegetated soil and root tissues was studied by X-ray Absorption spectroscopy (XAS). From Fig. 3.3 it can be observed that As(V) was the predominant species in the soil (rhizosphere and non-vegetated) whereas As(III) was dominant in the root tissues from both As(V) and As(III) treatments. The oxidation of As(III) to As(V) is an expected result in soils with predominant oxic conditions such as in this experiment [18]. Oxidation of As(III) in soils is favored by the presence of oxygen, Mn and Fe oxides, and bacteria [19]. This results explains why As accumulation was similar in plants from both As(III) and As(V) treatments (Fig. 3.1). Linear combination fittings showed the spectra from As in the soil had a contribution higher than 88% (combined) from the model compounds As(V)-ferrihydrite and pharmacosiderite ($KFe_4(AsO_4)_3(OH)_4 \cdot 6\text{-}7H_2O$). These two model compounds were used as proxys for sorbed (As(V)-ferrihydrite) and crystalline (pharmacosiderite) As species. The results indicate that As in the soil is predominantly found in the form of As(V) sorbed to amorphous Fe oxides followed by As in the form of a mineral consistent with structure of pharmacosiderite. Adsorption of As to amorphous Fe oxides is one the main biogeochemical processes affecting As mobility in soils [18]. The occurrence of pharmacosiderite suggests precipitation of As(V) and Fe(III) solutions close to neutral pH values. Pharmacosiderite minerals are extremely tolerant of cation exchanges in their channels, hence limiting As availability in the soil [20].

Speciation of As in the roots tissues was found to be similar to that of As-Cys_3 (used as a model compound for As-thiolate species), this results agrees well with the results from S accumulation. Also, these findings confirm the role of LMWT in the detoxification of As since no significant signs of toxicity were observed. However, it is worth noting that the results from

XAS studies do not differentiate As coordination to LMWT (such as glutathione or phytochelatins) and coordination to thiols from cysteine residues from functional proteins. Coordination of As to proteins may affect its proper folding or function leading to cellular toxicity [21].

3.3.4 μXAS studies

Soil cores from control and arsenic treated soils were embedded in LR white resin and cross sections from the cores (approx 1mm thick) were analyzed using a 15 x 5 μm synchrotron x-ray beam. In order to study the effect of the embedding methodology over As speciation, model compounds where embedded following the same method as samples and studied by XAS. From Fig. 3.4 it can be observed that the oxidation state of the embedded As(V) is affected but not the oxidation state of As(III). The spectra from the As(V) embedded model compound presents a feature at 11869 eV that corresponds to a contribution from an As(III) species. This reduced fraction from the As(V) embedded model compound indicates that the embedding methodology and/or the exposure to the X-ray beam affected the oxidation state. Despite this result, μXRF maps from the soil cores were obtained to study the distribution of As, Fe and Zn. Also, As k-edge μXANES data was collected at selected spots of interest. Tricolor μXRF maps and optical images from the soil core samples are shown in Fig. 3.5. From Fig. 3.5 (a, b) it can be observed that As was widely distributed across the soil matrix, although some hot pots (bright red speckles) can be observed, no regions of enrichment were detected. The mesquite root in Fig. 3.5(b) is revealed by an area with high blue contrast corresponding to the distribution of Zn. The sample is placed at a 45 º angle and the fluorescence detector is 90º relative to the x-ray beam. This orientation causes the beam in the case of Fig. 3.5(b) to interact with the soil matrix

surrounding the root tissue before reaching the root sample. Hence, the x-ray probe is most likely only detecting the surface layer of the root which in this case is rich in Zn. This is not the case for the As(III) μXRF map shown in Fig. 3.5(a) where the sample is perfectly positioned so the x-ray beam hits the cross section of the root showing a clear enrichment of As in the root tissues.

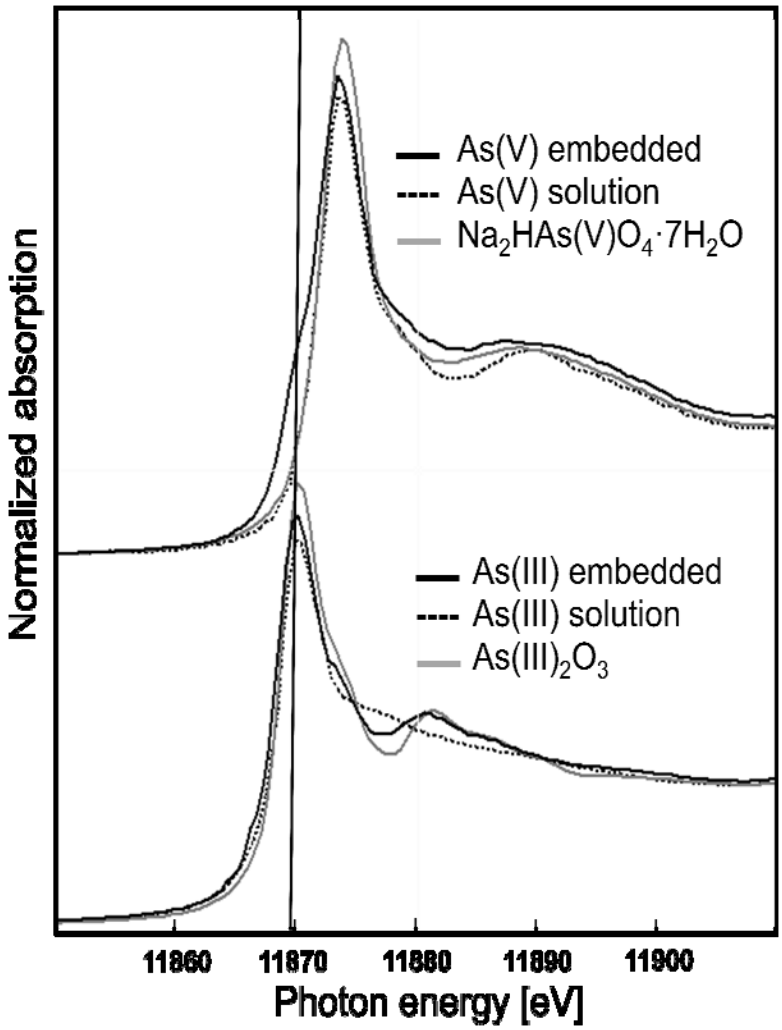

Figure 3.4 μXANES spectra of As(V) and As(III) references. Embedded references are As_2O_3 for As(III) and $NaHAs_2O_4 \cdot 7H_2O$ for As(V) fine powder in LR white resin. Solutions have pH 3.0 and 5.8 for As(III) and As(V) respectively.

The spots selected for μXANES are shown in Fig. 3.5 and the results from linear combination fittings (LC-XANES) are shown in Table 3.1. The results must be interpreted carefully due to the previously shown effect from embedding method and/or radiation damage (Fig. 3.4). The contribution from an As(III) species in the As(V) embedded model compound

was determined to be around 30%. The contribution from arsenolite ($As(III)_2O_3$) in the selected spot form the As(V) treated soil ranged from 9 to 46%. Spot 2 was fitted with only one As(III) component suggesting full As(V) reduction in this spot.

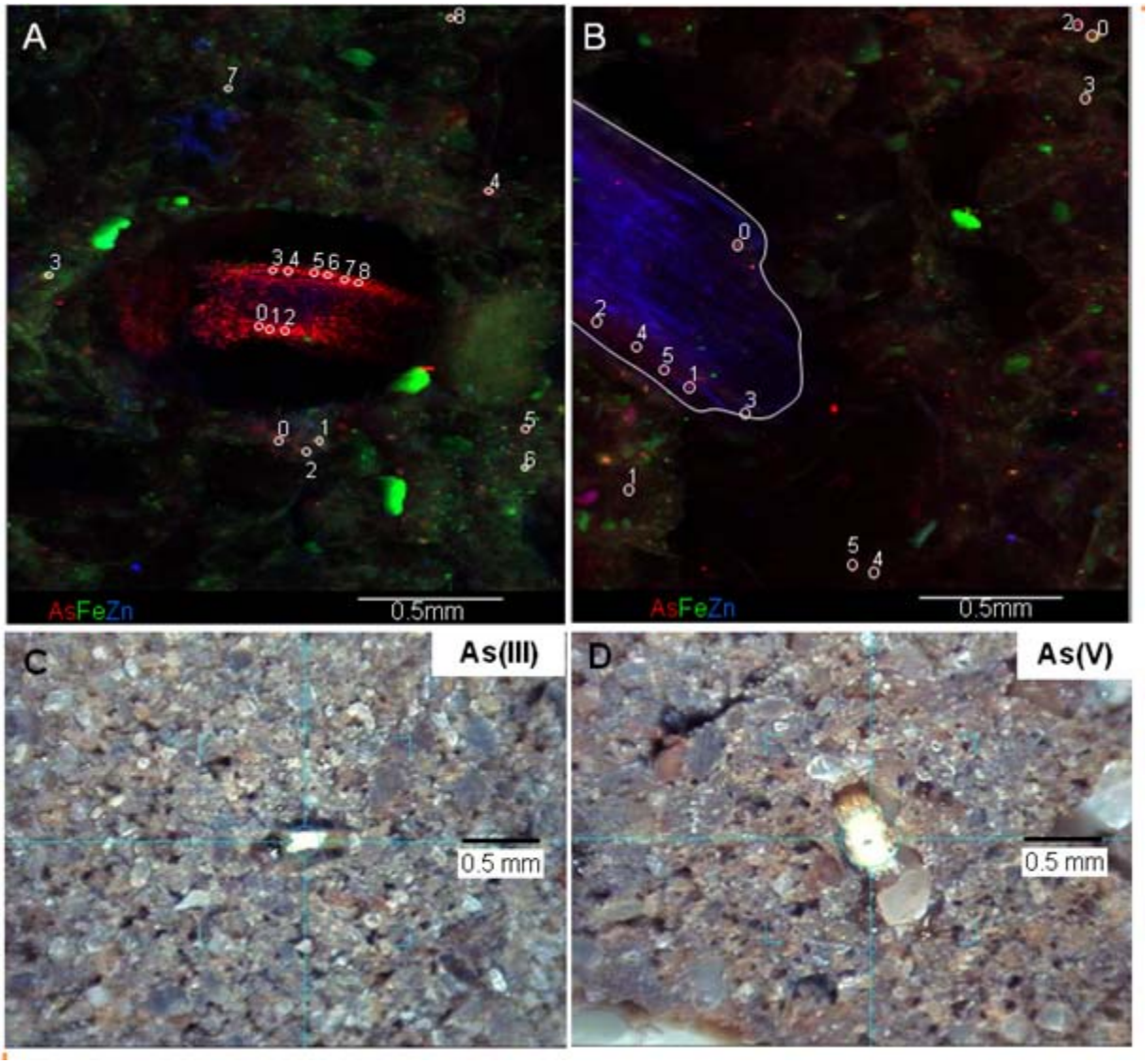

Figure 3.5 Tricolor μXRF maps and optical image of thin sections from the rhizosphere of mesquite plants grown in As contaminated soil for one month. (A) As(III) treatment. (B) As(V) treatment. (C) As(III) optical image. (D) As(V) optical image. Numbers in the map indicate spots selected for XANES data collection. Map acquisition performed at 12KeV with a 10μm pixel size and a dwell time of 120 ms.

The μXRF is a probe in the micrometer range subject to artifacts from microenvironments, a microenvironment in the sample with depleted oxygen and/or bacteria

present can lead to a full reduction of As(V) to As(III). However, this is not repeated in the rest of the spots and it does not represent the average speciation of As in this soil. Considering there is already a possible 30% contribution from As(III) in the spectra the data from the μXANES studies agrees with the findings from the bulk XANES (Fig. 3.3). In As(V) treated soil the oxidation state is preserved and predominantly found in the form of aqueous As(V) and the Fe arsenate pharmacosiderite. The percentage contribution from pharmacosiderite found in the μXANES (18-37%) studies is higher than the fraction found in bulk XANES (8-12%). However, due to the low As fluorescence signal from the soil, spectroscopy had to be performed in the brighter spots where the mineral formation can be promoted. Pharmacosiderite precipitation requires high As(V)/Fe(III) ratio; otherwise, Fe(III) arsenates (e.g., scorodite) or Fe oxyhydroxides would be preferentially formed [20]. The results from the spots in the As(III) treated soil are similar to the findings in the As(V) treated soil (Table 3.1). The As(III) was almost completely oxidized to As(V) and found in a form consistent with aqueous As(V) and pharmacosiderite.

Table 3.1 LC-XANES fitting results of mesquite root and soil spots from XRF maps in Figure 5 (A and B). Reference compounds used are aqueous solutions from As_2O_3 (pH= 3.0) and $Na_2HAsO_4 \cdot 7\ H_2O$ (pH=5.8) for As(III) and As(V), respectively. Pharmacosiderite, arsenolite, As_2O_5, As(V)-ferryhidrite, and As-Cys_3 were analyzed as dry fine powder.

	Pharmaco-siderite	Arsenolite	As_2O_5	AsV-Ferrihydrite	As-Cys_3	As(III)	As(V)	NSS
As(V) soil								
Spot 0	34	15					51	.000284
Spot 1	21	46				21		.00056
Spot 2		100						.00114
Spot 3	18	26					55	.000276
Spot 4	37	9					55	.000421
Spot 5	23	12		26			39	.000454
As(V) root								
Spot 0	29	26					45	.000468
Spot 1		100						.00126
Spot 2		88				12		.000758
Spot 3		100						.00138
Spot 4		22	23		54			.000755
Spot 5		17	14		67			.000601

	Pharmaco-siderite	Arsenolite	As_2O_5	AsV-Ferrihydrite	As-Cys_3	As(III)	As(V)	NSS
As(III) soil								
Spot 0	30	26					44	.00047
Spot 1	34	34					45	.00436
Spot 2	22	31					48	.00052
Spot 3	33	22					45	.000416
Spot 4		37	9				54	.000458
Spot 5	34	19					47	.00479
Spot 6	33	27		40				.000455
Spot 7	35					24	41	.00121
Spot 8	44					19	39	.0004
As(III) root								
Spot 0			4		96			.00043
Spot 1			5		80	14		.00028
Spot 2			4		95			.00033
Spot 3			6		93			.00032
Spot 4			6		94			.00024
Spot 5			5		94			.00036
Spot 6			4		96			.00035
Spot 7			6		94			.00028
Spot 8			6		93			.00011

One thing to notice is the lack of a contribution from As(V)-ferrihydrite in the fittings from μXANES (Table 3.1). The bulk XANES results show As(V)-ferrihydrite as the main contribution in the fittings (Fig. 3.3). The results from the bulk XANES should be interpreted as an average of the As forms in the soil where As(V)-ferrihydrite is the predominant form. In contrast, the μXANES reveals the presence of As forms that may have minor contribution in the total average speciation but that could be relevant in detecting specific reactions or mechanisms. In the case of this study the increase in the pharmacosiderite contribution in the μXANES fittings may be due to the criteria used for selecting the spots (bright spots).

The LC-XANES fittings from the root spots in As(III) treated soil showed the predominant form of As in the roots is consistent with As-Cys_3 (proxy for As-thiolate species). This is confirming the findings from the bulk studies that showed As in the form of an As-thiolate in the root tissues. In contrast, the LC-XANES fittings from the root spots in As(V)

showed only two spots with a significant contribution from As-Cys_3 (spot 4 and 5). However, as previously mentioned the orientation of the sample (specifically the root) in the beam prevented the x-rays from interacting with the cross section of the roots. As a result, these spectra is an average from As species in the soil surrounding the root and the epidermis of the root (rich in Zn, Fig. 3.5(b)).

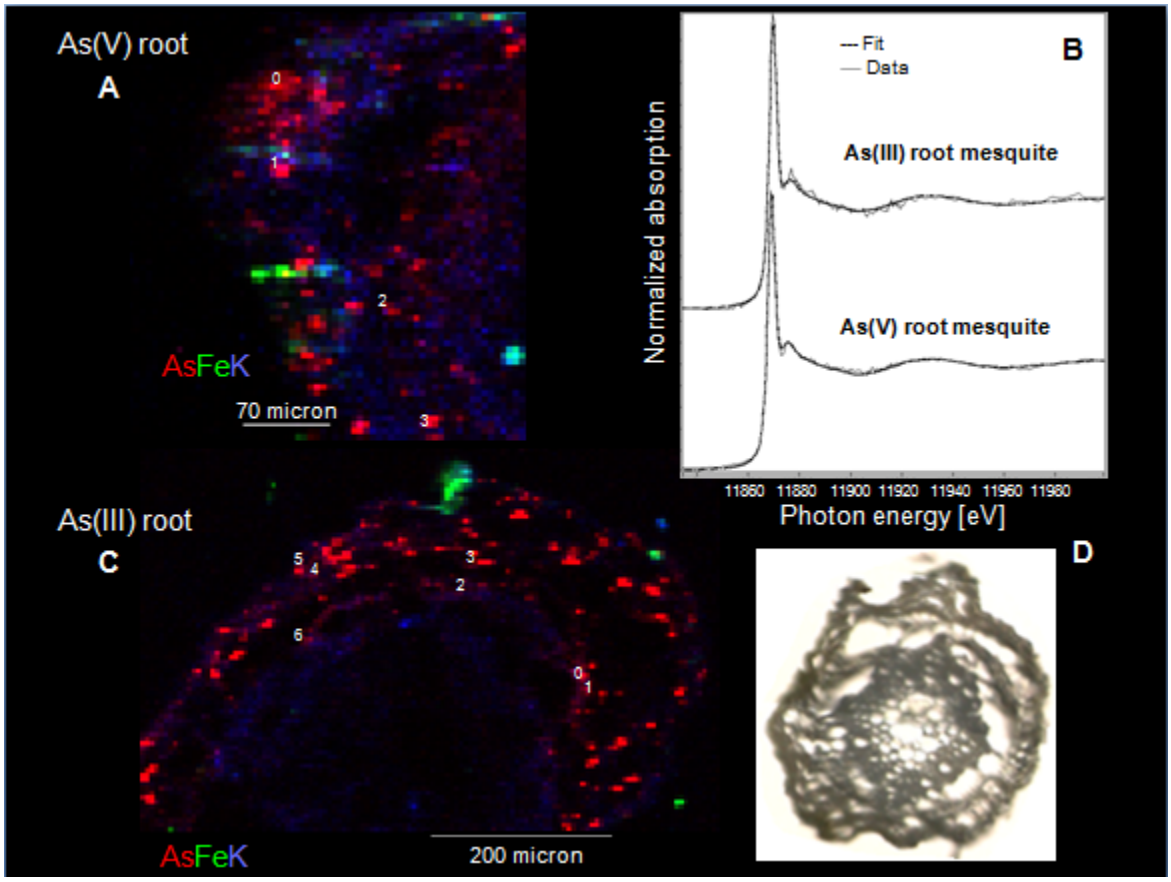

Figure 3.6 Tricolor XRF maps of root cross section from mesquite plants grown in As treated soil for one month. (A) As(V) root. (B) Example of LC-XANES fittings from As(V) spot 1 and As(III) spot 3. (C) As(III) root. (D) Optical image of a mesquite root cross section (30 µm thick).

To further investigate the speciation of As in the root tissues of mesquite plants thin cross sections (30 µm thick) from the roots were used for µXRF and µXANES analysis. Tricolor maps from the root thin sections and an optical image of one sectioned root is shown in Fig. 3.6. From Fig. 3.6 (A) and (C) it can be observed that As is mainly accumulated in the cortex of the roots.

This explains the low accumulation of As in the shoots, because the vascular tissue is where the transport from roots to shoots of soil solution with elements takes place. The LC-XANES fiitings from the spots marked in Fig. 3.6 (A) and (C) are shown in Table 3.2. These results confirm the coordination of As to S in the root tissues and sustain the hypothesis that LMWT play a key role in the accumulation and detoxification of As in the mesquite plants.

Table 3.2 LC-XANES fitting results of mesquite root and soil spots from XRF maps in Figure 4 (A and B). Reference compounds used are an aqueous solution from $Na_2HAs(V)O_4 \cdot 7\ H_2O$ (pH=5.8) and As-Cys_3 analyzed as dry fine powder.

	As(V)	As-Cys_3	NSS
As(V) root			
Spot 0	7	94	.00076
Spot 1	5	95	.00094
Spot 2	3	97	.0017
Spot 3	3	98	.00084
Spot 4	2	99	.00126
Spot 5	1	98	.0017
Spot 6	2	97	.00088
Spot 7	3	97	.00091
As(III) root			
Spot 0	6	95	.00116
Spot 1	3	97	.00188
Spot 2	4	95	.00172
Spot 3	3	97	.0016
Spot 4	3	98	.00229
Spot 5	3	97	.00166
Spot 6	5	96	.00116

3.4 Conclusions

Mesquite plants accumulated As mainly in the root tissues with very low concentrations found in the shoots (< 6 mg kg^{-1} dry biomass). Bulk XANES studies demonstrated the oxidation of As(III) to As(V) in the soil. The predominant form of As was consistent with As(V) sorbed in 2-L ferrihydrite followed by a crystalline Fe arsenate consistent with pharmacosiderite. LC-XANES from the bulk and μXAS studies were consistent in finding As(V) as the predominant

oxidation state of As. Similar to As, accumulation of S occurred mainly in the root tissues. Results from both bulk and micro LC-XANES demonstrated the coordination of As to S supporting the hypothesis that LMWT play a key role in As detoxification in mesquite plants. This work demonstrated the importance of combining bulk and μXAS techniques in the analysis of As speciation in soil and plant samples. The embedding methodology using LR white resin should be reassessed to find a method that does not affect the oxidation state of As in the sample.

CHAPTER 4

Coordination and speciation of cadmium taken up by corn seedlings and its effects on the uptake of some macro and micro nutrients

Abstract

This study investigated the uptake and speciation of Cd in corn plants and its effects on molybdenum, manganese, phosphorus, and sulfur uptake. Additionally, the link between S concentration, Cd uptake, and the synthesis of Low molecular weight thiols (LMWT) was investigated. ICP/OES determinations demonstrated that Cd concentration was higher in the roots compared to the shoots. Nutrient absorption of Mo and Mn remained normal in comparison to the control plants. P concentrations were found to increase in the roots of the exposed plants and remained at normal concentration levels in the shoots as compared to the control plants. However, the concentration of S in roots and shoot tissues increased with increasing uptake of Cd. S concentrations were found to increase significantly upon exposure to Cd and also the production the LMWT. X-ray absorption spectroscopy analyses were performed to demonstrate the link between Cd and sulfur ligands most likely from LMWT. The results indicate that Cd inside the corn roots and shoots is bound to sulfur ligands with interatomic distances of 2.51-2.52 Å. These results confirm a strong link between S uptake and the production of LMWT upon exposure to Cd.

4.1 Introduction

Cadmium is a heavy metal of high toxicity to plants. It occurs naturally at low levels in the environment [1] but tends to accumulate at high concentrations due to mining, industrial discharges, and as a by-product of mineral fertilizers. Cadmium toxicity, tolerance, uptake and translocation have been studied in many different plant species, including corn (*Zea mays*), in the field, in greenhouse soil, and hydroponic experiments [2-10]. Studies have identified few plant species as Cd hyperaccumulators (> 100 mg kg^{-1} dry tissue [11]), for instance, *Thlaspi caerulescens* can accumulate more than 1000 mg kg^{-1} and *Salsola Kali* almost 2400 mg kg^{-1} in dry root tissue [12, 13]. Among sensitive plant species corn is one with a high tolerance to cadmium concentrations (sorghum< cucumber< wheat< corn); the effective concentration value (EC50) (50% of the population exhibits response) for the corn plants in Cd-amended soils is in the range of 208-265 mg kg^{-1} of soil dry weight [14].

Plants basically exhibit two mechanisms against Cd toxicity which are either avoiding uptake of the metal or neutralization of its toxicity through specific mechanisms. The latter mechanism involves phytochelatins (PCs) and metallothioneins, which are sulfur rich low molecular weight compounds that can chelate heavy metals (such as Cd) through their cysteine residues [15]. It has been hypothesized that Cd is responsible for inducing the synthesis of phytochelatin and metallothionein compounds in different organisms. There is evidence in the literature that supports the hypothesis that Cd regulates/induces the expression of the enzyme phytochelatin synthetase (PCS; EC 2.3.2.15), which is in charge of the synthesis of PCs from glutathione (GSH) and cysteine monomers [16].

The determination of cysteine, GSH, PCs, and the structural coordination of these low molecular weight thiol (LMWT) compounds to Cd have been previously studied using high-performance liquid chromatography (HPLC) and X-ray absorption spectroscopy (XAS) techniques in extracts from corn plant tissues and frozen tissues from Indian mustard [17-19]. Pickering et al. [19] investigated the coordination of Cd to PCs in complexes extracted from corn roots and demonstrated a coordination of 4 sulfur ligands ($[Cd(SPh)_4]^{2-}$ model compound) with an interatomic distance of 2.54 Å using Cd K-edge extended fine structure XAS (EXAFS). Although, the coordination of Cd to PCs and LMWT has been proven, to our knowledge, none of the existent studies reports on the relative amounts of the different Cd species found in corn plants exposed to this heavy metal. Functional groups containing O (such as lignins) and N are other potential ligands that can coordinate and sequester Cd resulting in detoxification of the metal into the cell wall [20, 21].

In order to understand the mechanism(s) involved in the uptake, tolerance and translocation of Cd in corn plants, it is important to study the chemical species and relative amounts present inside its tissues. The present work investigated not only Cd uptake but also the uptake of important nutrients (Mo, Mn, S and P) by corn plants in hydroponic experiments using inductively coupled plasma optical emission spectroscopy (ICP-OES). Additionally, the concentration of LMWT in roots and shoots was determined using Ellman's reagent, and the Cd speciation and local coordination environment were determined in the tissues of the corn plants using X-ray absorption spectroscopy (XAS) analyses. XAS techniques allows the study of metal speciation and local coordination environment in vivo with minimal sample preparation, which ensures little to no change from structural environment [22].

4.2 Materials and Methods

4.2.1 Medium preparation and seed planting

Zea mays seeds were placed over the edge of paper towels, previously autoclaved (30 min at 120 ºC and 1.0 kg cm^{-2} pressure) under a laminar flow hood. The towels were bent and rolled to cover the seeds and transferred to 250 mL mason jars containing sterilized deionized water for five days. Next, the water was replaced by half strength modified Hoagland's nutrient solution (pH 5.8) for another 2 days. Germination and growth of the seedlings took place at room temperature using a 16-h photoperiod (two 34 W Phillips lamps).

After, *Zea mays* seedlings were exposed to cadmium treatments containing 0 (control), 10, 50 and 100 µM $Cd(NO_3)_2$ in hydroponics media containing full strength modified Hoagland's nutrient solution, which consisted of the following chemical composition: 0.35 mM $Ca(NO_3)_2 \cdot 4H_2O$, 2.1 mM $CaCl_2 \cdot 2H_2O$, 0.91 mM $Mg(NO_3)_2 \cdot 6H_2O$, 0.97 mM KH_2PO_4, 0.255 mM KNO_3, 23.13 µM H_3BO_3, 3.9 µM $MnCl_2 \cdot 4H2O$, 0.07 µM MoO_3, 0.44 µM $CuSO_4 \cdot 5H_2O$, 10 µM $Fe(NO_3)_3 \cdot 9H_2O$, 0.37 µM $Zn(NO_3)_2 \cdot 6H_2O$).

4.2.2 Elemental analysis

After seven days of exposure, the corn plants were rinsed with 0.1M HNO_3 and DI water, separated into roots, cotyledons, and shoots, which were subsequently freeze dried. The determination of cadmium and nutrient uptake (molybdenum, manganese, sulfur and phosphorus) was performed on freeze dried tissue samples using microwave assisted acid

digestion (CEM MarsX, CEM corporation, Mathews, NC). The lyophilized samples were digested using 6 mL of trace pure 70% HNO_3 following the USEPA 3051 method [23]. Samples were examined using an Inductive Coupled Plasma Optical Emission Spectrometer (ICP-OES) (Perkin-Elmer ICP-OES Optima 4300 DV with a Perkin-Elmer AS-90 plus autosampler rack; Shelton, CT). The ICP-OES parameters used were as follows: nebulizer flow, 0.80 L min^{-1}; power, 1450 W; peristaltic pump rate, 1.5 $mL.min^{-1}$; flush time, 15 s; delay time, 20 s; read time, 10 s; wash time, 60 s; and every sample was read in triplicate.

4.2.3 XAS sample preparation

Prior to lyophilization, the samples were first immersed in liquid nitrogen for 45 minutes until completely frozen. The samples were then placed into a LabConco Freeze Zone 4.5 System (LabConco Corporation, Kansas City, MO; USA) and lyophilized at -45°C and 0.069 mbar pressure. Subsequent to lyophilization, the samples were ground using a mortar and pestle to obtain a homogenous mixture and packed into 1.0 mm thick aluminum sample holders with Kapton Tape® windows.

4.2.4 XAS Sample collection

The sample spectra were collected at SSRL on beamline 10-2 using standard conditions at the cadmium K-edge 26.711 keV. The beamline conditions were as follows: a current ranging between 80-100 mA, a Si 220 (φ 90) double crystal monochromator, and beam energy of 3.0 GeV. The spectra of the samples and model compounds were collected in transmission mode

using nitrogen filled ion chambers and an internal Cd(0) metal foil for calibration purposes (E_0=26.711 keV). In addition, the beam was detuned by 30% to reduce higher order harmonics to aid in data analysis.

4.2.5 XAS Data Analysis

The XAS data was analyzed using the WinXAS (V 3.1) software and standard data reduction techniques [24]. The data was firs energy calibrated based on the internal Cd(0) metal foil (E_0 =26.711 keV) using a second degree derivative. The data was analyzed by the energy difference between the energy determined for the cadmium foil and the literature value for Cd(0) metal. Subsequent to energy calibration the samples were background corrected using a 2 polynomial fitting. The pre-edge region was fitted using a 1 degree polynomial and the post edge region was fitted using a 4^{th} degree polynomial and the sample spectra were subsequently normalized to one absorption unit. At this point the XANES spectra were extracted by sectioning the spectra from 26.650 keV to 26.800 keV.

The EXAFS were then extracted using the procedure described below. The sample spectra were first converted into k space (or wave number space $Å^{-1}$). The conversion into k space was performed by determining energy of the photoelectron ejected from the sample. The energy of the ejected photoelectron was determined by taking a second degree derivative of the sample spectra. Once the sample spectra were in k space the samples were μ fitted using a spline of 4 knots and a k weight of 3. The spectra were then Fourier transformed from 2 to 12.2 $Å^{-1}$, (with the exception of the Cd(II) cotyledon due to the poor signal to noise ratio this sample was Fourier transformed from 2.0 to 10.2 $Å^{-1}$) into R space (Å). The samples were subsequently back

transformed from 0.80 to 2.78 Å to extract the first shell of interacting atoms and fitted using least squared fittings based on calculations generated from FEFF 8.00 [25]. The fitting parameters included the interatomic distance (R), the coordination number (CN), the Debye Waller factor (σ^2), and the energy shifts (which were found to be approximately (1-2 eV). The inputs for the FEFF calculations were generated using the ATOMS software V 3.0 beta and crystallographic data from the literature [26].

4.2.6 Determination of Low Molecular Weight Thiols

Acid soluble thiols were determined as described by de la Rosa et al. [4]. Extractions were performed by grinding 50 mg of freeze-dry tissue in 2 mL of 5% (w/v) sulfosalicylic acid and 6.3 mM diethylenetriaminepentaacetic acid (DTPA). The samples were then centrifuged for 10 minutes at 14000 rpm at 4˚C using a refrigerated centrifuge (Eppendorf centrifuge 5417R, Westbury, NY). Supernatants were assayed after centrifugation. The concentrations of LMWT were determined using standards prepared from reduced glutathione (GSH). An aliquot of 100 µL of the supernatant or standard solutions was added to 200 µL of 0.525 mM KH_2PO_4 buffer previously placed into a microplate well. Later, 50 µl of DTNB solution (1.75 mM 5,5′-dithiobis(2-nitrobenzoic acid), 0.143 M K_2HPO_4, 6.3 mm DTPA, pH 7.5) were added to develop the characteristic Ellman's reagent yellow color. Background-sample blanks were prepared using 0.143 M K_2HPO_4 instead of the DTNB solution. The absorbance at 412 nm was measured using a microplate reader.

4.3 Results and Discussion

4.3.1 Cadmium concentration in plant tissues

The concentration of Cd in roots, cotyledons, and shoots of corn plants is shown in Fig. 4.1. Root tissues accumulated the highest amount of Cd for all the treatments, which was followed by the shoots.

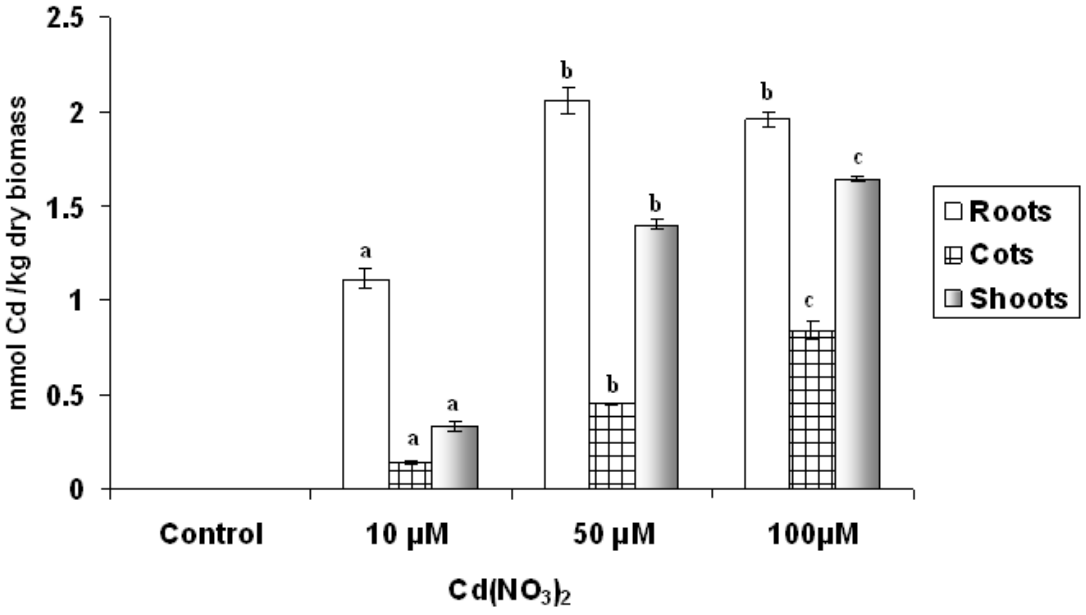

Figure 4.1 Cadmium uptake in the tissues of corn plants after seven days of exposure in hydroponic conditions. Values are average of three replicates ± standard error. Bars from the same tissue with different letter are significantly different (Tuckey alpha 0.05).

The concentration of Cd in the roots increased with increasing Cd concentration in the growth medium up to the 50µM $Cd(NO_3)_2$ treatment where it reached the maximum uptake. Shoots and cotyledons showed increased uptake with increasing concentration of Cd in the

treatments. Results are in agreement with other soil and hydroponics studies performed in tumbleweed, wheat, cucumber and sorghum where Cd showed a concentration dependent uptake and was mainly accumulated in roots [4, 13, 14]. The translocation factor (TF), defined as the proportion of Cd level in the shoots divided by that in the roots, increased with increasing concentration of Cd in the treatments (10 μM, 0.30; 50μM, 0.68; 100μM, 0.84). Wang et al. [27] also reported a similar increasing trend in the TF for two corn cultivars (Liyu No.6 and Nongda No.108) exposed to Cd in hydroponic conditions.

4.3.2 Effect of cadmium uptake on nutrients uptake

Molybdenum (Mo) is an essential micronutrient required in the cofactor complexes of key enzymes catalyzing reactions in carbon, nitrogen, and sulfur metabolism. Aldehyde oxidase (AO; EC 1.2.3.1), sulfite oxidase (SO; EC 1.8.3.1), and nitrate reductase (NR; EC 1.6.6.1) are enzymes that require Mo as part of their cofactor complexes. AO enzymes catalyze the final step in the synthesis of the important phytohormones indoleacetic acid (IAA) and abscisic acid (ABA). Hence, AO enzymes are important for physiological processes that involve the action of ABA and/or auxin hormones like the response to biotic and abiotic stress conditions [28]. NR can reduce nitrite to NO, an important signaling molecule that may contribute to plant growth, development, and protection against reactive oxygen species. Corn plants treated with 50μM $Cd(NO_3)_2$ significantly increased Mo uptake in the roots, whereas the rest of treatments maintained similar concentrations compared to control plants in nutrient solution (Table 4.1). Furthermore, it was also observed that the shoots of the corn plants exposed to Cd maintained a normal balance of Mo in comparison to the control plants (Table 4.1). A severe negative effect in

the water relationship, nitrate assimilation, and NR enzymatic activity was reported in bean plants exposed to Cd. Decreased uptake of water and nutrients due to Cd exposure showed a negative impact on the activity of key enzymes such as NR [29]. The present results demonstrate the ability of the tested corn plants to maintain normal concentrations of Mo in the tissues, which may aid in the plant's ability to tolerate to some extent the effects of Cd exposure.

Manganese is an essential micronutrient for plants. The superoxide detoxifying enzyme superoxide dismutase (SOD; EC 1.15.1.1) contains one atom of Mn as cofactor per enzyme [30]. Mn SOD enhances the resistance to oxygen radicals that are produced through the exposure of plants to toxic heavy metals. A unique role of Mn in green plants is the splitting of water molecules and O_2 production in photosynthesis. Therefore, a deficiency in Mn will seriously disrupt photosynthesis which is driven by the splitting of water molecules [30].

Table 4.1 Concentration of important nutrients in the tissues of corn plants exposed to Cd for seven days in hydroponic conditions. Values are average of three replicates ± standard error. Values from the same column with different letter are significantly different (Tuckey alpha 0.05).

$Cd(NO_3)_2$	Mo			Mn		
	Root	Cotyledon	Shoot	Root	Cotyledon	Shoot
0 µM	0.405 ± 0.012 a	0.141 ± 0.005 a	0.345 ± 0.007	0.292 ± 0.005	0.206 ± 0.003	0.408 ± 0.007
10 µM	0.547 ± 0.002 ab	0.121 ± 0.001 b	0.659 ± 0.029	0.399 ± 0.003	0.216 ± 0.002	0.429 ± 0.021
50 µM	0.647 ± 0.070 b	0.123 ± 0.004 b	0.594 ± 0.140	0.443 ± 0.062	0.212 ± 0.003	0.441 ± 0.017
100 µM	0.583 ± 0.053 ab	0.131 ± 0.003 ab	0.373 ± 0.002	0.422 ± 0.053	0.212 ± 0.003	0.403 ± 0.006
	S			P		
	Root	Cotyledon	Shoot	Root	Cotyledon	Shoot
0 µM	46.00 ± 0.06 a	26.25 ± 1.35 a	44.06 ± 0.76 a	11045.9 ± 54.3 a	1777.6 ± 139	9781.2 ± 106 a
10 µM	51.81 ± 1.02 b	25.59 ± 0.12 a	42.72 ± 1.99 a	12511.4 ± 199 b	1851.9 ± 80.1	9721.1 ± 476 a
50 µM	57.43 ± 1.86 c	30.17 ± 0.57 b	52.54 ± 0.32 b	14160.2 ± 322 b	1974.0 ± 56.6	12221.5 ± 109 b
100 µM	58.74 ± 1.30 c	25.43 ± 0.44 a	51.22 ± 0.75 b	10211.1 ± 74.5 a	1716.1 ± 23.6	9983.2 ± 118 a

Corn plants exposed to Cd maintained normal concentrations of Mn in the tissues when compared to the control plants (Table 4.1). The exposure to cadmium (Cd) has been found to decrease Mn uptake in different barley genotypes [31]. On the other hand, Cd stress symptoms were mild in the presence of Mn excess in plants of *Phytolacca Americana* demonstrating the importance of Mn in the heavy metal stress tolerance [32]. Studies performed with the Nongda No.108 and Liyu No. 6 cultivars of corn showed decreased Mn uptake when exposed to Cd under similar conditions as the ones used in this work [27]. Results from this work indicate no disturbance in the Mn balance due to Cd exposure. Maintaining normal concentrations of this important micronutrient is of great importance for the proper development of the plants even in the presence of a toxic heavy metal like Cd.

The nutritional importance of phosphorus (P) in plants is well established in terms of its role in phosphate functional groups, which are integral to cellular processes such as signal transduction, energy supply, and synthesis of DNA and RNA [30]. Additionally, other studies using corn plants have demonstrated the formation of P and Cd deposits in the plants roots vacuoles and the cell wall [33]. Thus, the uptake of P is important for the sequestration of Cd in the root tissues; whereas, external P may also decrease bioavailability of Cd [34]. The corn plants exposed to Cd showed a significant increas in the uptake of P in the roots from the 10 μM and 50 μM $Cd(NO_3)_2$ treatments (Table 4.1). However, the uptake of P in the roots of the 100 μM $Cd(NO_3)_2$ treatment was found to have normal concentrations when compared to the control plants. Furthermore, the uptake of P in the corn shoots was found to be lower than root uptake for all the Cd treatments (Table 4.1). Plant exposed to 50 μM $Cd(NO_3)_2$ significantly increased P uptake in the shoots compared to the control plants, whereas the plants exposed to 10 μM and 100 μM $Cd(NO_3)_2$ maintained normal concentrations of P when compared to the control (Table

4.1). It has been shown that the exposure to Cd in plants can damage the chloroplast structure and reduce the production of chlorophyll; P uptake can help to reduce both effects in corn plants by enhancing vacuolar and cell wall sequestration of Cd in the root tissues [33]. The results demonstrate the capacity of corn plants to maintain, at minimum, normal uptake of P in all tissues of plants exposed to Cd.

The uptake of S was studied in this work due to its high relevance in the tolerance and detoxification of Cd in plants. Reduced sulfur in the form of thiol groups (-SH) is present in the cysteine residues of the important peptide glutathione (GSH) and the metal-induced binding phytochelatins (PCs) and metallothioneins. All of the aforementioned sulfur rich compounds are used by plants to bio-inactivate heavy metals such as Cd [4, 35, 36]. Sulfur uptake in the roots of corn plants exposed to Cd significantly increase for all the treatments (Table 4.1). In addition, an increase in S concentration was found to correlate with increasing concentration of Cd found in the roots (Fig. 1). Thus, the data is suggesting a possible role of sulfur containing groups in the detoxification of Cd in the roots. One of the main responses reported in the literature for the roots of *Arabidopsis thaliana* was the induction of genes involved in sulfur assimilation–reduction and glutathione (GSH) metabolism [37]. Uptake of S in the shoots was also found to significantly increased in the 50 and 100 μM $Cd(NO_3)_2$ treatments (Table 4.1). The increase in S concentration was significant when considerable amounts of Cd (1.40 mmol Cd kg^{-1} dry biomass) were detected in the shoots suggesting a possible enhancement of S translocation from roots to shoots in the presence of Cd. These results suggest that corn plants may increase the assimilation of sulfur in the roots and translocation to the shoots to cope with Cd toxicity. An increase in the production of sulfur rich peptides (GSH and PCS) has been reported in other plant species such as *Salsola kali* and different genotypes of wheat [4, 38].

4.3.3 Effect of Cd uptake in the production of LMWT

The production of sulfur rich peptides such as cysteine, GSH and PCS was determined by the total acid soluble thiols method. This assay was performed in the roots and shoots tissues of the corn plants and the results are presented in Fig. 4.2. Synthesis of LMWT was mainly induced in the root tissues and was found to increase with increasing concentration of Cd in the treatment. The presence of a higher concentration of LMWT in the roots was also found to correlate to a higher concentration of Cd (Fig.4.1) and increasing concentration of S in these tissues (Table 4.1).

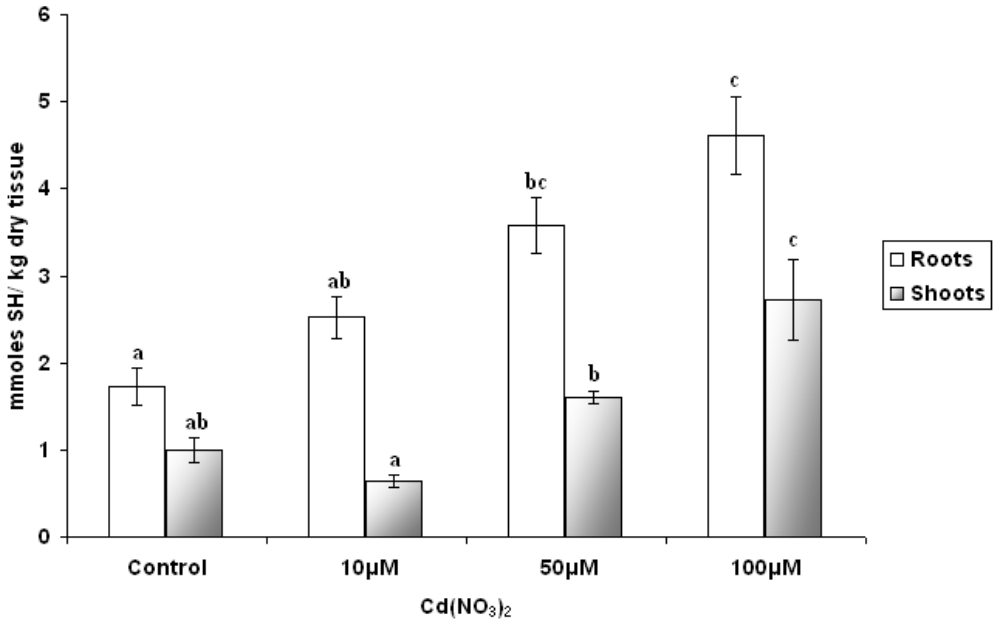

Figure 4.2 Production of LMWT in roots and shoots of corn plants exposed to Cd. Values are average of three replicates ± standard error. Bars from the same tissue with different letter are significantly different (Tuckey alpha 0.05).

Moreover, the stoichiometric relationship between Cd uptake and the production of LMWT presented a good linear correlation coefficient (R^2=0.9827) up to the 50µM $Cd(NO_3)_2$ treatment (Fig. 4.3). These results support the hypothesis that sulfur rich low molecular weight peptides are present in the roots of the corn plants and help to reduce the toxicity of Cd. The

sequestering of Cd in the root vacuoles may be one mechanism used by corn plants to avoid Cd toxicity and decrease translocation of this heavy metal to the shoots. Previous studies have also reported increasing synthesis of LWMT (such as GSH and PCs) upon exposure to Cd [4, 37, 38]. The shoots of the corn plants showed an increased production of LMWT in the 50 and 100 µM $Cd(NO_3)_2$ treatments compared to the control (Fig. 4.2). The same result was observed for total S (Table 4.1) uptake suggesting that the lag time in the LMWT synthesis response to Cd exposure in the shoots may be due to insufficient concentration of S in the shoots.

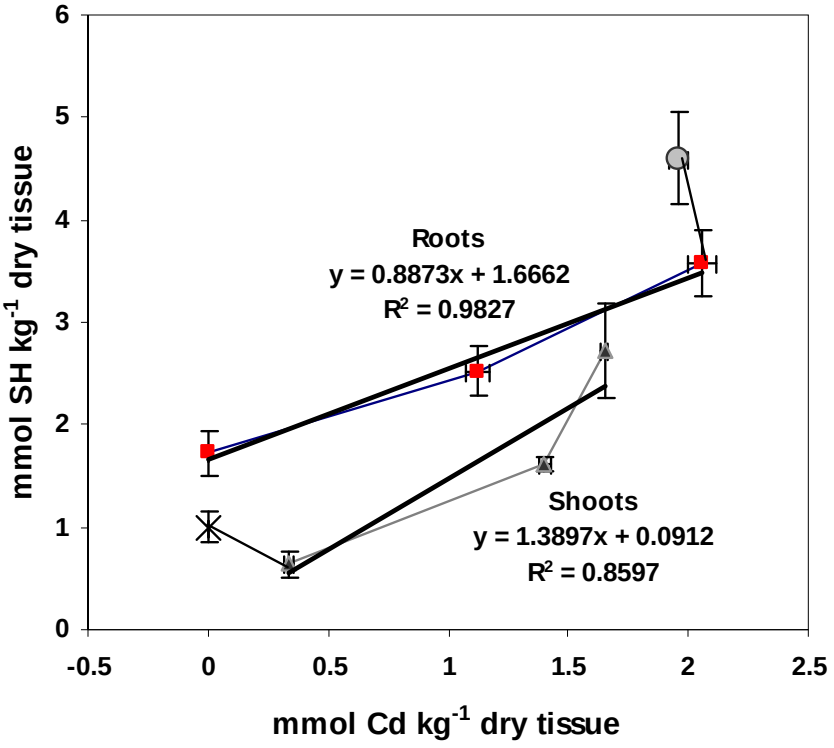

Figure 4.3 Stoichiometry of thiols and incorporated Cd^{++} in corn plants exposed for 7 days to 0– 100 µM $Cd(NO_3)_2$ in hydroponic culture. Bars represent S.E. ($n \geq 3$). First data point for the shoots and the last data point for the roots were discarded from the linear fittings.

From Figure 4.3 this lag time in the production of LMWT can be better observed. The data strongly suggests and induction in the sulfur accumulation pathway in order to induce the synthesis of LMWT to reduce Cd toxicity. This is a mechanism that has been studied and

described in other plant species such as *Arabidopsis thaliana* and wheat [37, 38]. The presence of PCS in the corn plants has been previously confirmed by Pickering et al. [18] however this study demonstrates the close link between S uptake, Cd exposure and the synthesis of LMWT. The presence of PCS in the corn plants has been previously confirmed by Pickering et al. [18] however this study demonstrates the close link between S uptake, Cd exposure and the synthesis of LMWT.

4.3.4 Coordination of Cd^{++} in the corn tissues

In order to confirm the role of Sulfur rich peptides in the detoxification of Cd in the corn plants samples were analyzed using XAS techniques, which includes XANES (x-ray absorption near edge structure) and EXAFS (extended x-ray absorption fine structure). Fig. 4.4 shows the XANES spectra of the Cd sulfide and the Cd in the roots, shoots, and the cotyledons of the corn plants. Within Fig. 4.4 there are 2 points designated as A and B, which indicate the edge positions of the cadmium in the different samples. The point A indicates the Cd edge position in the Cd sulfide model compound and the Cd found within the corn roots and shoots which has energy of 26.711 keV. Whereas point B indicates the cadmium edge position in the corn cotyledon sample and the Cd acetate model compound, which has an energy of 26.717 keV. The small shift in the edge energy between Cd-S bond and Cd-O bond is caused by the donation of electrons from the S to the Cd. The donation of electron density occurs between sulfur ligands and metal ions to cause a shift in the edge energy to approximately the same energy as the zero valent metal. This data indicates that the Cd inside the corn roots and shoots is bound to sulfur ligands.

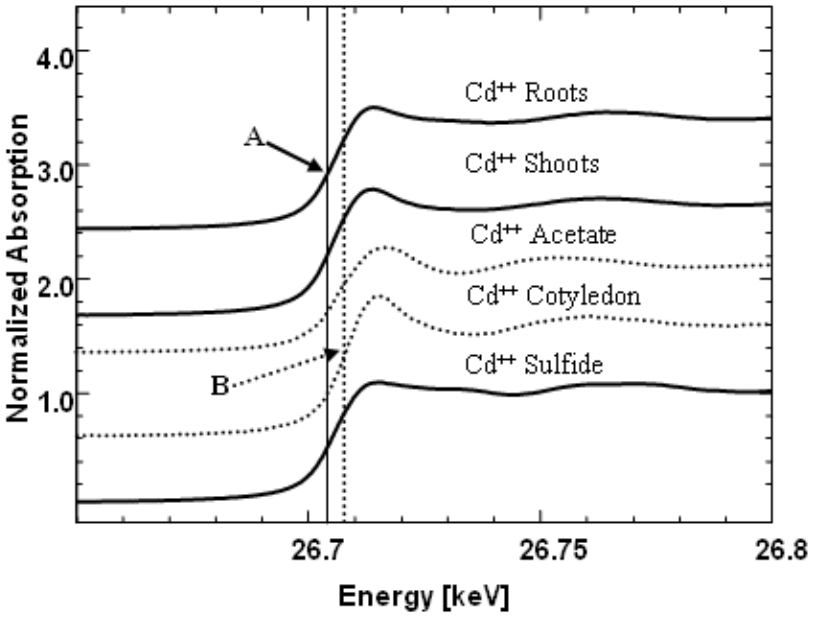

Figure 4.4 XANES region of cadmium sulfide and cadmium acetate model compounds and cadmium interaction with corn roots, shoots, and cotyledons taken from 26.650 keV to 26.800 keV.

The binding of Cd to sulfur ligands in the plants has been noted for a number of different species such as tumbleweed and *Arabidopsis thaliana* [13, 39]. It is also well known that Cd stresses the plants, which induces a PCs synthesis response in the plants to produce thiol rich ligands, which binds to the cadmium for transport and storage. However, in the cotyledon of the plants the XANES appear similar to the Cd acetate model compound indicating that complexation of Cd is through oxygen ligands, as indicated by the edge energy and the shape of the whiteline feature. The cotyledons are starch rich storage organs that act as a food source for the growing seedlings. The presence of Cd in this portion of the plant bound to oxygen ligands may be representing only the sorption of cadmium and not the transport. It is shown in the literature that when Cd sorbs onto non-living biological materials such as biomass of *Hydrilla verticillata*, *Pseudomona aeruginosa*, and organic soil, and that the coordination of Cd occurs to

some extent through O ligands of available carboxyl groups [40- 42]. The EXAFS of the Cd sulfide, Cd root, Cd shoots and Cd cotyledons are shown in Fig. 4.5, and the fittings of the EXAFS are shown in Table 4.2. As can be seen in Table 4.2 and Fig. 4.5 Cd sulfide and Cd in the corn roots and shoots are coordinated solely to sulfur ligands, within the first shell. The Cd sulfide model compound was found to have 4 sulfur ligands at an interatomic distance of 2.51 Å, as defined by the crystal structure [43].

Table 4.2 Least squared EXAFS fitting results using calculations generated from FEFF 8.00.

Sample	Interaction	CN	R(Å)	σ^2 (Å^2)	S_0^2
CdS	Cd-S	4.0	2.51(2)	0.0053	**0.85**
Cd Corn roots	Cd-S	4.0	2.51(7)	0.0070	**0.91**
Cd Corn shoots	Cd-S	4.1	2.49(6)	0.0084	**0.91**
Cd Corn cotyledons	**Cd-O**	**3.9**	**2.22(7)**	**0.0069**	**0.88**

The Cd root sample was determined to have 4 sulfur ligands at an interatomic distance of 2.51-2.52 Å. The Cd in the shoots of the corn plants was determined to have 4 sulfur ligands with an interatomic distance of 2.51 Å. These types of coordination in the first shell have been observed in Cd phytochelatin complexes [18]. In the phytochelatin-Cd system the Cd is complexed to 4 sulfur ligands in a cage type structure with sulfur ligands from four cysteine ligands coordinating the Cd^{++} ions and acting as bridges between Cd^{++} ions. However, due to the low signal to noise ratio observed in the data presented herein only the first shell were fitted. But from the Fourier transformed EXAFS shown in Fig. 4.5 one can see that there are interactions at longer interatomic distance at between 3.4 and 4.4 Å. These interactions at long interatomic distance could be indicating that there are Cd atoms at these distances, confirming the structure of Cd in the corn plant is in a cage structure. However, in the corn cotyledons the presence of

sulfur ligands was not observed, the binding was found to be through oxygen ligands only. The cotyledon samples were found to have approximately 4 oxygen ligands with an interatomic distanced of 2.22 Å. It is known that when sulfur ligands become saturated or less abundant than O ligands, as in the case of the corn cotyledons, Cd will bind through the O ligands from carboxylate groups to become a stable complex [42].

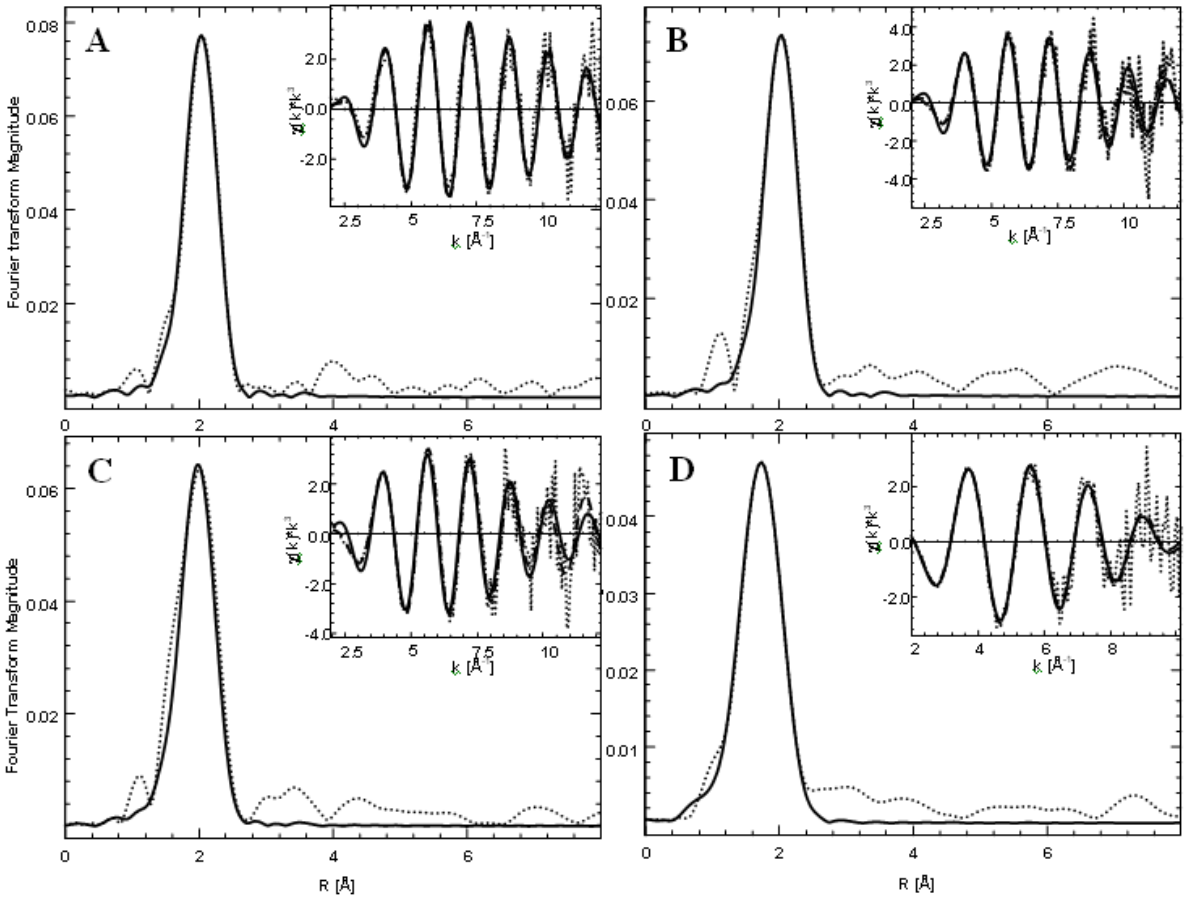

Figure 4.5. A) Fourier transformed EXAFS of cadmium sulfide model compound raw data (dotted line) and the Fourier transform of the fitting of the back transform (solid line). **B)** Fourier transformed EXAFS of cadmium corn roots sample raw data (dotted line) and the Fourier transform of the fitting of the back transform (solid line). **C)** Fourier transformed EXAFS of cadmium corn shoot sample raw data (dotted line) and the Fourier transform of the fitting of the back transform (solid line). **D)** Fourier transformed EXAFS of cadmium corn cotyledon sample raw data (dotted line) and the Fourier transform of the fitting of the back transform (solid line). (*Note: The insert in each of the figures shows the raw EXAFS, the back transform of the first coordination shell, and the fitting of the back transformed EXAFS.*)

4.4 Conclusions

This study investigated Cd uptake, translocation, and coordination state within the tissues of corn plants. Also the production of sulfur rich peptides such as cysteine, GSH and PCS upon exposure to Cd was determined. Corn root tissues accumulated the highest amount of Cd for all the treatments, which was followed by the shoots. The translocation factor (TF) increased with increasing concentration of Cd in the treatments. Mo uptake in the corn roots treated with 50μM $Cd(NO_3)_2$ significantly increased but was found at normal levels compared to the control for the rest of the treatments. It was also observed that the shoots of the corn plants exposed to Cd maintained a normal balance of Mo in comparison to the control plants. Results from this work indicate no disturbance in the Mn balance due to Cd exposure at the tested concentrations and demonstrate the capacity of corn plants to maintain, at least, normal uptake of P in all tissues. Sulfur uptake in the roots and shoots of corn plants exposed to Cd significantly increased upon Cd exposure. This is suggesting that corn plants may increase the assimilation of sulfur in the roots and translocation to the shoots to cope with Cd toxicity. The production of LMWT was induced mainly in the roots due to Cd exposure. A close link between Cd and S uptake, and the production of LMWT was confirmed by the results presented in this study. This was also confirmed by XAS analyses, which indicate that Cd inside the corn roots and shoots is bound to sulfur ligands with interatomic distances of 2.51-2.52 Å.

CHAPTER 5

DNA assessment of soybean roots exposed to ZnO and CeO_2 nanoparticles by RAPD

Abstract

The rapid development of nanotechnology has created an urge for the assessment of possible health and environmental hazards caused by metal NPs. Higher plants such as soybean can be used as bioindicators for toxicity of NPs. An essential area of study is genotoxicology, the study of genetic aberrations following exposure to NPs. In this work we studied the effect on DNA stability of ZnO and CeO_2 NPs in soybean plants using the RAPD assay. Soybean seeds were germinated in sterile petri dishes containing NPs suspension of 2000 and 4000 mg/L for 7d. The root tips of 9 plants were used for DNA isolation and PCR reactions. RAPD profiles from treated plants were compared to the control plants. Genetic similarity coefficients in untreated and treated plants were determined using the Nei's unbiased measure in POPGENE 1.6. Results showed that ZnO at 4000 mg/L and CeO_2 at 2000 and 4000 mg/L did affect the stability of the DNA with new bands appearing. Roots treated with ZnO NPs at 4000 mg/L presented a new band at 519bp. Roots treated with CeO_2 NPs at 2000 mg/L presented four new bands (1516, 581, 544, and 353bp), while three new bands appeared at 4000 mg/L (581, 411, and 353bp). RAPD has shown that the ZnO and CeO_2 NPs do affect the integrity of the DNA of soybean plants.

5.1 Introduction

Nanoparticles (NPs) are now being used for an expanding variety of applications including medicinal, electronics, and catalysis. The rapid development of nanotechnology has created an urge for the assessment of possible health and environmental hazards caused by metal NPs. Higher plants such as soybean can be used as bioindicators for toxicity of NPs. The wide range of NPs applications represent a challenge for researchers and government agencies, alike, who deal not only with scarce information about the fate and transport of NPs in the environment, but also with uncertainties about probable health hazards to living organisms [1, 2]. Of particular importance is the knowledge related to the plant response to NPs impacts, due mainly to their role of preserving environmental equilibrium as well as their importance as a food source.

An essential area of study is genotoxicology, the study of genetic aberrations following exposure to NPs. A few genotoxic studies have been performed on mammalian and human cell lines however there are hardly any reports in plant cells. Effects of genotoxins have been studied by using chromosome aberrations, micronucleus, or comet assays. An alternative new approach is the use of the random amplified polymorphic DNA (RAPD) assay. RAPD can potentially detect a wide range of DNA damage and mutations therefore it can be applied to NPs genotoxicity studies [3]. In this work we studied the genotoxic effects of ZnO and CeO_2 NPs in soybean (*Glycine max*) plants using the RAPD assay. Soybean is one of the major crops grown worldwide for human consumption. This plant is also an important precursor in the elaboration of several biomaterials and biodiesel [4]. Because of its high biomass production and easy

cultivation, soybean has been studied as a potential metal accumulator [5, 6]. Previous experiments performed at our lab have demonstrated the uptake, effect on germination and biomass production, and biotransformation of ZnO and CeO_2 in soybean plants. Briefly, accumulation of Zn peaked at 500 mg L^{-1} of ZnO NPs (229 mg Zn kg^{-1} DW) and Ce reached maximum accumulation at 4000 mg L^{-1} (462 mg Ce kg^{-1} DW). None of the ZnO and CeO_2 NPs treatments significantly affected the germination or the biomass production of soybean seedlings. X-ray absorption spectroscopy confirmed the presence of Ce and Zn in the tissues of soybean plants and showed the biotransformation of the primary Zn species (ZnO) into a coordination environment resembling zinc nitrate or zinc acetate. The speciation of Ce in the soybean plants was not altered. All our previous findings and the results from the present work have been reported in a peer reviewed journal [7].

5.2. Material and Methods

5.2.1 Preparation of ZnO and CeO_2 suspensions

Suspensions of ZnO and CeO_2 NPs were prepared at 0 (control), 500, 1000, 2000, and 4000 mg L^{-1} using Millipore water (MPW). To avoid aggregation, the NP suspensions were sonicated for 30 min after Lin and Xing [8], and the pH of each suspension was recorded.

5.2.2 Genomic DNA Isolation

For DNA isolation, seeds were treated with 2000 and 4000 mg L^{-1} of either ZnO or CeO_2 NPs. Control seeds were germinated with MPW. After 1 week, 9 root tips were treated with the Wizard™ Genomic DNA extraction kit (Promega A1120). DNA yield was determined using the Nanodrop spectrophotometer for quantification of double stranded DNA.

5.2.3 RAPD procedures

Polymerase chain reactions were performed in 25µL reaction mixtures containing 12.5µL of Green GoTaq® Green Master Mix. GoTaq® DNA Polymerase is supplied in 2X Green GoTaq® Reaction Buffer (pH 8.5), 400µM dATP, 400µM dGTP, 400µM dCTP, 400µM dTTP, and 3mM MgCl2 (Promega M7122). An aliquot of 2.5µL 10µM primer OPA03 (AGTCAGCCAC), and 20-50ng of genomic DNA were used for each PCR reaction from control and treated plants. Amplifications were performed in a Mycycler thermocycler system (BioRad, Hercules, CA) programmed for 5 min denaturation at 95˚C (initial denaturation); 40 consecutive cycles each consisted of 50s at 95˚C (denaturing), 50s at 45.8˚C (annealing), 1min at 72˚C (extension), followed by 1 cycle for 7 min at 72˚C. After amplification, RAPD reaction products were analyzed by electrophoresis on 1.6% agarose gels stained with ethidium bromide (1µg mL^{-1}) in 0.5X TBE (90mM Tris base, 90mM boric acid, and 2mM EDTA) buffer. The 100bp DNA ladder from Promega (G2101) was used as a molecular weight DNA standard. Gels were visualized and photographed under UV light on a Gel Doc XR system (BioRad, Hercules, CA, USA). The size of each amplification product was estimated using the Quantity One 4.6.8. band analysis feature.

5.2.4 RAPD profiles and data analysis

With the objective of investigating the genetic effect of ZnO and CeO_2 NPs on soybean seedlings, the RAPD analysis was performed using one random 10-mer. Reproducible amplification bands were scored for the construction of the data matrix. Only bands present in at least 70% of the 9 replicates were considered for the analysis. Changes in RAPD profiles were scored as present (1) and absent (0); changes in band intensities were not considered for the analysis. Genetic similarity coefficients among the roots of control and treated seedlings were estimated from Nei's unbiased measure [9] in POPGENE version 1.31. Cluster analysis was performed and a dendrogram was generated using the unweighted pair group method with the arithmetic means (UPGMA) algorithm of POPGENE 1.31.

5.3 Results and Discussion

Higher plants such as soybeans can be used as bioindicators for nanotoxicity. An essential area of study is genotoxicology, the study of genetic aberrations following exposure to NPs. A few genotoxic studies have been performed on mammalian and human cell lines; however, reports on plants are scarce [10]. Effects of genotoxins have been studied using chromosome aberrations, micronucleus, and comet assays [11]. An alternative new approach is the use of the RAPD assay. RAPD can potentially detect a wide range of DNA damage and mutations; it can therefore be applied to study NPs genotoxicity [3].

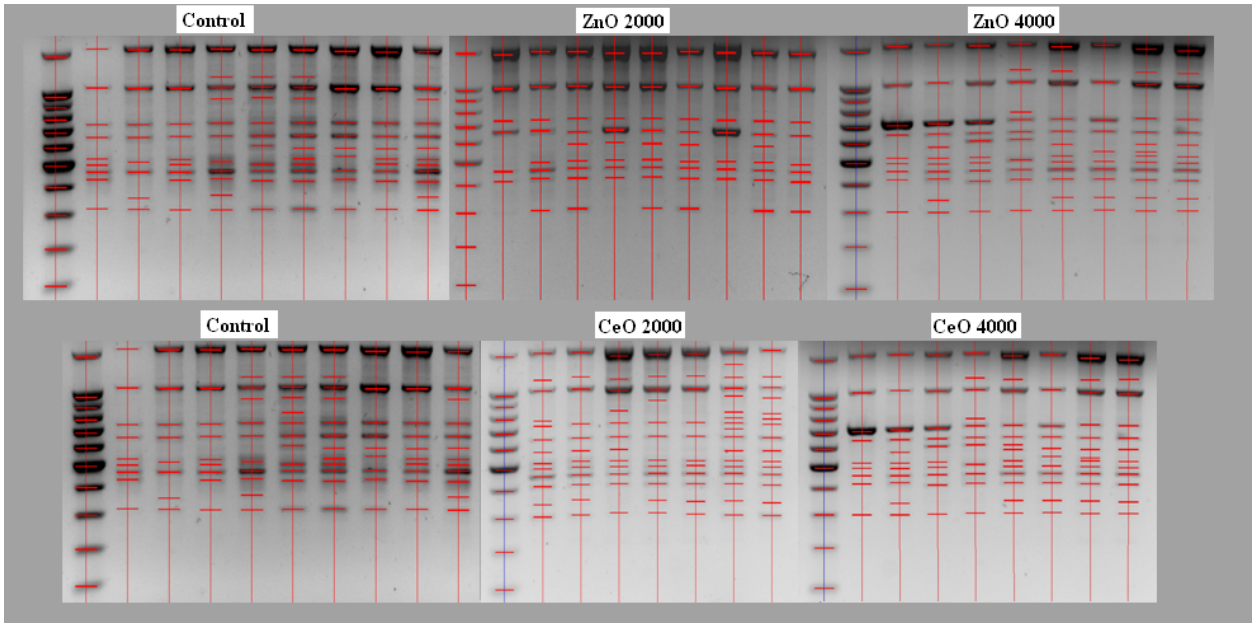

Figure 5.1 RAPD profiles in the roots of soybean seedlings treated with ZnO and CeO_2 nanoparticles at 0 (control), 2000 mg L^{-1}, and 4000 mg L^{-1}. RAPD profiles were generated using primer OPA03. First lane in all gels is 100 bp DNA Ladder (100–1500 bp).

In this study, the total number of representative bands identified in the control was 8 and ranged from 300 to 1600 bp. A total of 14 bands were detected (appearing and disappearing bands in all control and treated plants) using the band analysis feature of quantity one. Fig. 5.1 shows the RAPD profiles for all treatments and Table 5.1 shows the data matrix used for the genetic identity analysis. The RAPD profile from roots treated with ZnO at 2000 mg L^{-1} was similar to the one of control plants. However, at 4000 mg L^{-1}, a new band of 519 bp appeared in the profile. Unfortunately, there are no previous reports on the effects of ZnO NPs to plants. However, in other living systems such as Chinese hamster ovary (CHO) cells, Dufuor et al. [12] demonstrated the genotoxic effects of ZnO nanoparticles (100 nm diameter) using the chromosome aberration test. The lowest concentration that was tested (54 mg L^{-1}) produced a significant increase in DNA damage. Moreover, the authors demonstrated an enhancement of

ZnO NP genotoxicity by UV exposure. Zn is an important cellular nutrient and ZnO NPs are considered biocompatible; however, the results of the present study demonstrated that ZnO NPs could have an impact on the genetic material of terrestrial plants.

Table 5.1 Number and molecular size (base pair, bp) of bands detected in control, ZnO, and CeO_2 NP treated roots of soybean seedlings. (1) stands for present band (0) for absent bands for primer OPA03 (Gray box indicates appearing bands). Nei's genetic identity coefficient (NGI) was determined using the UPGMA method in Popgene 1.6.

	band size	control	ZnO 2000	ZnO 4000	CeO 2000	CeO 4000
1	1561	1	1	1	1	1
2	1216	0	0	0	1	0
3	1066	1	1	1	1	1
4	753	1	1	1	1	1
5	670	1	1	1	1	1
6	581	0	0	0	1	1
7	544	0	0	0	1	0
8	519	0	0	1	0	0
9	505	1	1	1	1	1
10	468	1	1	1	1	1
11	439	1	1	1	1	1
12	411	0	0	0	0	1
13	353	0	0	0	1	1
14	309	1	1	1	1	1
	NGI	1.00	1.00	0.93	0.71	0.79

The RAPD profile of soybean plants treated with 4000 mg ZnO NPs L^{-1} showed a new band. The presence of new bands may reveal a change in the priming sites leading to new annealing events. Also, large deletions and homologous recombination could lead to the appearance of new bands [3]. Zn ions released from NPs can convert cellular oxygen metabolic products such as H_2O_2 and superoxide anions into hydroxyl radicals, a primary DNA damaging species [10]. Through this mechanism, ZnO NPs could be affecting the genetic stability of soybean plants. Therefore, it is important to investigate the amount of Zn that could be leaching out of the NPs in order to confirm if the observed genotoxicity was due to the released Zn ions, or rather, was a direct interaction of the NPs with the DNA.

The exposure of soybean plants to CeO_2 NPs produced four new bands at 2000 mg L^{-1} and three at 4000 mg L^{-1} treatments. This result demonstrated the genotoxicity of CeO_2 NPs on soybean plants. Previous reports from toxicological studies of CeO_2 NPs in animal cells are controversial. Schubert et al. [13] demonstrated a ROS protective effect in HT22 cells derived from rodent nervous systems. The antioxidant effect of CeO_2 NPs was independent of the size (6nm, 12nm, and 1μm) but dependant of the concentration (from 0.0002 to 20 mg L^{-1}). On the other hand, Park et al. [14] reported induced oxidative stress by CeO_2 NPs in cultured human lung epithelial cells (BEAS-2B). It is well known that increasing oxidative stress leads to DNA damage that affects RAPD profiles. This could cause the appearance of the new bands in soybean plants. Park et al. [14] also found an increase in chromatin condensation in human lung cells treated with 30nm CeO_2 NPs. The dual oxidation state (III and IV) of CeO_2 NPs is responsible for the interesting redox chemistry exhibited by these NPs [15]. However, the ratio of (III) to (IV) ions in the NP surface depends on the size and preparation method of the NPs. Oxidative stress induced on BEAS-2B cells and the effect observed in soybean roots exposed to CeO_2 NPs may be due to the lack of enough Ce^{+3} ionic state to scavenge oxygen radicals leading to oxidative DNA damage.

Fig. 5.2 shows a dendrogram constructed based on UPGMA analysis of RAPD data. In the present study, the estimated genetic identity coefficient (NGI from Table 1) for 2000 mg ZnO L^{-1}, 2000 mg CeO L^{-1}, and 4000 mg CeO L^{-1} were found to be lower compared to the controls (Nei genetic identity (NGI) value is 1.00 for control treatments). Cluster analysis revealed two main groups: one composed of control and ZnO treated plants, and the other formed by CeO_2 treated plants. RAPD has shown that both ZnO and CeO_2 NPs do affect the integrity of the DNA, but CeO_2 NPs caused the highest effect on the genetic stability of soybean plants.

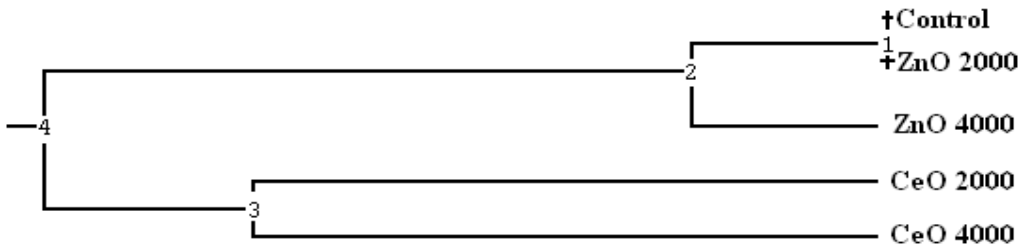

Figure 5.2 Dendrogram using the UPGMA based on DNA polymorphism among the roots of soybean seedlings exposed to untreated control, 2000 and 4000 mg L^{-1} treatments of ZnO and CeO_2 nanoparticles.

5.4 Conclusions

This work demonstrated the practicality of using the RAPD assay to screen DNA integrity in plants exposed to NPs. This technique uses genomic DNA as template and a random primer in a normal PCR reactions, these factors make it relatively easy and quick, after careful optimization, compared to other PCR-based techniques. It is also a perfect candidate for screening of organisms where there is no previous genetic information available. It has advantages over other techniques that can provide similar information, such as the comet assay, since one can decide to get the bands of interest sequenced and that could lead to more sophisticated studies in genetic expression. The results from this study demonstrated the effect of ZnO and CeO_2 NPs on the DNA stability of roots from soybean plants. The results here obtained come from the use of 4 random primers with only one primer providing consistent data for analysis, this work should be complimented with the study of more primer band patterns to be able to screen more areas of the genomic DNA for instabilities.

Chapter 6

General conclusions

The results from the present study have depicted the differential response to As of *P. florida* grown in soils with different physico-chemical properties and the accumulation of As in roots of mesquite plants. The desert plant species *P. florida* has demonstrated the ability to accumulate As in the root tissues from As contaminated soil. Furthermore, the results have shown that *P. florida* and mesquite plants coordinate As to S from thiol functional groups. These results suggest these plant species are possible candidates for phytostabilization of As in arid regions. Phytostabilization is a long-term remediation process where the contaminant is accumulated in root plant tissue and in the soil around the roots reducing its bioavailability and mobility.

Mesquite plants accumulated As mainly in the root tissues with very low concentrations found in the shoots (< 6 mg kg^{-1} dry biomass). Bulk XANES studies demonstrated the oxidation of As(III) to As(V) in the soil. The predominant form of As was consistent with As(V) sorbed in 2-L ferrihydrite followed by a crystalline Fe arsenate consistent with pharmacosiderite. LC-XANES from the bulk and μXAS studies were consistent in finding As(V) as the predominant oxidation state of As. This work demonstrated the importance of combining bulk and μXAS techniques in the analysis of As speciation in soil and plant samples. . The analysis of soil thin sections is an excellent approach for the study of the rhizosphere. However, the embedding methodology using LR white resin should be reassessed to find a method that does not affect the oxidation state of As(V) in the sample

Corn root tissues accumulated the highest amount of Cd for all the treatments, which was followed by the shoots. The translocation factor (TF) increased with increasing concentration of Cd in the treatments. Mo uptake in the corn roots treated with 50μM $Cd(NO_3)_2$ significantly increased but was found at normal levels compared to the control for the rest of the treatments. Results from this work indicate no disturbance in the Mo and Mn balance due to Cd exposure at the tested concentrations and demonstrate the capacity of corn plants to maintain, at least, normal uptake of P in all tissues. Sulfur uptake in the roots and shoots of corn plants exposed to Cd significantly increased upon Cd exposure. This suggests that corn plants may increase the assimilation of sulfur in the roots and translocation to the shoots and induce the production of LMWT due to Cd exposure. A close link between Cd and S uptake, and the production of LMWT was confirmed by the results presented in this study. This was also confirmed by XAS analyses, which indicate that Cd inside the corn roots and shoots is bound to sulfur ligands with interatomic distances of 2.51-2.52 Å.

Using the RAPD assay, the DNA integrity of soybean plants exposed to NPs was studied. The results from this study demonstrated the effect of ZnO and CeO_2 NPs on the DNA stability of roots from soybean plants. RAPD is a relatively easy and quick assay suitable for screening organisms where there is no previous genetic information available. It has advantages over other techniques that can provide similar information, such as the comet assay, since one can decide to get the bands of interest sequenced and that could lead to more sophisticated studies in genetic expression. The results obtained herein came from the use of 4 random primers with only one primer providing consistent data for analysis, this work should be complimented with the study of more primer band patterns to be able to screen more areas of the genomic DNA for instabilities.

References

Chapter 1

[1] Bunker, G., 2010. Introduction to XAFS. Cambridge University Press, New York, NY.

[2] Lombi, E., Susini, J., 2009. Synchrotron-based techniques for plant and soil science: opportunities, challenges and future perspectives. Plant Soil 320, 1-35. doi:10.1007/s11104-008-9876-x.

[3] Gardea-Torresdey, J., Peralta-Videa, J., de la Rosa, G., Parsons J.G., 2005. Phytoremediation of heavy metals and study of the metal coordination by X-ray absorption spectroscopy. Coord. Chem. Rev. 249, 1797-1810.

[4] Wójcik, M., Vangronsveld, J., D'Haen, J., Tukiendorf, A., 2005. Cadmium tolerance in Thlaspi caerulescens: II. Localization of cadmium in Thlaspi caerulescens. Environ. Exp. Bot. 53, 163-171.

[5] Ma, L.Q., Komar, K. M., Tu, C., Zhang, W.,Cai, Y., Kennelley, E. D., 2001. A fern that hyperaccumulates arsenic. Nature 409, 579.

[6] Isaure, M., Fayard, B., Sarret, G., Pairis, S., Bourguignon, J., 2006. Localization and chemical forms of cadmium in plant samples by combining analytical electron microscopy and X-ray spectromicroscopy. Spectrochimica Acta Part B: Atomic Spectroscopy 61, 1242-1252.

[7] Isaure, M., Sarret, G., Harada, E., Choi, Y., Marcus, M.A., Fakra, S.C., Geoffroy, N., Pairis, S., Susini, J., Clemens, S., Manceau, A., 2010. Calcium promotes cadmium elimination as vaterite grains by tobacco trichomes, Geochim. Cosmochim. Acta 74 (2010) 5817-5834.

[8] Pickering, I.J., Gumaelius, L., Harris, H.H., Prince, R.C., Hirsch, G., Banks, J.A., Salt, D.E., George, G.N., 2006. Localizing the Biochemical Transformations of Arsenate in a Hyperaccumulating Fern. Environ. Sci. Technol. 40, 5010-5014. doi:10.1021/es052559a.

[9] Marcus M.A., 2010. X-ray photon-in/photon-out methods for chemical imaging. TrAC Trends in Analytical Chemistry 29, 508-517.

[10] Meharg, A.A., Lombi, E., Williams, P.N., Scheckel, K.G., Feldmann, J., Raab, A., Zhu, Y., Islam, R., 2008. Speciation and Localization of Arsenic in White and Brown Rice Grains, Environ. Sci. Technol. 42, 1051-1057. doi:10.1021/es702212p.

[11] Lombi, E., Scheckel, K.G., Pallon, J., Carey, A.M., Zhu, Y.G., Meharg, A.A., 2009. Speciation and distribution of arsenic and localization of nutrients in rice grains. New Phytol. 184, 193-201. doi:10.1111/j.1469-8137.2009.02912.x.

[12] Smith, E., Kempson, I., Juhasz, A.L., Weber, J., Skinner, W.M., Gräfe, M., 2009. Localization and speciation of arsenic and trace elements in rice tissues. Chemosphere 76, 529-535.

[13] Seyfferth, A.L., Webb, S.M., Andrews, J.C., Fendorf, S., 2010. Arsenic Localization, Speciation, and Co-Occurrence with Iron on Rice (Oryza sativa L.) Roots Having Variable Fe Coatings. Environ. Sci. Technol. (In press). doi:10.1021/es101139z.

[14] Frommer, J., Voegelin, A., Dittmar, J., Marcus, M.A., Kretzschmar, R., 2010. Biogeochemical processes and arsenic enrichment around rice roots in paddy soil: results from micro-focused X-ray spectroscopy. Eur. J. Soil Sci. (In press). doi:10.1111/j.1365-2389.2010.01328.x.

[15] Hernandez-Viezcas J., Castillo-Michel H., Servin A.D., Peralta-Videa J., Gardea-Torresdey J., Spectroscopic verification of zinc absorption and distribution in the desert plant Prosopis juliflora-velutina (velvet mesquite) grown with ZnO nanoparticles, Chem. Eng. J. In Press, Accepted Manuscript.

Chapter 2

[1] Nriagu, J.O., 2002. Environmental Chemistry of Arsenic. W. T. Frankenberger Jr. Ed., New York, NY.

[2] Oremland, R.S., Stolz, J.F., 2003. The Ecology of Arsenic. Science 300, 939-944.

[3] National Research Council, 1999. Arsenic in Drinking Water. National Academy Press, Washington, DC.

[4] Environmental Protection Agency, 2006. Superfund Region 6: El Paso/ Dona Ana County Metals. http://www.epa.gov/region6/6sf/texas/el_paso/tx_el_paso_index.html. (accessed 01-6-2011)

[5] Bednar, A.J., Garbarino, J.R.; Ranville, J.F.; Wildeman, T.R., 2005. Effects of iron on arsenic speciation and redox chemistry in acid mine water. J. Geochem. Explor. 85, 55-62.

[6] Barcelo, J., Poschenrieder, C., 2003. Phytoremediation: Principles and perspectives. Contrib. Sci. 2, 81-126.

[7] Gardea-Torresdey, J. L., 2003. Phytoremediation where does it stand and where will it go? Environ. Prog. 23, A2–A4.

[8] Meharg, A.A., Hartley-Whitaker, J., 2002. Arsenic uptake and metabolism in arsenic resistant and nonresistant plant species. New Phytol. 154, 29-43.

[9] Rathinasabapathi, B., Ma, L.Q., Srivastava, M., 2006. Arsenic hyperaccumulating ferns and their application to phytoremediation of arsenic contaminated sites. Floriculture, Ornamental Plant Biotechnology; Global Science Books.

[10] Tu, S., Ma, L.Q., Fayiga, A.O., Zillioux, E.J., 2004. Phytoremediation of arsenic contaminated groundwater by the arsenic hyperaccumulating fern *Pteris vittata* L. Int. J. Phytorem. 6, 35-47.

[11] Castillo-Michel, H., Dokken, K., Peralta-Videa, J.R., Gardea-Torresdey, J.L., 2009. Localization and chemical forms of arsenic in three species of the *Parkinsonia* plant genus using X-ray spectromicroscopy. Proceedings of the 10th ICOBTE Conference, Chihuahua, Mexico, July 13-16.

[12] Wang S., Mulligan, C., 2006. Natural Attenuation processes for remediation of arsenic contaminated soils and groundwater. J. Hazard. Mater. B138, 459-470.

[13] Cances, B., Juillot, F., Morin, G., Laperche, V., Alvarez, L., Proux, O., Hazemann, J-L., Brown, G.E., Calas, G., 2005. XAS evidence of As(V) association with Iron oxyhydroxides in a contaminated soil at a former arsenical pesticide processing plant. Environ. Sci. Technol. 39, 9398-9405.

[14] Pickering, I.J., Gumaelius, L., Harris, H.H., Prince, R.C., Hirsch, G., Banks, J.A., Salt, D.E., George, G.N., 2006. Localizing the Biochemical Transformations of Arsenate in a Hyperaccumulating Fern. Environ. Sci. Technol. 40, 5010-5014.

[15] Seyfferth, A.L., Webb, S.M., Andrews, J.C., Fendorf, S., 2010. Arsenic Localization, Speciation, and Co-Occurrence with Iron on Rice (Oryza sativa L.) Roots Having Variable Fe Coatings. Environ. Sci. Technol. 44, 8108-8113.

[16] Smith, E., Kempson, I., Juhasz, A.L., Weber, J., Skinner, W.M., Gräfe, M, 2009. Localization and speciation of arsenic and trace elements in rice tissues. Chemosphere 76, 529-535.

[17] Bouyoucos, C. J., 1934. The hydrometer method for making mechanical analysis of soils. Soil Sci. 38,335–343.

[18] Kingston, H.M., Jassie, L.B., 1988. *ACS Professional Reference Book Series*, American Chemical Society, Washington, DC.

[19] Lopez-Moreno, M.L., Peralta-Videa, J., Parsons, J.G., Duarte-Gardea, M., Gardea-Torresdey, J., 2008. Concentration and biotransformation of arsenic by *Prosopis* sp. grown in soil treated with chelating agents and phytohormones. Environ. Chem. 5, 320-331.

[20] Marcus, M.A., MacDowell, A.A., Celestre, R., Manceau, A., Miller, T., Padmore, H.A., Sublett, R.E. Beamline 10.3.2 at ALS: a hard X-ray microprobe for environmental and materials sciences. J. Synchrotron Rad. 11, 239-247.

[21] Parikh, S.J., Lafferty, B.J., Meade, T.G., Sparks, D.L., 2010. Evaluating Environmental Influences on AsIII Oxidation Kinetics by a Poorly Crystalline Mn-Oxide. Environ. Sci. Technol. 44, 3772-3778.

[22] Manning, B.A., Fendorf, S.E., Goldberg, S., 1998. Surface structures and stability of arsenic(III) on goethite: Spectroscopic evidence for inner-sphere complexes. Environ. Sci. Technol. 32, 2383-2388.

[23] Han, F.X., Kingery, W.L., Selim, H.M., Gerard, P.D., Cox, M.S., Oldham, J.L., 2004. Arsenic solubility and distribution in poultry waste and long-term amended soil. Sci. Total Environ. 320, 51-61.

[24] Roberts, L.C., Hug, S.J., Dittmar, J., Voegelin, A., Kretzschmar, R., Wehrli, B., Cirpka, O.A., Saha, G.C., Ashraf, A.M., Badruzzaman, A.B., 2010. Arsenic release from paddy soils during monsoon flooding. Nature Geosci. 3, 53-59.

[25] Cances, B., Juillot, F., Morin, G., Laperche, V., Alvarez, L., Proux, O., Hazemann, J., Brown, G.E., Calas, G., 2005. XAS Evidence of As(V) association with iron oxyhydroxides in a contaminated soil at a former arsenical pesticide processing plant. Environ. Sci. Technol. 39, 9398-9405.

[26] Gräfe, M., Tappero, R.V., Marcus, M.A., Sparks, D.L., 2008. Arsenic speciation in multiple metal environments: I. Bulk-XAFS spectroscopy of model and mixed compounds. J. Colloid Interface Sci. 320, 383-399.

[27] Melo, E.E.C., Costa, E.T.S., Guilherme, L.R.G., Faquin, V., Nascimento, C.W.A., 2009. Accumulation of arsenic and nutrients by castor bean plants grown on an As-enriched nutrient solution. J. Hazard. Mater. 168, 479-483.

[28] Meharg, A. A., Macnair, M. R., 1992. Suppression of the high-affinity phosphate-uptake system- a mechanism of arsenate tolerance in *Holcus lanatus* L. J. Exp. Bot. 43, 519–524.

[29] Ullrich-Eberius, C. I., Sanz, A., Novacky, A. J., 1989. Evaluation of arsenate-associated and vanadate-associated changes of electrical membrane potential and phosphate transport in *Lemna gibba* G1. J. Exp. Bot. 40, 119–128.

[30] Ma, J. F., Yamaji, N., Mitani, N., Xu, X.-Y., Su, Y.-H., McGrath, S. P., Zhao, F.-J., 2008. Transporters of arsenite in rice and their role in arsenic accumulation in rice grain. Proc. Natl. Acad. Sci. 105, 9931–9935.

[31] Ali, W., Isayenkov, S., Zhao, F., Maathuis, F, 2009. Arsenite transport in plants. Cell. Mol. Life Sci. 66, 2329-2339.

[32] Raven, J.A., 2003. Cycling silicon – the role of accumulation in plants. New Phytol. 158, 419–430.

[33] Mokgalaka-Matlala, N., Flores-Tavizón, E., Castillo-Michel, H., Peralta-Videa, J., Gardea-Torresdey, J., 2009. Arsenic tolerance in mesquite (*Prosopis sp*.): Low molecular weight thiols synthesis and glutathione activity in response to arsenic. Plant Physiol. Biochem. 47, 822-826.

[34] Srivastava, S., D'Souza, S.F., 2010. Effect of variable sulfur supply on arsenic tolerance and antioxidant responses in *Hydrilla verticillata* (L.f.) Royle. Ecotoxicol. Environ. Saf. 73, 1314-1322.

[35] Zhang, J., Zhao, Q., Duan, G., Huang, Y., 2010. Influence of sulphur on arsenic accumulation and metabolism in rice seedlings. Environ. Exp. Bot., doi:10.1016/j.envexpbot.2010.05.007.

[36] Mendez, M.O., Maier, R.M., 2007. Phytostabilization of mine tailings in arid and semiarid environments—an emerging remediation technology. Environ. Health Perspect. 116, 278-283.

[37] Castillo-Michel, H., Zuverza-Mena, N., Parsons, J.G., Dokken, K.M., Duarte-Gardea, M., Peralta-Videa, J., Gardea-Torresdey, J., 2009. Accumulation, speciation, and coordination of arsenic in an inbred line and a wild type cultivar of the desert plant species *Chilopsis linearis* (Desert willow). Phytochemistry 70, 540-545.

[38] Rey, N.A., Howarth, O.W., Pereira-Maia, E., 2004. Equilibrium characterization of the As(III)-cysteine and the As(III)-glutathione systems in aqueous solution. J. Inorg. Biochem. 98, 1151-1159.

Chapter 3

[1] Cances, B., Juillot, F., Morin, G., Laperche, V., Alvarez, L., Proux, O., Hazemann, J-L., Brown, G.E., Calas, G., 2005. XAS evidence of As(V) association with Iron oxyhydroxides in a contaminated soil at a former arsenical pesticide processing plant. Environ. Sci. Technol. 39, 9398-9405.

[2] Kidd, P., Barcelo, J., Bernal, M.P., Navari-Izzo, F., Poschenrieder, C., Shilev, S., Clemente, R., Monterroso, C., 2009. Trace Element behaviour at the root-soil interface: Implications in phytoremediation. Environ. Exp. Bot. 67, 243-259.

[3] Voegelin, A., Weber, F., Kretzchmar, R., 2007. Distribution and speciation of arsenic around roots in a contaminated riparian floodplain soil: Micro-XRF element mapping and EXAFS Spectroscopy. Geochem. Cosmochim. Acta 71(23), 5804-5820.

[4] Aldrich, M.V., Peralta-Videa, J.R., Parsons, J.G., Gardea-Torresdey, J.L., 2007. Examination of Arsenic(III) and (V) uptake by the desert plant species Mesquite (*Prosopis spp.*) using X-Ray Absorption Spectroscopy. Sci. Total Environ. 379(2-3), 249-255.

[5] Mokgalaka-Matlala, N.S., Flores-Tavizon, E., Castillo-Michel, H., Peralta-Videa, J.R., Gardea-Torresdey, J.L., 2008. Toxicity of arsenic(III) and (V) on plant growth, element uptake, and total amylolytic activity of mesquite (Prosopis spp.) Inter. J. Phytorem 10 (1), 47-60.

[6] Lopez-Moreno, M.L., Peralta-Videa, J., Parsons, J.G., Duarte-Gardea, M., Gardea-Torresdey, J., 2008. Concentration and biotransformation of arsenic by *Prosopis* sp. grown in soil treated with chelating agents and phytohormones. Environ. Chem. 5, 320–331..

[7] Mokgalaka-Matlala, N.S., Flores-Tavizón, E., Castillo-Michel, H. Peralta-Videa, J.R., Gardea-Torresdey, J.L., 2009. Arsenic tolerance in mesquite (*Prosopis* sp.): Low molecular weight thiols synthesis and glutathione activity in response to arsenic. Plant Physiol. Biochem. 47, 822-826

[8] Cai, Y., Su, J., Ma, L.Q., 2004. Low molecular weight thiols in arsenic hyperaccumulator *Pteris vittata* upon exposure to arsenic and other trace elements. Environ. Pollut. 129, 69-78.

[9] De la Rosa, G., Martinez-Martinez, A., Pelayo, H., Peralta-Videa, J.R., Sanchez-Salcido, B., Gardea-Torresdey, .JL., 2005. Production of low-molecular weight thiols as a response to cadmium uptake by tumbleweed (*Salsola kali*). Plant Physiol. Biochem. 43, 491-498.

[10] Zhang, W., Cai, Y., Downum, K.R., Ma, L.Q., 2004. Thiol synthesis and arsenic hyperaccumulation in *Pteris vittata* (Chinese brake fern). Environ. Pollut. 131, 337-345.

[11] Pickering, I.J., Gumaelius, L., Harris, H.H., Prince, R.C., Hirsch, G., Banks, J.A., Salt, D.E., George, G.N., 2006. Localizing the biochemical transformations of arsenate in a hypeaccumulating fern. Environ. Sci. Technol. 40, 5010-5014.

[12] Beesley, L., Moreno-Jimenez, E., Clemente, R., Lepp, N., Dickinson, N., 2010. Mobility of arsenic, cadmium and zinc in a multi-element contaminated soil profile assessed by *in-situ* soil pore water sampling, column leaching and sequential extraction. Environ. Pollut. 158(1), 155-160.

[13] Strawn, H., Doner, M., Zavarin, S., McHugo., 2002. Microscale investigation into the geochemistry or arsenic, selenium, and iron in soil developed in pyretic shale materials. Geoderma 108, 237-257.

[14] Marcus, M.A., MacDowell, A.A., Celestre, R., Manceau, A., Miller, T., Padmore, H.A., Sublett, R.E., 2004. Beamline 10.3.2 at ALS: a hard X-ray microprobe for environmental and materials sciences. J. Synchrotron Rad. 11, 239-247.

[15] Cances, B., Juillot, F., Morin, G., Laperche V., Alvarez, L., Proux, O., Hazemann, J., Brown, G.E., Calas, G., 2005. XAS Evidence of As(V) Association with Iron Oxyhydroxides in

a Contaminated Soil at a Former Arsenical Pesticide Processing Plant. Environ. Sci. Technol. 39, 9398-9405.

[16] Schmöger, M.E.V., Oven, M., Grill, E., 2000. Detoxification of arsenic by phytochelatins in plants. Plant Physiol. 122, 793–801.

[17] Schat, H., Llugany, M., Vooijs, R., Hartley-Whitaker, J., Bleeker, P.M., 2002. The role of phytochelatins in constitutive and adaptive heavy metal tolerances in hyperaccumulator and non-hyperaccumulator metallophytes. J. Exp. Bot. 53, 2381–2392.

[18] Gräfe M., Tappero R.V., Marcus M.A., Sparks D.L., 2008. Arsenic speciation in multiple metal environments: I. Bulk-XAFS spectroscopy of model and mixed compounds. J. Colloid Interface Sci. 320, 383-399.

[19] Amstaetter K., Borch T., Larese-Casanova P., Kappler A., 2010. Redox Transformation of Arsenic by Fe(II)-Activated Goethite (α-FeOOH). Environ. Sci. Technol. 44, 102-108. doi:10.1021/es901274s.

[20] Drahota P., Filippi M., 2009. Secondary arsenic minerals in the environment: A review. Environ. Int. 35, 1243-1255.

[21] Ramadan D., Rancy P.C., Nagarkar R.P., Schneider J.P., Thorpe C., 2009. Arsenic(III) Species Inhibit Oxidative Protein Folding in Vitro. Biochem. 48, 424-432. doi:10.1021/bi801988x.

Chapter 4

[1] Wagner, G.J., 1993. Accumulation of cadmium in crop plants and its consequences to human health. Adv. Agron. 51, 173–212.

[2] Gardea-Torresdey, J. L., Peralta-Videa, J. R., Montes, M., De la Rosa, G., Corral-Diaz, B., 2004. Bioaccumulation of cadmium, chromium and copper by Convolvulus arvensis L.: impact on plant growth and uptake of nutritional elements. Bioresource Technol. 92, 229-235

[3] Sharma, S.S., Kaul, S., Metwally, A., Goyal, K.C., Finkemeier, I., Dietz K.J., 2004. Cadmium toxicity to barley (Hordeum vulgare) as affected by varying Fe nutritional status. Plant Sci. 166, 1287-1295

[4] De la Rosa G., Martinez-Martinez A., Pelayo H., Peralta-Videa J.R., Sanchez-Salcido B., Gardea-Torresdey J.L., 2005. Production of low-molecular weight tilos as a response to cadmium uptake by tumbleweed (*Salsola kali*). P. Physiol. Biochem. 43, 491-498.

[5] Wójcik, M., Vangronsveld, J., Tukiendorf, A., 2005. Cadmium tolerance in Thlaspi caerulescens: I. Growth parameters, metal accumulation and phytochelatin synthesis in response to cadmium. Environ. Exp. Bot. 53, 151-161

[6] Liu, H.J., Zhang, J.L., Zhang F.S. 2007. Role of iron plaque in Cd uptake by and translocation within rice (Oryza sativa L.) seedlings grown in solution culture. Environ. Exp. Bot. 59, 314-320.

[7] Liu, J., Qian, M., Cai, G., Yang, J., Zhu, Q., 2007. Uptake and translocation of Cd in different rice cultivars and the relation with Cd accumulation in rice grain. J. Hazard. Mat. 143, 443-447.

[8] Liu, Y., Wang, X., Zeng, G., Qu, D., Gu, J., Zhou, M., Chai, L., 2007. Cadmium-induced oxidative stress and response of the ascorbate–glutathione cycle in *Bechmeria nivea* (L.) Gaud. Chemosphere 69, 99-107.

[9] Murakami, M., Ae, N., Ishikawa, S., 2007. Phytoextraction of cadmium by rice (*Oryza sativa* L.), soybean (*Glycine max* (L.) Merr.), and maize (*Zea mays* L.). Environ. Pollut. 145, 96-103.

[10] Van Engelen, D.L., Sharpe-Pedler, R.C., Moorhead, K.K., 2007. Effect of chelating agents and solubility of cadmium complexes on uptake from soil by *Brassica juncea*. Chemosphere 68, 401-408.

[11] McGrath, S.P., Lombi, E., Zhao, F.J., 2001. What's New about Cadmium Hyperaccumulation? New Phytol. 149, 2-3.

[12] Brown, S.L., Chaney, R.L., Angle, J.S., Baker, A.J.M., 1994. Phytoremediation potential of Thlaspi caerulescens and bladder campion for zinc and cadmium-contaminated soil. J. Environ. Qual. 23, 1151–1157.

[13] De la Rosa, G., Peralta-Videa, J.R., Montes, M., Parsons, J.G., Cano-Aguilera, I., Gardea-Torresdey, J.L., 2004. Cadmium uptake and translocation in tumbleweed (Salsola kali), a potential Cd-hyperaccumulator desert plant species: ICP/OES and XAS studies. Chemosphere 55, 1159-1168

[14] Youn-Joo, A., 2004. Soil ecotoxicity assessment using cadmium sensitive plants. Environ. Pollut. 127, 21-26.

[15] Clemens, S., Palmgren, M.G., Krämer, P., 2002. A long way ahead: understanding and engineering plant metal accumulation, Trends Plant Sci. 7, 309–315.

[16] Lee, S., Korban, S.S., 2002. Transcriptional regulation of *Arabidopsis thaliana* phytochelatin synthase (AtPCS1) by cadmium during early stages of plant development. Planta 215, 689–693.

[17] Salt, D.E., Prince, R.C., Pickering, J., Raskin, I., 1995. Mechanisms of cadmium mobility and accumulation in Indian mustard. Plant Physiol. 109, 1427–1433.

[18] Pickering, I.J., Prince, R.C., George, G.N., Rauser, W.E., Wickramasinghe, W.A., Watson, A.A., Dameron, C.T., Dance, I.G., Fairlie, D.P., Salt, D.E., 1999. X-ray absorption spectroscopy of cadmium phytochelatin and model systems. Biochim. Biophys. Acta 1429, 351-364.

[19] Potesil, D., Petrlova, J., Adam, V., Vacek, J., Klejdus, B., Zehnalek, J., Trnkova, L., Havel, L., Kizek, R., 2005. Simultaneous femtomole determination of cysteine, reduced and oxidized glutathione, and phytochelatin in maize (Zea mays L.) kernels using high-performance liquid chromatography with electrochemical detection. J. Chromatogr. A 1084, 134-144

[20] Varga, A., Zaray, G., Fodor, F., 2002. Determination of element distribution between the symplasm and apoplasm of cucumber plant parts by total reflection X-ray fluorescence spectrometry. J. Inorg. Biochem. 89, 149–154.

[21] Dupont, L., Bouanda, J., Dumonceau, J., Aplincourt, M., 2003. Metal ions binding onto a lignocellulosic substrate extracted from wheat bran: a NICA-Donnan approach. J. Colloid Interf. Sci. 263, 35–41

[22] Gardea-Torresdey, J.L., Peralta-Videa, J.R., De la Rosa, G., Parsons, J.G., 2005. Phytoremediation of heavy metals and study of the metal coordination by X-ray absorption spectroscopy. Coord. Chem. Rev. 249, 1797-1810.

[23] Kingston, H.M., Jassie, L.B., 1988. ACS Professional Reference Book Series, American Chemical Society, Washington, DC.

[24] Ressler, T., 1998. WinXAS: a program for X-ray absorption spectroscopy data analysis under MS-Windows. J. Synchrotron Radiat. 5, 118–122.

[25] Ankudinov, A.L., Ravel, B.J., Rehr, J.J., Conradson, S.D.,1998. Real Space Multiple-scattering Calculation and Interpretation of X-ray Absorption Near-Edge Structure. Phys. Rev. B, 7565.

[26] Ravel B., 2001. ATOMS: crystallography for the X-ray absorption spectroscopist. J. Synchrotron Radiat. 8, 314-316.

[27] Wang, M., Zou, J., Duan, X., Jiang, W., Liu, D., 2007. Cadmium accumulation and its effects on metal uptake in maize (Zea mays L.). Bioresource Technol. 98, 82-88.

[28] Sreenivasulu, N., Sopory, S.K., Kavi Kishor, P.B., 2007. Deciphering the regulatory mechanisms of abiotic stress tolerance in plants by genomic approaches. Gene 388, 1-13.

[29] Gouia, H., Ghorbal, M.H., Meyer, C., 2000. Effects of cadmium on activity of nitrate reductase and on other enzymes of the nitrate assimilation pathway in bean. P. Physiol. Biochem. 38, 629-638.

[30] Mengel, K., Kirkby, E.A., 2001. Principles of plant nutrition. Kluwer Academic Publishers, Massachussets.

[31] Wu, F., Dong, J., Cai, Y., Chen, F., Zang, G., 2007. Differences in Mn uptake and subcellular distribution in different barley genotypes as a response to Cd toxicity. Sci. Total Environ. 385, 228-234.

[32] Peng, K., Luo, C., You, W., Lian, C., Li, X., Shen, Z., 2007. Manganese uptake and interactions with cadmium in the hyperaccumulator – *Phytolacca Americana.* J Hazard. Mat. doi:10.1016/j.jhazmat.2007.10.080

[33] Jiang, H.M., Yang, J.C., Zhang, J.F., 2007. Effects of external phosphorus on the cell ultrastructure and the chlorophyll content of maize under cadmium and zinc stress. Environ. Pollut. 147, 750-756.

[34] Hettiarachchi, G.M., Pierzynski, G.M., 1999. Effect of phosphorus and other soil amendments on soil lead, cadmium and zinc bioavailability. Proc. Extended Abstr., fifth Int. Conf. on the Biogeochem. Trace Elements (ICOBTE), Vienna, Austria, 11-15 July, 1999. Int. Soc. for Trace Element Res., Vienna, Austria, pp. 514-515.

[35] Połeć-Pawlak, K., Ruzik, R., Lipiec, E., 2007. Investigation of Cd(II), Pb(II) and Cu(I) complexation by glutathione and its component amino acids by ESI-MS and size exclusion chromatography coupled to ICP-MS and ESI-MS. Talanta 72, 1564-1572.

[36] Seth, C.S., Chaturvedi, P.K., Misra, V., 2007. The role of phytochelatins and antioxidants in tolerance to Cd accumulations in *Brassica juncea* L. Ecotoxicol. Environ. Safety, Article in press.

[37] Herbette, S., Taconnat, L., Hugouvieux, V., Piette, L., Magniette, L.M., Cuine, S., Auroy, P., Richaud, P., Forestier, C., Bourguignon, J., Renou, J.P., Vavasseur, A., Leonhardt, N., 2006. Genome-wide transcriptome profiling of the early cadmium response of Arabidopsis roots and shoots. Biochimie 88, 1751-1765.

[38] Stolt, J.P., Sneller, F.E.C., Bryngelsson, T., Lundborg, T., Schat, H., 2003. Phytochelatin and cadmium accumulation in wheat. Environ. Exp. Bot. 49, 21-28.

[39] Isaure, M.P., Fayard, B., Sarret, G., Pairis, S., Bourguignon, J., 2006. Localization and chemical forms of cadmium in plant samples by combining analytical electron microscopy and X-ray spectromicroscopy. Spectrochim. Acta 61, 1242-1252.

[40] Komy, Z.R., Gabar, R.M., Shoriet, A.A., Mohammed, R.M., 2006. Characterisation of acidic sites of Pseudomonas biomass capable of binding protons and cadmium and removal of cadmium via biosorption. World J. Microbiol. Biotechnol. 22, 975-982.

[41] Bunluesin, S., Kruatrachue, M., Pokethityook, P., Upatham, S., Lanza, G.R., 2007. Batch and continuous packed column studies of cadmium biosorption by Hydrilla verticillata biomass. J. Biosci. Bioeng. 103, 509-513.

[42] Karlsson, T., Elgh-Dalgren, K., Bjorn, E., Skylberg, U., 2007. Complexation of cadmium to sulfur and oxygen functional groups in an organic soil. Geochim. Cosmochim. Acta 71, 604-614.

[43] Ulrich, F.; Zachariasen, W., 1926. The crystal structure of α and β cadmium sulfide and wurtzite. Zeitschrift fuer Kristallographie, Kristallgeometrie, Kristallphysik, Kristallchemie 62, 260-73.

Chapter 5

[1] Darlington, T. K., Neigh, A. M., Spencer, M. T., Nguyen, O. T., Oldenburg, S. J., 2009. Nanoparticle characteristics affecting environmental fate and transport through soil. Environ. Toxicol. Chem. 28, 1191-1199.

[2] Pidgeon, N., Harthorn, B. H., Bryant, K., Rogers-Hayden, T., 2009. Deliberating the risks of nanotechnologies for energy and health applications in the United States and United Kingdom. Nature Nanotech. 4, 95-98.

[3] Atienzar, F.A., Jha, A.N., 2006. The random amplified polymorphic DNA (RAPD) assay and related techniques applied to genotoxicity and carcinogenesis studies: A critical review. Mutation Research 613, 76-102.

[4] Czernichowski, A., Czernichowski, M., Wesolowska, K., 2006. Generation of 1 kg/h of hydrogen from soybean biodiesel. Preprints of Symposia: ACS, Division of Fuel Chemistry 51, 619-620.

[5] Murakami, M.; Ae, N., Ishikawa, S., 2007. Phytoextraction of cadmium by rice (*Oryza sativa* L.), soybean (*Glycine max* (L.) Merr.), and maize (*Zea mays* L.). Environ. Pollut. 145, 96-103.

[6] Maejima, Y., Makino, T., Takano, H., Kamiya, T., Sekiya, N., Itou, T., 2007. Remediation of cadmium-contaminated paddy soils by washing with chemicals: Effect of soil washing on cadmium uptake by soybean. Chemosphere 67, 748-754.

[7] Lopez-Moreno M.L., de la Rosa G., Hernandez-Viezcas J.A., Castillo-Michel H., Botez C.E., Peralta-Videa J., Gardea-Torresdey J., 2010. Evidence of the Differential Biotransformation and Genotoxicity of ZnO and CeO_2 Nanoparticles on Soybean (Glycine max) Plants. Environ. Sci. Technol. 44, 7315-7320.

[8] Lin, D., Xing, B., 2007. Phytotoxicity of nanoparticles: inhibition of seed germination and root growth. Environ. Pollut. 150, 243-250.

[9] Nei, M., 1978. Estimation of average heterozygosity and genetic distance from a small number of individuals. Genetics 89, 583–590.

[10] Singh, N., Manshian, B., Jenkins, G. J., Griffiths, S. M., Williams, P. M., Maffeis T. G., Wright, C. J., Doak, S. H., 2009. NanoGenotoxicology: The DNA damaging potential of engineered nanomaterials. Biomaterials 30, 3891–3914.

[11] Landsield, R., Maike, D. K., Schulz, M., Wiench, K., Oesch, F., 2009. Genotoxicity investigations on nanomaterials: Methods, preparation and characterization of test material, potential artifacts and limitations—Many questions, some answers. Mutat. Res. 681, 241–258.

[12] Dufour, E. K., Kumaravel, T., Nohynek, G. J., Kirkland, D., Toutain, H., 2006. Clastogenicity, photo-clastogenicity or pseudo-photo-clastogenicity: genotoxic effects of zinc oxide in the dark, in pre-irradiated or simultaneously irradiated Chinese hamster ovary cells. Mutat. Res. 607, 215–24.

[13] Schubert, D., Dargusch, R., Raitano, J., Chan, S., 2006. Cerium and yttrium oxide nanoparticles are neuroprotective. Biochem. Biophys. Res. Comm. 32, 86–91.

[14] Park, E. J., Choi, J., Park, Y. K., Park, K., 2008. Oxidative stress induced by cerium oxide nanoparticles in cultured BEAS-2B cells. Toxicology 245, 90-100.

[15] Robinson, R. D., Spanier, J. E., Zhang, F., Chan, S. W., Herman, I. P., 2002. Visible thermal emission from sub-band-gap laser excited cerium dioxide particles. J. App. Phys. 92, 1936–1941.

CURRICULUM VITAE

Hiram Castillo-Michel was born in Chihuahua, Chih., México on February 1, 1979, the first son of Armando Castillo and Rosa Michel. He received his Bachelor of Science degree in Chemical Engineering in 2003 from the Universidad Autónoma de Chihuahua. He joined the chemistry department at UTEP in January 2004 as a master student in chemistry. His thesis "Biochemical aspects of chromium and arsenic uptake by peas (*Pissum sativum*): Effect on amylase activity and elemental reduction" was supervised by Dr. Jorge Gardea-Torresdey. He was selected as the "Outstanding graduate" in December 2005 at the UTEP College of Science Pre-Commencement. In the spring of 2006 he joined the ESE PhD program. While at UTEP, he authored and coauthored over 13 manuscripts published in some of the most prestigious international journals in the environmental field. He has also presented his work at numerous national and international conferences

PUBLICATIONS

1. Montes-Holguin, M.O., Peralta-Videa, J.R., Meitzner, G., Martinez-Martinez, A., de la Rosa, G., **Castillo-Michel, H.**, Gardea-Torresdey, J.L. (2006). Biochemical and spectroscopic studies of the response of Convolvulus arvensis L. to Cr(III) and Cr(VI) stress. Environmental Toxicology and Chemistry 25 (1), 220-226.

2. **Castillo-Michel, H.**, Parsons, J.G., Peralta-Videa, J.R., Martínez-Martínez, A., Dokken, K.M., Gardea-Torresdey, J.L. (2007). Use of X-ray absorption spectroscopy and biochemical techniques to characterize arsenic uptake and reduction in pea (Pisum sativum) plants. Plant Physiology and Biochemistry 45, 457-463.

3. Lopez M.L., Peralta-Videa, J.R., **Castillo-Michel, H.**, Martinez-Martinez, A., Gardea-Torresdey, J.L. (2007). Lead toxicity in alfalfa plants exposed to phytohormones and ethilenediaminetetracetic acid monitored by peroxidase, catalase and amylase activities. Environmental Toxicology and Chemistry 26, 2717 - 2723.

4. Mokgalaka-Matlala, N.S., Flores-Tavizon, E., **Castillo-Michel, H.**, Peralta-Videa, J.R., Gardea-Torresdey, J.L. (2008). Toxicity of arsenic(III) and (V) on plant growth, element uptake, and total amylolytic activity of mesquite (Prosopis spp.) International Journal of Phytoremediation 10(1), 47 - 60.

5. De la Rosa, G., Martínez, A., **Castillo-Michel, H.**, Fuentes-Ramírez, R. Gardea-Torresdey, J. (2009). Insights into the mechanisms of Cd hyperaccumulation in S. kali, a desert plant species. Nova Scientia 2(1), 33-53.

6. **Castillo-Michel, H.**, Zuverza-Mena, N., Parsons, J.G., Dokken, K.M., Duarte-Gardea, M. Peralta-Videa J.R., Gardea-Torresdey, J.L. (2009). Speciation and coordination of arsenic in two phenotypes of the desert plant species Chilopsis linearis. Phytochemistry 70(4), 540-545.

7. **Castillo-Michel, H.**, Valente, N., Martinez-Martinez, A., Parsons, J.G., Peralta-Videa, J.R., Gardea-Torresdey, .L. (2009). Coordination and speciation of cadmium in corn seedlings and its effects on macro and micro nutrients uptake. Plant Physiology and Biochemistry 47(9), 822-826.

8. Parsons, J.G., Lopez, M.L., **Castillo-Michel, H.**, Peralta-Videa, J.R., Gardea-Torresdey, J.L. (2009). Arsenic Speciation in Biological Samples Using XAS and Mixed Oxidation State Calibration Standards of Inorganic Arsenic. Applied Spectroscopy 63(8), 961-970.

9. Mokgalaka-Matlala, N.S., Flores-Tavizón, E., **Castillo-Michel, H.**, Peralta-Videa, J.R., Gardea-Torresdey, J.L. (2009). Arsenic tolerance in mesquite (Prosopis sp.): Low molecular weight thiols synthesis and glutathione activity in response to arsenic. Plant Physiology and Biochemistry 47, 822-826.

10. De la Rosa, G., Torres, J., Parsons, J.G., Peralta-Videa, J.R., **Castillo-Michel, H.**, Lopez, M.L., Cruz-Jiménez, G., Gardea-Torresdey, J.L. (2009). X-ray Absorption Spectroscopy Unveils the Formation of Gold Nanoparticles in Corn (Zea mays) Acta Universitaria 19, Special Volume 2, 76-81.

11. Arias, J., Peralta-Videa, J.R., Ellzey, J.T., Viveros, M.N., Ren, M., Mokgalaka-Matlala, N.S., **Castillo-Michel, H.**, Gardea-Torresdey, J.L. (2009). Plant growth and metal distribution in tissues of *Prosopis juliflora-velutina* grown on chromium contaminated soil in the presence of *Glomus deserticola*. Environmental Science and Technology 44 (19), 7272–7279.

12. López-Moreno, M. L., De la Rosa, G., Hernández-Viezcas, J. A., **Castillo-Michel, H.**, Botez, C., Peralta-Videa, J. R., Gardea-Torresdey, J. L. (2010). Evidence of the differential biotransformation and genotoxicity of ZnO and CeO_2 nanoparticles on soybean (Glycine max) plants. Environmental Science and Technology 44 (19), 7315–7320.

13. Hernandez-Viezcas, J.A., **Castillo-Michel, H.,** Servin, A.D., Peralta-Videa, J.R., Gardea-Torresdey. J.L. (2010). Verification through ICP-OES, μXRF, and XANES of the absorption, distribution, and biotransformation of ZnO nanoparticles in the desert plant mesquite (*Prosopis juliflora-velutina*). Environmental Science and Technology (accepted in revision).

PRESENTATIONS

1. Castillo-Michel H., Martinez-Martinez A., Peralta-Videa J.R., Gardea-Torresdey J.L. Actividad Amilasa en respuesta a la toma de arsenico y cromo en Pisum sativum (Chicharos). Poster 3F. Internacional Conference "El conocimiento botanico en la gestion ambiental y el manejo de ecosistemas", September 22, 2005. Durango, Dgo, Mexico.

2. Castillo-Michel H., Martinez-Martinez A., Peralta-Videa J.R., Gardea-Torresdey J.L. Amylase activity in response to arsenic and chromium uptake in Pisum sativum (peas). Poster D-34. SACNAS national conference, October 2, 2005. Denver, Colorado.

3. Castillo-Michel H., Martinez-Martinez A., Mokgalaka N.S., Peralta-Videa J.R., Gardea-Torresdey J.L. Amylase activity in response to chromium and arsenic uptake in Pisum sativum. Oral presentation. CREST-RESSACA Conference "Emerging Technologies for a Sustainable Environment", October 21, 2005. South Padre Island, Texas.

4. Castillo-Michel H., Parsons J., Peralta-Videa J.R., Gardea-Torresdey J.L. Chromium(VI) and arsenic(V) reduction in Pisum sativum (peas): X-ray absorption spectroscopy analysis. Oral presentation. ACS national meeting, March 28, 2006. Atlanta, Georgia.

5. Castillo-Michel H., Zuverza-Mena N., Parsons J.G., Peralta-Videa J.R., Gardea-Torresdey J.L. Effect of arsenic uptake on macro and micronutrient absorption and total amylolitic activity in peas. Oral presentation. South Central SETAC Regional Meeting, May 19, 2006. Denton, Texas.

6. Castillo-Michel H., Zuverza-Mena N., Parsons J.G., Peralta-Videa J.R., Gardea-Torresdey J.L. Effect of arsenic uptake on macro and micronutrient absorption and total amylolitic activity in peas. Oral presentation. SACNAS national conference, October 28, 2006. Tampa, Florida.

7. Castillo-Michel H., Parsons J.G., Peralta-Videa J.R., Martinez-Martinez A., Dokken K.M., Gardea-Torresdey J.L. Actividad amilolitica total y alfa-amilasa en respuesta a la toma de arsenico en plantas de chicharo. Poster presentation. XXVI Congreso Nacional de la Sociedad Mexicana de Bioquímica, November 14, 2006. Guanajuato, Gto., Mexico.

8. Castillo-Michel H., Peralta-Videa J.R., Dokken K.M., Gardea-Torresdey J.L. Effect of As(III) exposure on the activity of starch degrading enzymes in the pea leaf. Poster presentation. ACS national meeting, March 28, 2007. Chicago, Illinois.

9. Castillo-Michel H., Dokken K.M., Martinez-Martinez A., Peralta-Videa J.R., Gardea-Torresdey J.L. Effect of arsenite on the activity of oxidative stress enzymes and DNA integrity in the root zone of pea plants. Oral presentation. SACNAS National Conference, October 13, 2007. Kansas City, Missouri.

10. Castillo-Michel H. Dokken K.M., Peralta-Videa J.R., Gardea-Torresdey J.L. Study of localization and chemical forms of arsenic in three species of the Parkinsonia plant genus using X-ray spectromicroscopy. Oral presentation. SACNAS National Conference, October 14, 2008. Salt Lake City, UTAH.

11. Castillo-Michel H., Dokken K.M., Peralta-Videa J.R., Gardea-Torresdey J.L. Study of localization and chemical forms of arsenic in three species of the Parkinsonia plant genus using X-ray spectromicroscopy. Oral presentation. International Conference on the Biogeochemistry of Trace Elements, July 13, 2009. Chihuahua, Chih. Mexico.

12. Castillo-Michel H., Dokken K.M., Peralta-Videa J.R., Gardea-Torresdey J.L. Phytostabilization of arsenic by three species of the parkinsonia plant genus. Poster presentation. SACNAS National Conference, October 15, 2009. Dallas, Texas.

13. Castillo-Michel H., Dokken K.M., Peralta-Videa J.R., Gardea-Torresdey J.L. Use of Synchrotron Techniques to Determine Coordination and Speciation of Arsenic in the Desert Plant Parkinsonia florida. Oral presentation. ACS Southwest Regional Meeting, November 5, 2009. El Paso, Texas.

14. Castillo-Michel H., Hernandez-Viezcas J.A., Dokken K., Peralta-Videa J., Gardea-Torresdey J.L. Local coordination and speciation of arsenic in the root-soil interface of the desert plant *Prosopis juliflora*. Poster presentation. ALS User's meeting October 13, 2010.